Characterization of myeloid-derived suppressor cells during acute Friend retrovirus infection of mice

Inaugural Dissertation

for

the Doctoral Degree of

Dr. rer. nat.

from the Faculty of Biology

University of Duisburg-Essen,

Germany

Submitted by

Malgorzata Drabczyk-Pluta, née Drabczyk

from Warsaw, Poland

August 2016

Die der vorliegenden Arbeit zugrunde liegenden Experimente wurden am Institut für Virologie in der Abteilung für experimentelle Virologie der Universität Duisburg-Essen durchgeführt.

1. Gutachter: Prof. Ulf Dittmer
2. Gutachter: Prof. Wiebke Hansen

Vorsitzender des Prüfungsausschusses: Prof. Ralf Küppers
Tag der mündlichen Prüfung: 19.10.2016

Content

1. Introduction

1.1 The immune system

The immune system is a complex of mechanisms and structures which protects an organism from infectious agents and pathologic processes. The disease can be caused by pathogens, like viruses, bacteria, fungi, but may be also caused by internal mechanisms, like autoimmunity or cancer. Protection in invertebrates is provided by an innate immune system, whereas vertebrates have developed an additional, adaptive immune system, which can provide a specific immune response against a pathogen.

1.1.1 The innate immune system

The innate immune system represents first line of immune response and becomes immediately activated after an organism is invaded with a pathogen. The mechanisms of innate immune system are not specific to a certain pathogen. They can be recognized by molecular structures, called pathogen associated molecular patterns (PAMPs). The parts of the innate immune system include: molecular (antimicrobial compounds), cellular (macrophages and neutrophils) and more complex (skin). The innate immune system can be further subdivided into four types of defense: anatomical barriers, physiological barriers, phagocytosis and inflammation. (99)

1.1.1.1. Cellular components and function of the innate immune response

The development of immune response occurs in bone marrow and leads to formation of different immune cells. PAMPs are recognized by pattern recognition receptors (PRRs) and these molecules can either be soluble or cell-associated. Examples of PRRs are the macrophage mannose receptor, complement, toll-like-receptors (TLRs) nucleotide-binding oligomerization domain receptors, cytoplasmic RNA sensors like RIG-I and MDA-5 (recognizes dsRNA) and cytosolic DNA sensors like cGAS (recognizes dsDNA) (2, 99). These receptors trigger various responses, like

phagocytosis, chemotaxis, and upregulation of co-stimulatory molecules or secretion of cytokines (2, 99).

Natural killer (NK) cells are a part of the innate immune response. They are able to respond to pathogens immediately in a non-specific manner. When activated, NK release of cytotoxic granules, containing granzymes (Gzm) and perforin. This leads to the induction of apoptosis in the target cells. NK cells express ligands for death receptors like TRAIL (tumor-necrosis factor-related-apoptosis-inducing ligand) or FasL, which kill cells through binding to their receptors on the target cells. (99)

Phagocytosis is another feature of the immune system, which is performed by specialized immune cells, such as dendritic cells (DCs) macrophages/monocytes, and granulocytes (especially neutrophils). These cells can destroy pathogens in phagosomes. Monocytes (in the blood) or macrophages (in tissues) are long-lived phagocytic cells which secrete signaling proteins like cytokines and chemokines to attract other immune cells. Activated macrophages initiate the process of inflammation. Additionally, DCs can take up large amounts of extracellular fluid and its content (macropinocytosis). Their main function is the recognition and degradation of invading pathogens. DCs present antigens within the major histocompatibility complex (MHC) molecules on their surface to naïve T lymphocytes. The first encounter happens in peripheral lymphoid organs to initiate the adaptive immune response. DCs are also able to produce cytokines that influence the innate and adaptive immunity. The mechanism of antigen presentation provides the crucial connection between innate and adaptive immunity and is essential to initiate an effective immune response against a pathogen (2, 99). The innate immune response provides the first and quick defense against foreign structures. Components of innate immunity may be divided in natural and mechanical barriers (e.g., skin, surface epithelia, cilia), chemical protection (e.g., proteases, lysozyme), the complement system, which are both humoral and cellular units (99).

1.1.1.2 Humoral components of the immune system

The humoral immune response consists of different soluble factors, such as complement and cytokines. Complement system is an enzymatic cascade of different proteolytic enzymes. This system consists of opsonization, local

inflammation, chemoattractant or by binding the pores on the cell membrane in order to destroy the cell (99).

Cytokines are various soluble, immunoregulatory factors, such as interleukins (IL), interferons, colony stimulating factors, chemokines, and tumor necrosis factors. Cytokines are the key factors in the cell-cell communication and affect cell growth, migration, development, differentiation and apoptosis of cells. They have an important function as signaling molecules during the tumor development and are important for the tissue damage repair (2, 99). They also modulate the immune response, control the virus replication and thus contribute to an effective immune response (99). One of these groups is interferons, (IFN), which can be induced as a result of PRR stimulation by its ligand resulting from different infections. Type I interferons (IFNα and IFNβ) are important players in the immediate anti-viral response. Almost all cells express the interferon receptor. Upon binding of its ligand an anti-viral state is induced, which is characterized by the expression of hundreds of interferon stimulated genes that are able to reduce viral replication and modulate immune cell responses (2, 99).

1.1.1.3 Myeloid-derived suppressor cells

Myeloid-derived suppressor cells (MDSCs) is a heterogeneous population of activated, immature myeloid cells, which show robust suppressive function. First, these cells was described around 30 years ago (150), but only lately got deserved attention due to evidence about suppressive function in distinct models, such as cancer (59), infectious diseases (HBV, HCV, HIV), autoimmunity etc..

Myeloid-derived suppressor cells are characterized in different models, both *in vitro* and *in vivo*. In murine model they are defined by co-expression of Gr1 (which consists of 2 epitopes Ly6G and Ly6C) and CD11b (α_M-integrin). In healthy, murine bone marrow, cells with this phenotype take 20%-30% of cell suspension. Spleen contains only small amount of MDSCs, around 1-3%, of Gr1$^+$ CD11b$^+$ cells. MDSCs are absent in lymph nodes. MDSCs are, in mice, divided in two distinct populations: granulocytic or polymorphonuclear (gMDSCs) and monocytic (mMDSCs). gMDSCs are characterized with expression of CD11b$^+$ and high expression of Gr1, or as

CD11b$^+$ Ly6G$^-$ Ly6C$^+$ cells. This population shows morphological and phenotypical similarities to neutrophils. Monocytic MDSCs morphologically and phenotypically resemble monocytes. mMDSCs are defined by expression of CD11b$^+$ and dim expression of Gr1 or as CD11b$^+$ Ly6G$^-$ Ly6C$^+$ cells.
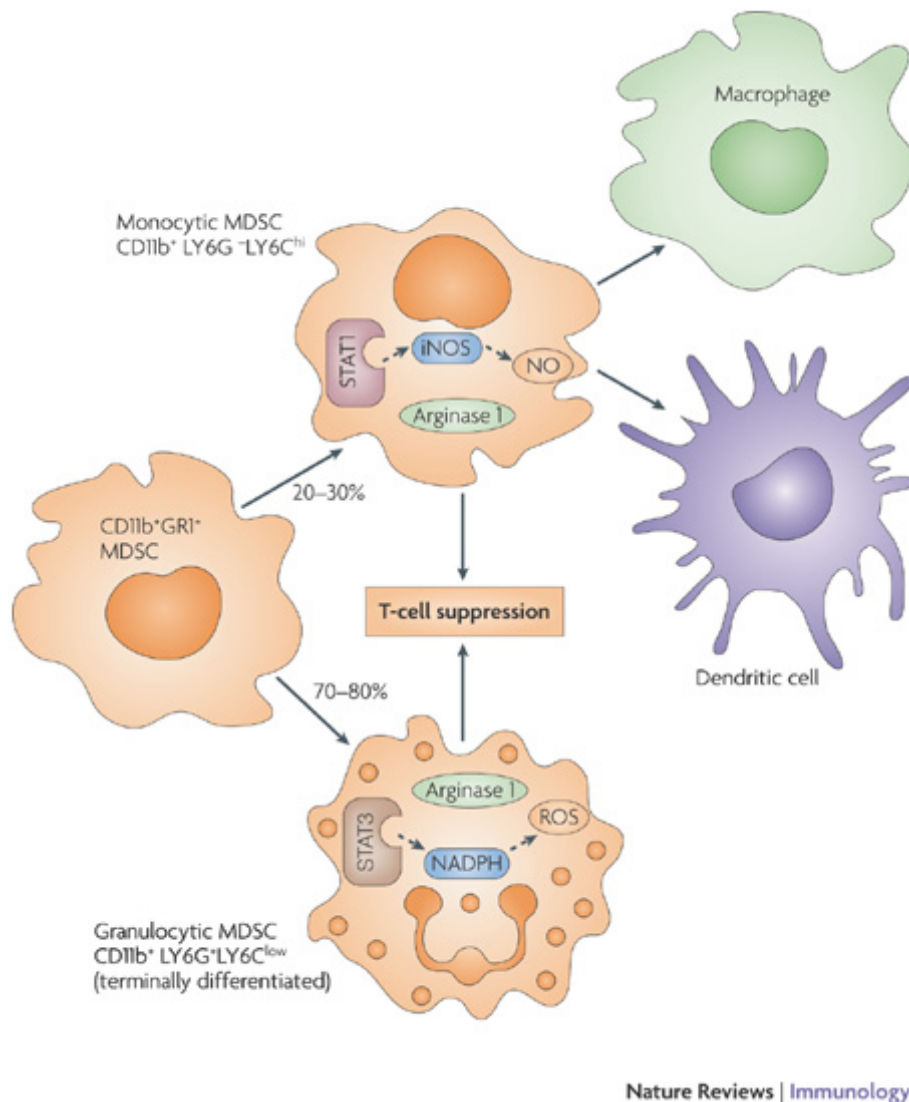
Figure 1.1 Murine granulocytic and monocytic MDSCs

Murine MDSCs consist of two main subsets with distinct functions: granulocytic and monocytic. gMDSC suppress the T cell response mainly via ROS and arginase activity, and mMDSCs the T cell response via NO and arginase.

In human system, MDSCs are mainly characterized by expression of the common myeloid marker CD33, CD11b, and lack of CD14 expression. They also not express maturation markers for myeloid and lymphoid cells, as well as MHC-class-II molecule HLA-DR. CD15^{+} is also used for characterization of MDSCs in peripheral blood. PBMCs of healthy individuals contain mostly ~0.5% of cells with this phenotype. (59)

MDSCs are generated from common myeloid progenitor cells in bone marrow (BM). This process is regulated by series of signals, which may be divided into two categories: promotion of accumulation of immature myeloid cells, and provision for the pathological activation of these cells.

1.1.1.4 Mechanisms of MDSCs suppressive activity

MDSC action is conducted either though cell-cell contact or is mediated though soluble factors.

MDSC suppressive activity is historically associated with ı-arginine metabolism. In this processes ı-arginine may by converted by two enzymes: arginase-1 (ARG1) and inducible nitric oxide synthase-2 (iNOS or NOS2). In first process ı-arginine is metabolized by ARG1 into urea and ı-ornithine, while NOS2 converts it into nitric oxide (NO) and ı-citrulline. MDSCs are expressing high levels of these enzymes, due to exposure to specific cytokines, where Th2 cytokines TGF-β and IL-10 and associated with ARG1, and Th1 cytokines IFNγ, IL-1, IFNα and TNFα with NOS2. High activity of these enzymes was shown to inhibit T cell function through distinct mechanism. (21, 141)

High MDSCs related arginase activity leads to arginine depletion from microenvironment, which absence leads to decreased expression of T cell-CD3ζ, and through this unable transmission of signal for T cell activation. It may also suppress the cell cycle regulatory protein cyclin D3 and cyclin-dependent kinase 4, which is shown to block proliferation of T cells (111). On the other hand NOS2 mediated production of NO by MDSCs may interfere with JAK/STAT signaling proteins,

required for distinct T cell functions, suppress MHC II expression and induce T cell apoptosis. (21, 59, 84, 149)

Described above mechanism are ɪ-arginine dependent. The other mechanisms involved in MDSCs mediated suppression, such as reactive oxygen species (ROS) production, TGF-β production, cysteine depletion, CD62L downregulation, are ɪ-arginine independent (141).

Another important function of MDSCs mediated immune suppression is reactive oxygen species (ROS) production. Increased production of ROS is one of the characteristics of MDSCs. The increased ROS production by MDSC is mediated by up-regulated activity of NADPH oxidase (NOX2). Inhibition of ROS production by MDSCs in murine and human model efficiently abrogated suppressive effect of MDSC *in vitro*. Interestingly, the interaction of T cells with MDSCs was shown to increase ROS levels due to ligation of integrins expressed on the surface of MDSCs. The production of ROS by MDSCs may be further induced by several known tumor-derived factors, such as TGFβ, IL-10, IL-6, IL-3, platelet-derived growth factor (PDGF) and GM-CSF.(141)

1.1.1.5 Immune regulation and depletion of MDSCs

Different attempts to study the function of MDSCs *in vivo* have been proposed. First, transfer experiments were performed, in which freshly isolated, lipopolisaccharid (LPS) or IFNγ induced MDSCs were transferred into recipient mice. This attempt was shown to inhibit inflammation (147) and reduce CD8+ T cell responses in a melanoma model (128). Another approach to study the function of MDSCs *in vivo* is a specific depletion of these cells. There are different ways to modulate MDSC by reduction of numbers or blockade of the function of MDSCs *in vivo*. The most commonly used way of depletion is by administrating αLy6G or αGr1 antibodies into mice. This procedure allows the efficient depletion of all MDSCs (αGr1 antibody) or of granulocytic MDSCs only (αLy6G antibody). Nevertheless, as lately shown, long term

administration of either αGr1 or αLy6G antibody leads to reappearance of immature Ly6G+ cells (45).

The modulation of immune responses offers promising results for the therapy of different diseases, including cancer and viral infections (91, 144).

Different methods were described to deactivate (influencing MDSCs accumulation by TLR agonists) or deplete MDSCs (depletion by 5-Fluorouracil), as well as differentiate them into mature cells (maturating granulocytic MDSCs by ATRA) or block their development (144). Many of these agents, like 5-Fluorouracil (5FU), ATRA, PDE-5 inhibitors, NO-aspirins, CSF-1R inhibitors, Zoledronic Acid, JAK/STAT3 inhibitors and Multi-Kinase inhibitors, as well as VEGF inhibitors, are already under clinical investigation in cancer treatment (91, 144).

5-FU is an analog of uracil, anti-cancer drug, which operates as antimetabolite by inhibiting thymidylate synthase. 5FU selectively deplete MDSCs. The 5FU what leads to increased IFNγ production by tumor-specific CD8^{+} T cells.

An overview of different strategies used for MDSC immunomodulation is presented in Table 1.1.

Table 1.1 Strategies of MDSC inhibition under investigation (144)

Strategies of MDSC Inhibition Under Investigation

Deactivation of MDSC	Differentiation of MDSC into mature cells	Blocking Development of MDSC	Depletion of MDSC
NO Inhibitors •PDE-5 inhibitors* • NO-aspirins* •L-NAME **Arginase Inhibitors** •PDE-5 Inhibitors* •COX2 inhibitors •NOHA •L-NAME **ROS Inhibitors** •Synthetic Triterpenoids **MDSC Migration Inhibitors** •Anti-glycan antibodies •CSF-1R inhibitors* **Others** •Histamine inhibitors •Anti-IL-17 Antibodies	**Vitamins** •ATRA* •Vitamin A •Vitamin D3* **Cytokines** •IL-12 **Others:** •CpG	**Bisphosphonates** •Zoledronic Acid* **Modulators of Cell Signaling** •JAK2/STAT3 inhibitors* •Multi-Kinase Inhibitors* •VEGF Inhibitors*	**Cytotoxic Agents** •Gemcitabine •Cisplatin •Paclitaxel •5-Fluorouracil **HSP 90 Inhibitors** •17-DMAG **•Others** •IL-6R blockers •Antibody Drug Conjugates (ex IL-13-PE)

Figure 1 Graphical representation of MDSC inhibition strategies. (Abbreviations: NO – Nitric Oxide; PDE-5 – Phosphodiesterase 5; NO-Aspirin – Nitro-aspirin; L-Name – N(G)-Nitro-L-Arginine Methyl Ester; COX2 – Cyclooxygenase 2; CSF-1R – Colony Stimulating Factor Receptor 1; ATRA – All Trans Retinoic Acid; CpG – Deoxycytosine-Deoxyguanine Dinucleotide; JAK2 – Janus-Activated Kinase-2; STAT3 – Signal Transducer and Activator of Transcription 3; VEGF – Vascular Endothelial Growth Factor; 17-DMAG – 17-Dimethylaminoethylamino-17-Demethoxygeldanamycin; IL-6R – IL-6 Receptor); * – Agents that are presently under clinical investigation as MDSC inhibitors.

1.1.2. The adaptive immune system

While the innate immune response is activated within hours, it takes days to weeks for the adaptive immune system to develop its protective effects. Adaptive immunity is different to innate immunity in the way that it is pathogen specific, it takes time to develop and a memory response can be launched at second encounter with an antigen. The adaptive immune system can be divided into the cellular (T and B cells) and humoral (antibodies) components. Recognition of invading pathogens by DCs leads to their activation, causing the upregulation of MHC class I and class II, as well as co-stimulatory molecules to initiate an effective T cell response. After migration to lymphoid organs, DCs present nonself- peptides bound to MHC molecules on their surface to naïve CD4$^+$ and CD8$^+$ T cells. CD4+ T cells only interact with peptide bound to MHC class II and CD8$^+$ T cell only recognize peptides bound to MHC class I. Whereas almost all nucleated body cells express MHC class I, MHC class II is only present on professional antigen presenting cells (APCs), like DCs. There are two different pathways that lead to the presentation of a peptide on an MHC molecule. Peptides presented on MHC class I molecules are of cytosolic or endoplasmic

reticulum (ER) origin, whereas peptides presented on MHC class II molecules are derived from endosomes. All peptides are usually of pathogenic origin and the result from different routes of infection or pathogen encounter. For MHC class I loading endogenous antigens are generated. These are derived from misfolded proteins of cellular or pathogenic origin, or proteins produced within an infected cell. These proteins are cleaved into smaller peptides by the proteasome. The unloaded MHC class I molecule is initially located in the luminal side of the ER membrane. Therefore, peptides must be transported into the ER lumen via the transporter associated with antigen processing (TAP). TAP has the highest affinity for peptides with a length of 8 to 10 amino acids and with hydrophobic and basic carboxy-terminal amino acids, which present the optimal size and anchor charge for MHC class I binding. The process of MHC class I:peptide-complex assembly is highly chaperone guided. The fully assembled complex is then transported to the surface of the cell via the Golgi apparatus, where it can be recognized by specific CD8+ T cells. (99) MHC class II loading occurs in a different process with peptides derived from exogenous antigens captured through phagocytosis or endocytosis. The internalized antigens become degraded in increasingly acidified compartments (early endosome – endolysosome – lysosome) containing hydrolytic enzymes. In this process oligopeptides with a length of 13 to 18 amino acids are produced, which are able to bind to the peptide binding groove of the MHC class II complex. The assembly of the two chains of the MHC class II complex takes place in the ER, where an invariant chain blocks the peptide binding groove from binding endogenous peptides and stabilizes the complex. After passing through the Golgi apparatus, the MHC class II: invariant chain-complex is included in the endosomal-lysomsomal pathway. The invariant chain is degraded, leaving only a small fragment blocking the peptide binding groove (CLIP, class II-associated invariant chain peptide). In a chaperon-mediated pathway, the CLIP is released and replaced by a peptide produced from the endosomal-lysosomal pathway. The MHC class II:peptide-complex is then presented on the surface of APCs, where it can be recognized by specific CD4+ T cells. (79, 99)

B cells are APCs and thereby able to activate naive CD4$^+$ T cells. Their principle role is in the production of antibodies, as part of the humoral immune response to pathogens. B cells mature into antibody-producing plasma cells and memory B cells

in an antigen-driven way. B cells can be activated in two different ways: by thymus independent antigens and thymus-dependent antigens, which is mediated with the help of CD4^{+} T cells. In response to stimulation, B cells produce antibodies and this process can be divided into primary and secondary responses. In the primary response, naïve B cells become activated to produce antibodies, whereas in the secondary response, plasma cells are activated to produce more specific antibodies of different classes. These antibodies from the secondary response are more specific because the B cells have undergone clonal selection, expansion and differentiation in germinal centers. Antibody production is important for specific pathogen recognition and elimination (complement activation, opsonization and neutralization of pathogens and phagocytosis of pathogens). (99)

1.1.2.1 Effector CD8^{+} T cells

CD8^{+} T cells, also called cytotoxic T lymphocyte (CTL), are a subset of T lymphocytes, showing effector function. To achieve their function cytotoxic cell CD8+ T cell acquire activation. To achieve this naïve CD8^{+} T cell need to recognize antigen peptides presented by MHC Class I molecule on activated antigen presenting cells (APCs). MHC I molecules are present on all nucleated cells and present epitopes of viral peptides. CD43 and CD62L are the two glycoproteins used for identification of cytotoxic T lymphocytes. The CD62L molecule is the adhesion and homing receptor, it derives naive T cells through interaction with endothelial cells to secondary lymphoid organs. In case of an encounter of the naïve T cell with its specific antigen the expression of the cell surface molecule CD62L is downregulated. Lack of expression of CD62L classifies the CD8^{+} T cell as activated CD8^{+} effector cell [100, 101]. After activation the CD8^{+} T cells play a role not only in the elimination of infected cells, but they also secrete different cytokines (e.g. IFN-γ, TNF-α) and chemokines and thus also have a regulatory character (99). Cytotoxic CD8^{+} T cells can kill infected cells by exocytosis of lytic granules, as for example, proteases (granzyme), lytic enzymes such as perforin or cytokines (IFN-γ, TNF-α, etc.), or TRAIL (CD253) / TRAIL receptor and Fas (CD95) / Fas (CD95L) mediated apoptosis. During a primary immune response CTLs expand over several hundred folds and

form a very efficient antigen-specific effector immune response and are able to kill several target cells (15).

Cytotoxic CD8+ T cells maintain their function by several cellular mechanisms or secreted molecules. After forming immunological synapse with target cell, CTL may act on two distinct ways: calcium dependent or calcium independent. First and principal of them, is the calcium-dependent secretion of cytotoxic granules, such as granzymes and perforins, upon antigen recognition.

Gzms are serine proteases that are stored in specialized lytic granules of CTLs and NK cells along with perforin. In mice, ten Gzms (A-G, M and gene duplications) and in humans five Gzms (A, B, H, K and M) have been described. When CD8$^+$ T cells become activated and recognize their antigen in an MHC class I context, these granules can be released and the Gzms can kill the target cell. For the Gzms to enter the target cell, perforin pores are formed in the target cell membrane in a calcium dependent manner. Upon entry into the target cell, Gzms induce proteolytic cleavage of caspases eventually leading to DNA fragmentation and cell apoptosis. In addition to activating caspases, Gzms can also activate caspase-independent mitochondrial collapse, resulting in the release of cytochrome c, a pro-apoptotic protein (24, 99).

The Fas (CD95) – FasL (CD95L) pathway is another pathway through which CTLs can induce apoptosis in target cells. Fas is a member of the TNFR family and contains an intracellular death domain to deliver an apoptotic signal upon FasL binding. Fas expression is induced by TNFα and IFNγ or the activation of lymphocytes and FasL is expressed after TCR engagement on CD8+ T cells. The activation of the Fas – FasL pathway results in the activation of caspases and leads to apoptosis (154).

In addition to the above mechanisms, cytokines like IFNγ and TNFα are secreted by activated CD8$^+$ T cells. It should, however, be noted that these cytokines can be secreted by a variety of other immune cells as well (T cells, NK cells, APCs). IFNγ is the only member of the type II interferons with a wide range functionality, like: leukocyte attraction, maturation and differentiation of many cell types, NK cell activity enhancing action and regulation of B cell functions and altering macrophage function during infections. IFNγ also up-regulates factors involved in CD4$^+$ T cell recognition

and induces further MHC class II expression on APCs and other cells. IFNγ is also involved in the up-regulation of MHC class I and the immunoproteasome, therefore providing efficient recognition of virus-infected cells by CTLs. It also elicits direct antiviral effects by regulating antiviral proteins (induces an antiviral state) and has pro-apoptotic and anti-proliferative effects (45, 99).

The surface expression of CD107a (lysosomal-associated membrane protein-1) is a way to determine if cells recently de-granulated. CD107a is located on the surface of intracellular granules designated for exocytosis. Upon degranulation of these intracellular bodies CD107a becomes exposed on the cell surface until it is recycled (99, 119).

1.1.2.3 The different CD4$^+$ T cell subsets

After activation and several rounds of division naïve CD4$^+$ T cells differentiate into various CD4$^+$ T helper subsets. The function and effector or helper mechanism of the CD4$^+$ T cell response is dependent on the cytokine milieu. The best described subsets are Th1 and Th2 cells, which are characterized by strong IFNγ or IL4 production, respectively. Th1 cells activate macrophages and drive inflammation and Th2 cells induce an effective humoral antibody-mediated immune response. In a viral infection, the Th cell response consists mainly of Th1 cells, where they are important for enhancing the CD8+ T cell responses and memory cell development. Many different Th subsets have been described, like T follicular helper cells (Tfh) (specialized B helper cells), Th17 (pro-inflammatory), Th22 (potentially involved in skin homeostasis and pathology), cytotoxic CD4$^+$ T cells (mediating direct killing) and induced regulatory T cells (iTreg) (immunosuppressive). Th cell subsets have a certain level of plasticity and can convert under special change of cytokine milieu into other Th subsets (99).

1.1.2.3.1 T regulatory cells

Tregs are specialized subpopulation of CD4$^+$ T cells, which are naturally present in the immune system. Normally 10-15% of CD4$^+$ T cells in mice are Tregs. The main function of Tregs, also known as suppressor T cells, is to maintain immune homeostasis (99). Like other T cells, one subset of Tregs matures in the thymus

where they are characterized by the expression of CD4, CD25 and Foxp3. These are the natural Tregs. Natural Tregs express IL-2Rα chain (CD25) and the transcriptional repressor forkhead box protein 3 (Foxp3). Natural Tregs are characterized by selective, surface expression of Neuropilin-1 (Nrp-1) (85). Tregs that arises in the periphery are called inducible Tregs. This cell population is generated from naïve $CD25^+$ or $CD25^-$ T cells in the periphery upon antigen presentation by semi-mature DCs and under the influence of IL-10, transforming growth factor β (TGF-β) and possibly IFN-α (63). Higher numbers of $CD4^+$ Tregs in cancer patients compared to normal healthy controls have been reported in recent in head and neck, hepatocellular, gastric, breast, ovarian, lung, melanoma, renal cell, and pancreatic cancer (150). Increased numbers of Tregs have also been observed in numerous human and animal studies of chronic viral infections, in Hepatitis C virus (HCV) (91), HIV (17) and herpes simplex virus (HSV) (131) infections. There are four suppression mechanisms, which are utilized by Tregs. Tregs can secrete inhibitory cytokines, such as IL-10, TGF-β, and IL-35, and apply these soluble factors as a main mechanism of suppression. Recent studies showed that Tregs may use perforin/granzyme-mediated cytotoxicity. Metabolic disruption by Tregs includes high-affinity CD25 dependent cytokine-deprivation-mediated apoptosis, cyclic adenosine monophosphate (cAMP)-mediated inhibition, and $CD39^-$ and/or $CD73^-$ generated, adenosine receptor 2A (A2AR)-mediated immunosuppression. Another mechanisms are targeting DCs and include the modulation of maturation and function of DCs through lymphocyte-activation gene 3 (LAG-3)–MHC-class-II-mediated suppression of DC maturation, and CTLA4–CD80/CD86-mediated induction of indoleamine 2,3-dioxygenase (IDO) (29).

1.1.2.4 Humoral immune response

Antibodies in the blood and extracellular fluids provide humoral immunity of the adaptive immune system. They show diverse biological functions, they can bind extracellular pathogens or their products. They can be further neutralized, opsonized or the complement system can be activated. Activated B cells produce pathogen-specific antibodies. They are required for their activation, proliferation and differentiation into antibody-secreting plasma cells. As a stimulus for production of

these pathogen specific antibodies serve a specific antigen contact and interaction with Th cells. (99)

1.1.2.5 Costimulatory and co-inhibitory molecules

Co-stimulatory and inhibitory molecules are important for the activation of T cells through DCs. Many of these molecules have been identified and this section focuses on the ones that have been well characterized. The TCR-inducible co-stimulatory receptor (ICOS), homologous to CD28 and cytotoxic T lymphocyte antigen-4 (CTLA-4), interacts with its ligand on APCs thereby enhancing effector T cell responses (65). ICOS becomes up-regulated within 6 to 48 hours after stimulation on T cells and delivers a co-stimulatory signal to T cells. This enhances T cell dependent antibody production and cytokine secretion by CD4$^+$ T cells (49). The glucocorticoid induced tumor necrosis factor receptor (TNFR) family related gene (GITR) is a costimulatory molecule expressed on T cells (59).

T cell immunoglobulin mucin 3 (TIM3) is usually expressed on Th1 and some CD8+ T cells and acts as a negative regulator on these cells, inducing apoptosis. TIM3 is up regulated during a late stage of T cell differentiation and is expressed on dysfunctional or exhausted CD8$^+$ T cells (98, 136).

Programmed cell death-1 (PD-1) is described to be a co-inhibitory receptor expressed on T cells and signaling through it attenuates TCR signaling and inhibits cytotoxic functions. Following TCR stimulation, PD-1 is expressed on T cells and binds members of the B7 family (PD-L1 (B7-H1) and PD-L2 (B7-DC)). Its ligand PD-L1 is up-regulated on hematopoietic and non-hematopoietic cells and its signaling down-regulates TCR signaling, inhibiting proliferation and cytokine secretion which promotes anergy and apoptosis, leading to immune suppression (10, 105). CTLA-4 is an inhibitory molecule and a homolog of the co-stimulatory molecule CD28. It has higher affinity than CD28 to the B7 family ligands CD80 and CD86. CTLA-4 becomes transiently up-regulated on T cells shortly after activation and interaction with its ligands prevents continuous T cell co-stimulation and activation (147).
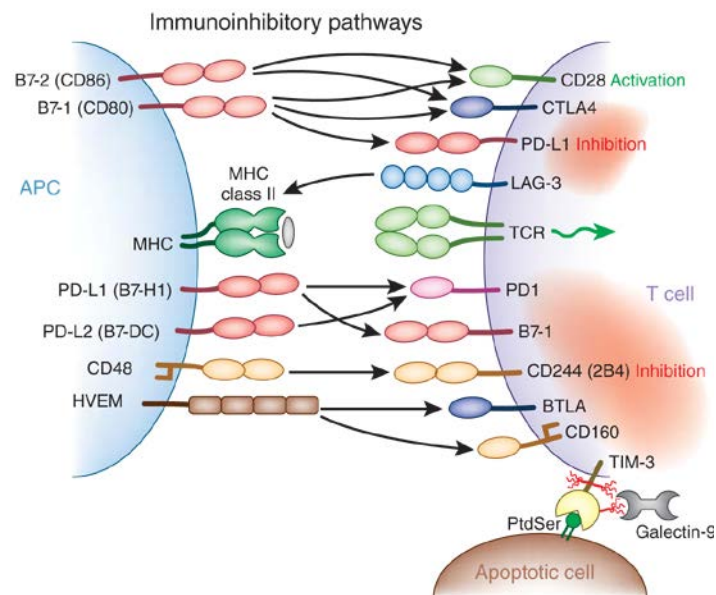
Figure 1.2 Coinhibitory pathways (121)

Exhausted T cells can express multiple inhibitory receptors, which modify the outcome of a T cell antigen receptor signal and limit the population expansion, functional activity and survival of T cells.

The lymphocyte-activation gene 3 (Lag3) is a CD4 homolog which binds MHC class II molecules with a higher affinity than CD4 (124). It is up-regulated on T cells after activation and negatively regulates T cell expansion and activation (40).

1.1.2.6 Adenosine metabolism

An interesting and newly described mechanism of T cell immunosuppression involves the two ecto-enzymes CD39 (ecto-nucleoside triphosphate diphosphohydrolase 1 or ATPase/ADPase) and CD73 (ecto-5'-nucleotidase), which removes the proinflammatory signal ATP from extracellular spaces and generates anti-inflammatory adenosine (65). CD39 is the rate-limiting enzyme in the cascade. It converts immune activating extracellular ATP or ADP into AMP, which can then be used by CD73 to generate adenosine. Adenosine is an immune suppressive molecule and binds to the A2A receptor on effector T cells, which then become

suppressed because of elevated intracellular production of cyclic AMP (cAMP) (49, 50).
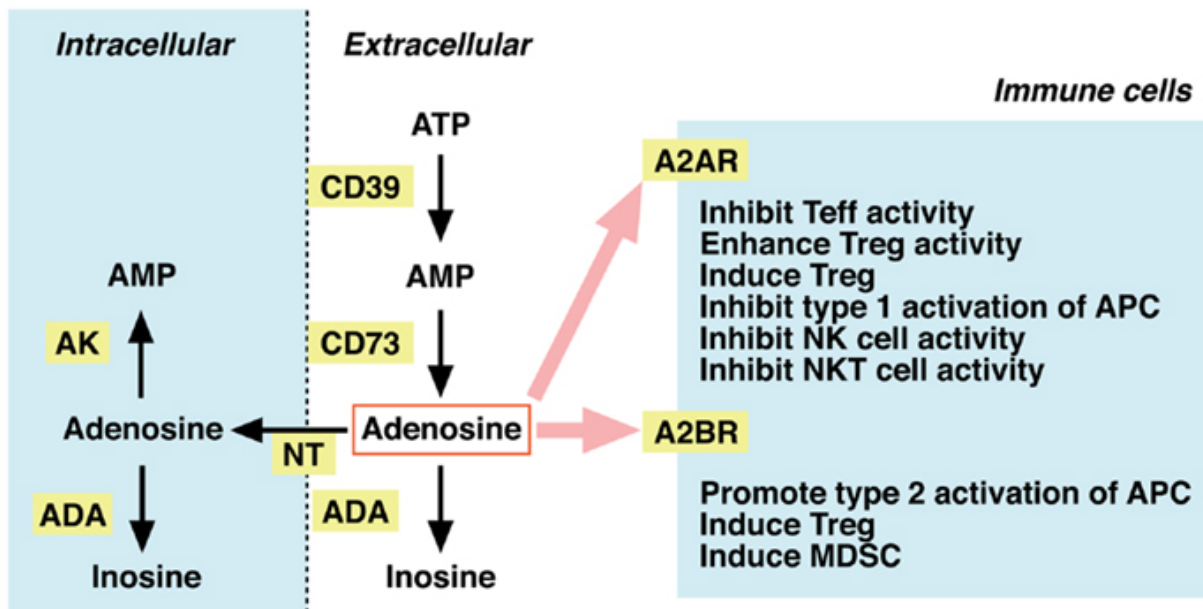
Figure 1.3 Metabolism of extracellular adenosine and its effect of cellular immunity (18)

The activities of CD39 and CD73 lead to production of extracellular adenosine, which is decreased by adenosine deaminase (ADA)- dependent catabolism or by cellular uptake through nucleoside transporters (NT). Increased level of extracellular adenosine stimulates A2AR and A2BR on immune cells. Adenosine is suppressive to effector T cells, NK cells and NKT cells. These suppressive activities may by further enhanced by adenosine-mediated Treg, tolerogenic APCs or MDSC suppression.

Adenosine has also been shown to modulate DC maturation and thereby favor a tolerogenic phenotype (137). Adenosine has a very short half-life, which makes close proximity necessary for effective suppression through this pathway. Interestingly, it has also been shown that the transfer of cAMP from Tregs through gap junctions into effector cells or DCs can directly inhibit these cells (17, 19).

1.1.2.7 Proliferation markers

Different markers are described to indicate proliferation of T cell. The most commonly used marker is a Ki67. Ki67 is a nuclear protein present in the active stages of the cell cycle (G1, S, G2 and M phase), but absent in resting cells (G0 phase) (109). Therefore, it can be used to determine the proliferative potential of cell populations. Different techniques allow determining cell proliferation, such as the incorporation of BrdU, a thymidine analogue, into the chromosomal DNA. (72)

1.2 Retroviruses

Retroviruses are a large group of RNA viruses. Their virions are 80-100 nm diameter, their envelope consist of and display viral glycoproteins. Retroviruses are broadly divided into two groups: simple and complex. Retroviruses are composed of 3 domains, which encode different virion proteins: *gag*, from which are derived internal viron proteins which form the matrix, the capsid, and the nucleoprotein structures, *pol*, which consist of information of reverse transcriptase and integrase enzymes and *env*, which directs the synthesis of surface and transmembrane envelope proteins. Additional, smaller domain, called *pro,* encodes virion protease. As simple viruses consist mainly of the above genes, complex viruses contain also of different genes encoding further regulatory and accessory proteins. (41)
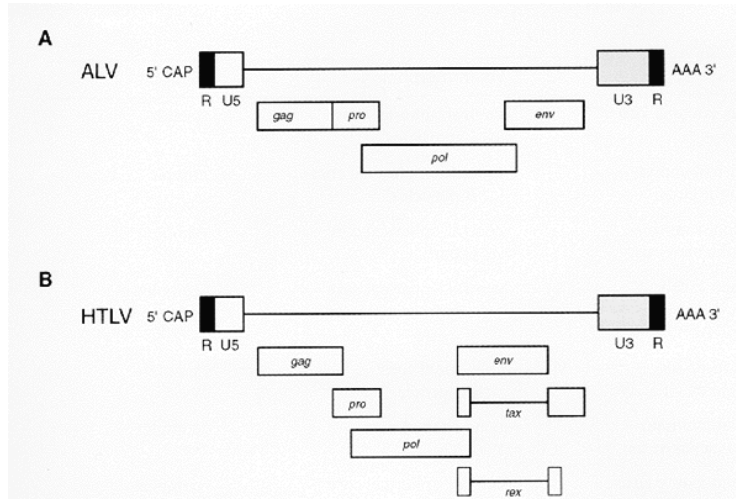
Figure 1.4 Retroviral genome

A. A genome of simple retrovirus consisting of four major domains: gag, pro, pol and env.

B. A genome of complex retrovirus containing, additionally, information for other regulatory proteins.

Retroviruses are divided in 3 different groups: oncoviruses, lentiviruses and the spumaviruses. Furthermore, oncoviruses are divided in 5 subgroup (α,β,γ,δ,ε – viruses). (41)

1.2.1 Retroviral life cycle

Retroviral replication starts by binding viral envelope proteins to entry receptor of a host cell. The replication of retroviruses takes place in several stages.

First, retroviral replication starts by binding the viruses with their glycoproteins in the lipid bilayer specific surface receptors of the host cell (1). After adsorption and fusion of the viral membrane with the host cell membrane, the capsid reaches the cytoplasm of the host cell (2). In the cytosol, the viral proteins as well as the RNA strands are released. Using reverse transcriptase, the viral RNA in double-stranded (ds) DNA is rewritten (3), which is further transported into the nucleus by viral and cellular proteins (4). In the nucleus, the viral DNA is integrated into the host cell genome by the Integrase (5). The DNA of the host cell of the provirus is transcribed by the RNA polymerases II and other transcription factors (6). Next, the mRNA of the provirus is transported back to the cytosol and there translated (7). Newly formed nucleocapsids attach to the plasma membrane and it comes at the cell surface using the proteins for packaging of viral particles. The budding at the cell membrane or the release of the viral particles is also called budding (8).
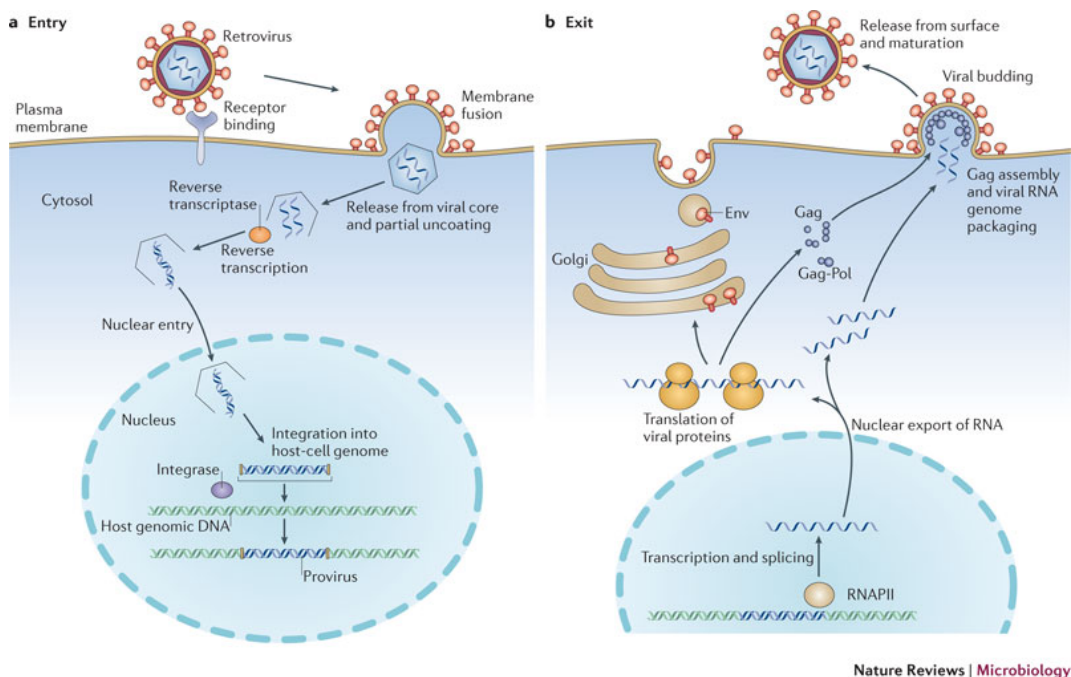
Figure 1.5 Retroviral life cycle (133)

a. Steps of viral entry: binding to a specific receptor on the cell surface; membrane fusion either at the plasma membrane or from endosomes (not shown); release of the viral core and

partial uncoating; reverse transcription; transit through the cytoplasm and nuclear entry; and intergration into cellular DNA to give a provirus

b. Steps of viral exit: transcribtion by RNA polymerase II (RNAPII); splicing and nuclear export of viral RNA; translation of viral proteins, Gag assembly and RNA packaging; budding through the cell membrane; and release from the cell surface and virus maturation.

1.2.2 Human Immunodeficiency Virus-1

HIV-1 the causative agent of AIDS (acquired immunodeficiency syndrome) was discovered in 1983 (19, 105). It is a complex retrovirus (lentivirus) and possesses all components of a simple retrovirus with the addition of regulatory (Tat and Rev) and accessory (Nef, Vif, Vpr and Vpu) proteins. HIV-1 infects cells by binding of gp120 to CD4, present on CD4$^+$ T cells, macrophages and DCs as well as by interaction with a co-receptor. There are two co-receptors which can potentiate infection, CXCR4 and CCR5. Different strains of HIV-1 can utilize these two co-receptors to varying degrees which is a major determinant of viral tropism. HIV-1 infection causes a long lasting disease characterized by a long incubation period, which is usually asymptomatic, and eventual progression to AIDS, if untreated (69). The routes of transmission are either horizontally; by sexual contacts or contact to contaminated blood (blood transfusion, intravenous drug use); or vertically (mother to child) (142). (140).

The first antiretroviral drugs were developed in the nineties and given in single or dual combination. However, this could only control viral loads temporarily due to drug resistance by viral escape mutants. In the following years, the highly active antiretroviral therapy (HAART) a combination of three different antiretroviral drugs was developed. There are different antiretroviral drugs available targeting different stages of the retroviral life cycle: reverse transcriptase inhibitors (nucleoside or nonnucleoside), protease inhibitors, entry blockers and integrase inhibitors. This combination therapy has been shown to be more efficient in suppressing viral loads and reducing the levels of drug resistant HIV-1 strains in infected individuals. Some retroviral drugs have severe side effects, but due to the development of new drugs and better treatment regimes, these side effects have been greatly reduced. This makes HIV-1 infection a chronic but treatable disease in the western world where the access to HAART is available. However, due to the high costs of HAART and

insufficient education about HIV-1 infection routes, there is still a high incidence of HIV-1 infection and AIDS-induced death in developing countries, with millions of new infections every year. (70, 140)

1.2.3 Friend virus as a model of retroviral infection

Friend virus, discovered in 1957 by Charlotte Friend, belongs to γ-retroviruses. It is a retroviral complex of two viruses: Friend murine leukemia virus (F-MuLV), which is the apathogenic, replication competent helper virus and Spleen Focus Forming Virus (SFFV), which is the pathogenic, but replication defective helper virus. Due to various deletions in *env* gene the SFFV is not able to build viral particles. (41) Therefore F-MuLV is required for replication and packaging SFFV genome into the viral particles[i]. During the course of infection erythroid precursor cells are infected, as wells as other cell types, as lymphocytes, monocytes, dendritic cells *etc*. F-MuLV infection in adult mice is aphatogenic. If newborns are infected with F-MuLV they suffer anemia, splenomegaly and erythroleukemia due to immature adaptive immune response.

In the beginning of FV infection SFFV viral envelope protein gp55 binds to erythropoietin receptor (EpoR) on the cell surface of erythroid precursor cells, giving a false signal for proliferation of them. During next 48 hours in susceptible mice uncontrolled proliferation occurs and infected erythroblasts migrate from bone marrow to the spleen, causing enlargement of the spleen. This is followed by integration of SFFV into site-specific target, *spi-1* gene (SFFV proviral integration site-1). This leads to activation and overexpression of transcription factor PU.1 erythroid cells and inhibition of their differentiation. Tumor suppressor gene p53 loss take place, what effect with uncontrolled proliferation of transformed cells.

In adult susceptible mice FV complex induces severe splenomegaly and lethal erythroleukemia. In resistant strains FV infection leads to strong immune response in acute face of infection, however mice are not able to completely eliminate the virus, which persists lifelong. (41, 58)

1.2.4 Immunoresponce against retroviral infection

Mice susceptible to FV develop during FV infection malignant erythroleukemia, however mice resistant to FV develop merely shortly splenomegaly. There are different genes responsible on FV-susceptibility. The resistance to FV infection is due to 6 genes *Fv 1-6*. *Fv 1,4* prevent from cell infection, *Fv 2,5* regulate proliferation and differentiation of erythroblast, *Fv 3* modify the immune response. Four MHC genes, which were described in H-2 mouse mediate resistance and may influence immune response (*Rfv 1-3*). For the presentation of viral T cell epitope H-2 genes are essential. The protection against FV-induced erythroleukemia consists of efficient interplay between FV-specific CD8$^+$ T cells, Th cells and neutralizing antibodies. Due to haplotype H-2^b, C57BL/6 mice are resistant to FV-induced erythroleukemia, they contain *Fv 2* gen, which restricts proliferation of erythroblasts. [139]. On the contrary to C57BL/6 mice, BALB/c mice contain susceptible H-2^d haplotype. Through the cross between both of this population, the new F1 generation, CB6F1 mice (*Fv 2$^{s/r}$*, haplotype H-2$^{b/d}$), can be created,. The CB6F1 mice are susceptible to FV-induced erythroleukemia [140, 141]. Heterozygotes own H-2 gens, therefore the FV-specific immune response occurs slower. The infection cannot be fully eliminated from the virus. [142].

Aim and scope of work

Subpopulations of myeloid cells are key players in the regulation of cellular immune responses. During retroviral infection, cytotoxic virus-specific CD8$^+$ T Lymphocytes (CTLs) efficiently control acute virus infections but become exhausted when a chronic infection develops. A recently discovered population of myeloid derived suppressor cells (MDSCs) can restrain T cell responses by showing suppressive activity. The inhibition of T cells by MDSCs was first observed in tumor models. Although first information about the role of MDSCs in infectious diseases was generated, their function has to be studied in much more detail.

The main aim of this project was to characterize the expansion of different MDSC subpopulations during acute Friend virus (FV) infection. As the mechanisms of T cell suppression by MDSC during retroviral infection are still elusive, phenotypic and functional properties of FV-induced MDSCs were assessed. Furthermore, it was of interest to establish a model for assessing functionality of these cells *in vitro*. In order to characterize mechanisms involved in MDSCs mediated T cell suppression several pathways were investigated with the help of cells from knockout animals or chemical inhibitors. To confirm the suppressive function of MDSCs in the living mouse and establish protocols for *in vivo* functionality of MDSC during acute FV infection, specific depletion experiments were performed.

Different inhibitory mechanisms, such as T regulatory cells (Tregs) and inhibitory receptors play an important role in the regulation of immune responses during chronic infections. In order to show the contribution of MDSCs in T cell suppression the interplay between MDSC, Tregs and inhibitory receptors and their ligands was assessed. Simultaneous depletion of different inhibitory mechanisms allowed us to gain deep insight into mechanisms of immunoregulation and new approaches for restoration of T cell responses.

Therefore, this study contributes to existing knowledge on the biology of MDSC, providing new insights into the role of these cells in chronic infections and possible new immune therapy of retroviral infections.

2. Materials

2.1 Laboratory animals

All animal experiments were performed in strict accordance with the German regulations of the Society for Laboratory Animal Science (GV-SOLAS) and the European Health Law of the Federation of Laboratory Animal Science Associations (FELASA). Protocols were approved by the North Rhine-Westphalia State Agency for

Nature, Environment and Consumer Protection (LANUV). For all the experiments mice were older than six weeks. The mice were kept in a pathogen-free environment with free access to water and standard mouse food. All mice were under controlled and regular examination by veterinarians of the University Hospital Essen.

The mice used in this PhD thesis had the resistance genotype of *H-2D^{b/b}, Fv-1b/b, Fv- 2^{r/r}, Rfv3^{r/r}* and were bred on C57BL/6 (B6) background. The exceptions are BALB/c mice, which are susceptible to FV-induced leukaemia and splenomegaly and were used to produce virus stocks *in vivo,* and Y10A (F1: A.BY x C57BL/10A) mice, which are also susceptible to FV and were used to titrate the virus stocks.

2.1.1 Wild type mice

BALB/c	Harlan Winkelmann GmbH, Borchen, Germany,	Resistance genotype: *H-2D^{d/d}, FV-2^{s/s}*
C57BL/6 (B6)	Harlan Winkelmann GmbH,	Resistance genotype: *H-*

	Borchen, Germany	$2D^{b/b}$, $FV\text{-}2^{r/r}$
F1: A.BY x C57BL/10A	Bred at the Animal Facility, University Hospital Essen, (Y10A) Germany	Resistance genotype: $H\text{-}2D^{a/b}$, $FV\text{-}2^{r/s}$

2.1.2 Knock out mice

TCRtg CD8 TCR transgenic mice	The D^bGagL TCR Tg (T cell receptor transgenic) mice were specific for the D^bGagL FV epitope (30). Mice were maintained at animal facilities, University Hospital Essen, Germany.
DEREG	DEREG (depletion of regulatory T cell) mice were generated from bacterial artificial chromosome (BAC) technology. These mice express a *diptheria toxin* receptor (DTR) enhanced green fluorescent protein (eGFP) fusion protein under the control of the *foxp3* locus. DEREG mice allows both detection and inducible depletion of Foxp3^{+} Treg cells. Kindly provided by Dr. Tim Sparwasser (Institut für Medizinische Mikrobiologie, Immunologie und Hygiene, Technische Universität München, Munich, Germany) and maintained at animal facilities of University Hospital Essen.

PD-L1 KO	In this mice exon 1 and a large part of exon 2 in the endogenous B7-H1 allele is replaced with a Neo-resistance cassette by a gene-targeting vector, which leads to deleting the sequences encoding the signal peptide and the majority of the extracellular IgV domain of PD-L1. (32) Mice were originally generated by Lieping Chen (Department of Immunology, Mayo Clinic College of Medicine, Rochester, USA) and maintained at animal facilities of University Hospital Essen, Germany
CD39 KO	Mice with a targeted disruption of exon 1 in the ectonucleotide triphosphate diphosphohydrolase (*entpd1*) gene, which leads to a shorter transcript of the gene and no detectable function of the enzymatic protein product CD39. Mice were kindly provided by Verena Jendrossek (Institute for Cell Biology, University Hospital Essen,Germany). Mice were generated by Simon C. Robson (Department of Medicine, Beth Israel Deaconess Medical Center, Harvard Medical School, Boston, MA, USA) (50) and inbred at the animal facilities, University Hospital Essen, Germany.

2.2 Cell lines and viruses

2.2.1 Cell lines

Mus dunni cell line is susceptible to infection with FV was used to determine the productivity of virus infected cells *in vitro*. *Mus dunni* cells were maintained in complete RPMI medium supplemented with 10% FCS and 0.5% Penicillin/Streptomycin.

2.2.2 Friend virus

The FV stock used for the experiments was a FV complex containing B-tropic Friend Murine Leukemia Helper Virus (F-MuLV) and polycythemia-inducing spleen focus-forming virus (SFFV) (19).Two different virus stocks were used: the virus containing only FV complex (31), for acute infections, and the virus containing additionally lactate dehydrogenase-elevating virus (LDV), for experiments with combinatorial treatment. The addition of LDV enables a more stable chronic infection with the FV to be established (127).

2.3 Chemicals and media

Chemicals, buffers and media were purchased from Applichem, Invitrogen, Merck, Roth and Sigma-Aldrich unless otherwise stated.

3-amino-9-ethylcarbazole (AEC), 4-(2-hydroxyethyl)-1-piperazineethanesulfonic acid (HEPES), 5-bromo-4-chloro-3-indolyl-β-D-galactopyranoside (X-gal), adenosine 5'- (α,β-methylene)diphosphate (AMPCP), acetic acid, autoMACS run and wash buffer (Miltenyi Biotec), β-mercaptoethanol (β-ME), bovine serum albumin (BSA), brefeldin A (BFA), calcium chloride, dextran, dimethyl sulfoxid (DMSO), disodium hydrogen phosphate, Dulbecco´s modified Eagle medium (DMEM) (Gibco) and DMEM high glucose (Gibco), ethanol, ethylendiaminetetraacetic acid (EDTA), FACS Clean (BD Bioscience), FACS Flow (BD Bioscience), FACS Rinse (BD Bioscience), fetal calve serum (FCS) (Biochrom), Ficoll (GE Healthcare), 37 % formaldehyde, formalin, FuGENE® transfection reagent (Promega), glucose, hydrogen peroxide (H_2O_2), incidine 8%, isopropanol, L-Glutamine, magnesium chloride ($MgCl_2$), N-Ndimethylformamid, penicillin-streptomycin (PenStrep), phosphate buffered saline (PBS) (Gibco), picric

acid, polybrene A, potassium ferricyanide, potassium ferrocyanide, RPMI-1640-Media (Gibco), saponin, sodium carbonate, sodium acetate, sodium azide (NaN3), sodium pyruvate, trypan blue, trypsin-EDTA.

2.3.1 Antibiotic

Penicillin / Streptomycin (Gibco)

2.3.2 Buffer and supplemented cell culture media

If not stated otherwise all buffer and media were prepared using bi-distilled H_2O.

Table 2.1 Buffer and supplemented cell culture media

Media	Composition
Culture medium	500 ml RPMI 1640 (Gibco) 10% FCS (Gibco) 0.5% Penicillin/Streptomycin mixture
FACS buffer	1l Phosphate buffered saline (PBS) 0.02% Na-azide 0.5% BSA
Freezing mediums	40% FCS 10% DMSO 50% RPMI medium
MACS buffer	1 l (PBS) 0.5 % BSA 2 mM EDTA

PBBS	1 l (PBS)
	1.0 g glucose

2.4 Antibodies and staining reagents

2.4.1 Characteristics of fluorophores

Antibody-coupled fluorochromes and their absorption- and emission maxima are described in a table.

Table 2.2 Characteristics of fluorophores

Fluorochrom		Absorption	Emission
Fluorescein-isothiocyanat	FITC	488	525
R-Phyccoerythrin	PE	488	575
Peridinin-Chlorophyll-Protein Komplex	PerCP	488	670
Phycoerythrin-Cy7	PE-Cy7	488	785
Allophycocyanin	APC	633	660
Allophysocyanin-Cy7	APC Cy7	635	785
Alexa Fluor 700	AF 700	635	723

eFluor 450	eF 450	405	455
eFluor 605	eF 605	590	605
eFluor 650	eF 650	635	650

2.4.2 Antibodies

Anti-mouse antibodies were purchased from eBioscience (Affymetrix), BD Bioscience or BioLegend unless otherwise stated.

Table 2.3 Antibodies

		Fluorochrom	Clone	Manufacturer
AB720 (α-MuLV Env, Isotype IgG2b)				
AB720 (α-MuLV Env, Isotype IgG2b)*		AF647		
Arg1 anti-human/mouse		FITC		R&D Systems
CD3 anti-mouse		Alexa Fluor 700	17A2	eBioscience
CD11b anti-mouse		BV 650	M1/70	BioLegend

30

CD11b **Rat anti-mouse**		PE CF594	M1/70	BD Horizon
CD11c **anti-mouse**		BV510	N418	BioLegend
CD16/32	Fc-Block	-	Clone 93	eBioscience
CD19 anti-mouse		eFluor 605 NC	eBio1D3	eBioscience
CD19 anti-mouse		PE	eBio1D3	eBioscience
CD39 anti-mouse		PerCP eFluor 780	24DMS1	eBioscience
CD43 anti-mouse		PerCP	1B11	BioLegend
CD49b **anti-mouse**		PE	Dx5	eBioscience
CD73 anti-mouse		PE Cy7	TY/11.8	eBioscience
CD80 anti-mouse		APC	16-10A1	eBioscience
CD274 **anti-mouse**	(PD-L1)	PE	MIH5	eBioscience
FVD		APC-Cy7		eBioscience
Gr1 **(Ly6G/Ly6CLy6G)** **anti-mouse**		eFluor 450	RB6-8C5	eBioscience
Gr1 **(Ly6G/Ly6CLy6G)**		FITC	RB6-8C5	BioLegend

anti-mouse		32		
Gr1 (Ly6G/Ly6CLy6G) anti-mouse		APC	RB6-8C5	BioLegend
GzmB anti-human/mouse		APC	GB12	invitrogen
IL-2 anti-mouse				
IFNγ anti-mouse		APC	XMG1.2	eBioscience
KI67 anti-mouse/rat		PE Cy7	SolA15	eBioscience
Ly6C anti mouse		PerCP Cy5.5	HK1.4	eBioscience
Ly6G		AF700	1A8	BioLegend
NK1.1 anti-mouse		BV421	PK136	BioLegend
NK1.1 anti-mouse		eFluor 605	PK136	BioLegend
NOS2 anti-mouse		PE-eFluor 610	CXNFT	eBioscience
Streptavidin		eF610	-	eBioscience

TER119		PE-Cy7	TER-119	eBioscience
TNFα anti-mouse		PE-Cy7	MP6-XT22	BioLegend

2.5 MHC tetramers and F-MuLV specific peptide

2.5.1 MHC I tetramer

PE labelled MHC class-I H-2D^b tetramer loaded with the peptide AbuAbuLAbuLTVFL (DbGagL tetramer, FV gag CD8$^+$ epitope gPr80gag85-93) recognised by DbGagLspecific CD8$^+$ T cells (2, 124, 134). The MHC class-I tetramer was purchased from Beckman and Coulter (Krefeld, Germany) or MBL International Corporation (Woburn, MA, USA).

2.5.2 CD8 peptide

The F-MuLV CD8$^+$ T cell peptide was synthesised by PAN Tecs (Tübingen, Germany) and reconstituted in 100 % sterile DMSO. Peptide name: FMR-H-2Db GagL CD8 epitope. Sequence: AbuAbuLAbuLTVFL (30).

2.6 Discrimination of dead cells

To discriminate dead from live cells, either propidium iodide (PI) or fixable viability dye (FVD) eF780 were used.

2.7 Staining reagents

Table 2.4 Staining reagents

Staining reagent	Manufacturer
FVD eF780	eBioscience
CFSE	Invitrogen
Violet tracer	Invitrogen

2.8 Standard kits

Table 2.5 Standard kits

Kit	Manufacturer
Cytofix/ Cytoperm Intracellular staining kit	BD Pharmingen, Heidelberg
Foxp3 staining set	eBioscience, San Diego, USA
Cytofix/cytoperm intracellular staining kit	BD Pharmingen, Heidelberg, Germany
Mouse CD8α (Ly-2) isolation kit	Miltenyi Biotec, Bergisch Gladbach, Germany
Myeloid-Derived Suppressor Cell Isolation Kit (mouse)	Miltenyi Biotec, Bergisch Gladbach, Germany

2.9 Depletion antibody and treatment reagents

Table 2.6 Depletion antibody and treatment reagents

*InVivo*MAb anti m Ly6G	Ly6G antibody, Clone 18A, purchased from BioXcell
*InVivo*MAb anti m Tim3	Tim3 antibody, Clone RMT3-23 purchased from BioXcell
*InVivo*MAb anti m PD-L1	PD-L1 antibody, Clone 10F.9G2 purchased from BioXcell
5-Fluorouracyl (5FU)	**2,4-Dihydroxy-5-fluoropyrimidine, purchased from** Sigma-Aldrich
Diphteria toxin (DT)	Diphtheria toxin, Corynebacterium diphtheria – Calbiochem, purchased from Merck.

3. Methods

3.1 Animal trials

The animal experiments were conducted according to the guidelines of the Federation of European Laboratory Animal Science Association.

3.2 Infection

The infection of mice with Friend Virus was conducted by intravenously (i.v) injection in the lateral tale vein using 25G-hollow needle. Virus stock used for infection was thawed, centrifuged and the supernatant diluted in sterile PBS. For acute FV infection of mice 20 000 SFFU (Spleen Focus Forming Units) were used. For experiment with combinatory treatment with DT, αPD-L1 and αTim3, FV + LDV was used in concentration 20 000 SFFU of FV.

3.3 Intraperitoneal injection (i.p.)

The *in vivo* depletion antibodies as well as 5FU and *Diphtheria toxin* were administered via intraperitoneal (i.p) injection. Mice were hold by the skin at the back of the neck and the tail was held back. Mice were hold with the ventral side exposed and tense, therefore internal organs are not harmed by the injection. The injection was done in a 45° angle into the lower abdomen and slowly administered.

3.4 Dissection of mice

Mice were sacrificed using cervical dislocation after anesthesia with isofloran. Then, the mice were then fixed with needles and carefully cut open in order not to destroy internal organs. First the cervical, axillary and inguinal lymph node were removed. Next the peritoneal cavity was opened. The spleen was removed by excising both blood vessels. To dissect the bone marrow, hind legs were cut loose

and the flesh was removed. All organs and tissues were kept in PBBS on ice until further preparation.

3.5 Preparation of single cell suspension

Spleen and lymph nodes were homogenized through a 70 μm cell strainer with help plunger of a syringe. The strainer was washed from the strainer using PBBS. An aliquot of cell suspensions was removed to count the cells. Cells were then centrifuged at 300 xg for 10 min and the supernatant was discarded. Based on the cell count, cells were re-suspended in an appropriate volume of PBBS.

A bone marrow cell suspension was delivered by flushing the femur and tibia of hind leg with a 23G-hollow needle with PBBS. An aliquot of cell suspension for counting the cells was removed. The cells were subsequently centrifuged at 520 xg for 10 min and the supernatant discarded. Based on the cell number the cells were re-suspended in an appropriate volume of PBBS.

3.6 Preparation of bone marrow derived dendritic cells

To generate mouse DCs, the bone marrow from a naïve B6 mouse was prepared as described above and re-suspended in 50 mL mouse DC media supplemented with 1 ng/mL mrIL4 and 5 ng/mL mrGM-CSF. 10 mL were then seeded into a 10 cm cell culture dish and incubated at 37 °C and 5 % CO2 for seven days. After 24 hours an additional 10 mL of supplemented mouse DC media was added to the culture. Five days after seeding, the cells were washed once by centrifuging the cell culture media at 400 xg for 6 min (these cells are non-adherent). The cells were then re-suspended in 20 mL supplemented mouse DC media and cultured for another two days. Seven days after initially seeding the bone marrow cells, the differentiated DCs could be used for other applications.

3.7 Peptide stimulation of mouse CD8$^+$ T cells with peptide-loaded mouse DCs

Bead-isolated CD8$^+$ T cells from naïve TCRtg mice (55) were incubated for different lengths of time with F-MuLV CD8$^+$ T cell peptide loaded onto mouse DCs in complete RPMI. DCs were loaded with 5 µg peptide (AbuAbuLAbuLTVFL) for 1 hour at 37 °C. After loading, the DCs were washed, counted and seeded at a ratio of 1 DC to 5 CD8$^+$ T cells.

3.8 *In vivo* production of a FV stock

To obtain a FV stock, susceptible BALB/c mice were infected intra venously (i.v.) with 3000 spleen focus forming units (SFFU) of FV. Nine days post infection the mice were sacrificed and the spleens removed. A 15 % spleen homogenate was prepared in PBBS with 1 mM EDTA. The homogenate was then aliquoted and stored at -80°C until use.

3.9 Titer determination of a FV stock

Titration of a FV stock was done by infecting Y10A mice i.v. with different amounts of virus stock. The spleens were removed 14 days post infection. During the course of FV infection, malignant cell populations develop on the surface of the spleen. These foci can be visualized by incubation of the whole spleens in Boulin´s solution which enhances the visual contrast of foci on the spleen surface. SFFUs can be determined by counting these foci.

3.10 *In vivo* depletion of cell populations

To deplete MDSCs two depletion methods were used. First, 5-Fluorouracil was diluted to concentration 10mg/kg per mouse in 500µl PBS and injected i.p. once,

four days prior sacrifice. With this method depletion of all MDSCs was performed (Figure 4.6).

To deplete only gMDSCs αLy6G (Clone 1A8) was in vivo antibody was diluted 100µg per mouse in PBS and administrated i.p. four times every third day (Figure 4.6).

T regulatory cells were depleted using a diphtheria toxin, mice were injected with DT diluted in PBS i.p. three times every third day (Figure 4.6).

For immune checkpoint blockade in vivo antibody for αPD-L1 (10F.9G2) and Tim3 (RMT3-23) were used. Mice were injected with 250µg αPD-L1 three times every third day, and with 100µg Tim3 three times every second day. µg per i.p. injection was used (Figure 5.5).

The depletion efficiency was assessed via cell specific markers using flow cytometry.

3.11 *In vivo* cytotoxicity assay

In vivo cytotoxicity assay allows determining cytotoxic function of T cells after MDSCs depletion during FV infection. (182) Lymphocytes were isolated from lymph nodes and spleens from naive mice (donor mice). Single cell suspensions were prepared and the cells were washed with 40 ml of PBS. Mononuclear cells from the spleens were separated additionally by erythrocytes lysis. Consequently, cells were washed twice in 50 ml of PBS. Cell suspensions from lymph nodes and erythrocyte lysed spleen cells were mixed and divided into equal volumes of 15 ml of RPMI medium into two tubes. The cells from one tube were loaded with the class I-restricted peptide recognized by $CD8^+$ T cells for 1,5 h at 37°C and afterwards were stained with 40nM CFSE (carboxyfluorescein succinimidyl ester) dye for 10 min at 37°C and then for 5 min on ice (target cells, experimental). The second tube was incubated for 1,5 h at 37°C and stained with 7,5µM Violet Tracer The phenotype of these cells would be CFSE- high . The unloaded cells remained intact and would be separated from the target cells as CFSE-low (control cells).

Peptide loaded and unloaded cells were counted using Trypan blue exclusion microscopy and suspended in sterile PBS in the ratio 1:1. 1.0×10^7 cells of each population (per mouse) were injected intravenously (i.v.) into FV infected and 5FU treated mice. One hour after i.v. injection of the donor cells, recipient mice were sacrificed. Subsequently, *in vivo* killing activity was quantified in single-cell suspensions from the spleen, lymph nodes and bone morrow of each FV infected mouse. The percentage of killing was calculated as follows: 100 − {[(% of peptide loaded in infected cells / % of peptide unloaded in infected cells) / (% peptide loaded in uninfected cells / % peptide loaded in uninfected cells)] × 100}.

3.12 Infectious center assay (IC assay)

To detect the number of infectious centers of FV-infected cells, 2×10^4 *Mus dunni* cells in 3 ml complete RPMI were seeded into each well of a 6-well plate. The cells were then incubated over night at 37 °C with 5 % CO_2. The following day mouse cell suspensions (derived from spleen of FV-infected mice) were prepared, a 10-fold dilution series formed (starting with 1×10^7 cells) and 1 ml of each dilution was added to a single well of the 6-well plate. The plate was then incubated for three days under the same conditions. During this incubation period, infected cells spread the infection to the *Mus dunni* cells via cell-cell contacts. Cell division of the *Mus dunni* transfers the provirus to their daughter cells what form an infected cell colony. To visualize the infected cell clones, the media on the *Mus dunni* cells was discarded and the cells were fixed by incubating them with 95 % ethanol for 10 min. The ethanol was discarded and the plates washed twice with PBS plus 0.1 % BSA. The cells were then incubated for 2 hours at room temperature with 600 µl of culture supernatant of an AB720 producing hybridoma cell line. This hybridoma cell line produces an antibody (AB720) which specifically binds to the env-protein of F-MuLV recognizing FV-infected cells. After two hours the plates were washed twice with PBS plus 0.1 % BSA. 600 µl of a 1:400 dilution (into PBS) of secondary antibody conjugated to HRP (goat-α-mouse- IgG2b-HRP (0.05 mol/l)) was added to the cells for 90 min. After the incubation, the antibody was discarded and the plates were washed twice with PBS. The cells were then incubated for 20 min in

the dark with 2 ml of fresh AEC substrate solution. A red precipitate is formed by conversion of the soluble substrate AEC in the substrate solution into an in-soluble precipitate catalyzed by the HRP coupled to the secondary antibody. The substrate solution was discarded and the plates were washed twice with H_2O. After the plates had dried over night the red spots in each well were counted and calculated for $1x10^6$ added cells. To determine the IC count per $1x10^6$ spleen cells the mean off all dilutions was formed. As a control an additional plate of *Mus dunni* cells was prepared a day before the experiment. Three wells of this plate were left uninfected and the other three wells were infected with free F-MuLV (with 8 µg/ml polybrene A to facilitate virus uptake). The appearance of red dots after developing the assay indicated functionality.

3.13 Stimulation of freshly isolated mouse cells for cytokine production

For the intracellular staining of cytokines (like TNFα, IFNγ and IL-2), freshly isolated mouse cells were stimulated *in vitro*. The wells of a Nunc MaxiSorp 96-well plate were coated with 50 µL purified αCD3 antibody (10 µg/ml) in sodium carbonate coating buffer. The coating of the plate was done for overnight at 4°C. After αCD3 coating, the plate was washed three times with PBS. For stimulation of freshly isolated mouse cells, $1x10^7$ cells were added to each well in duplicates. The cells were re-suspended in complete RPMI medium supplemented with 50 µM β-ME, 2 µg/ml purified αCD28 and 2 µg/ml BFA and incubated for 5 hours at 37°C. After stimulation, the cells were transferred into new wells and stained for surface molecules and intracellular cytokines. For controls, a sample was left unstimulated but stained with intracellular antibodies and a stimulated sample did not get stained with the intracellular antibodies. (183)

3.14 Flow cytometry

3.14.1 Principle of flow cytometry

Flow cytometry is a method used for the characterization and quantification of heterogeneous cell populations in solution. Using fluorescence labelled antibodies or fluorescently tagged proteins it allows to detect surface and intracellular molecules. Labelled and prepared cells are then measured on a fluorescence-activated cell sorting (FACS) machine. The main components of a FACS analyzer can be divided in the fluidic system, the optical system and the detection system. In a cell solution the cells are randomly distributed in a three dimensional space. To detect the fluorescence signal of labelled molecules they need to be focused in a stream of single cells. The fluidic system is responsible for this process, whereby the cell suspension is taken up by the sample injection port and then usually hydrodynamically focused. (184-188)

After focusing, the cells pass through the optical system and can be analyzed. FACS machines are equipped with different lasers, mirrors and filters. Two initial parameters are acquired by all FACS analyzers: forward scatter (FSC) and side scatter (SSC). To measure the size of cells, light that is scattered in a forward direction (FSC) is used. The granularity of cells is measured by the SSC channel, which is the light measured at a 90° angle. Combining the information of the FSC and the SSC is used for a pre-selection of cell types in a heterogeneous sample (Figure).
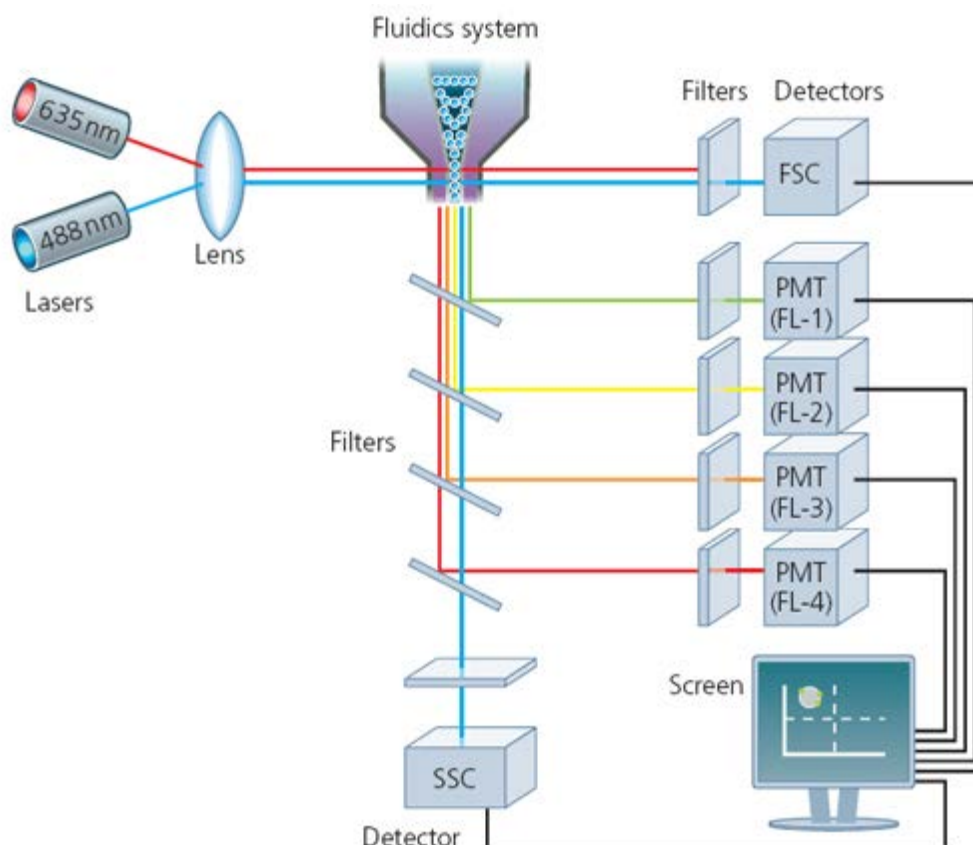
Figure 3.1 Principle of Flow Cytometry

Two lasers (635 and 488 nm) send light trough the sample. The light emitted by the sample is then isolated by different filters and sent to the different PMT detectors. The PMT detectors transform and enhance the optical signal into an electric signal, which can then be visualized in the analysis software on a computer.

If an antibody labelled cell passes through a light beam emitted by a single laser, the different fluorophores sensitive to that specific wavelength of light are specifically excited. When the electrons in the fluorophores become excited by the laser light they are lifted to a higher energy level and shortly after this they fall back to the original energy state emitting energy in the form of photons. The wavelength of these released photons is longer than that of the excitation light source, which is part of the phenomenon known as Stoke´s shift. The emitted light is reflected, filtered and detected with specific sets of optical mirrors, filters and detectors. The mirrors reflect the light onto filters, which filter light of specific wavelength. Short pass or long pass filters only allow light under or above a

certain wavelength (respectively) to pass and band pass filters are used to filter a certain range of wavelengths (Figure 3.1). The emitted and filtered light is then detected by the detectors (usually photomultiplier tubes (PMTs)). These detectors measure the amount of photons and their output signal is proportional to the amount of antibody bound to the cell. This type of measurement allows to collect the necessary information about quantify and characterization of the cells within a sample. The optical signal is then amplified and converted into an electric signal. This can be visualized in the analysis software (Figure 3.1). Multicolor flow cytometry is made possible by using different fluorophores which emit at wavelengths that can be discerned from each another. In this thesis an LSR II with four lasers (488 nm, 633 nm, 355 nm and 405 nm) and the software FACS DiVa BD bioscience) and FlowJo7.6.5 (Treestar) were used for acquiring and analyzing, respectively. It is also possible to sort cells, for this method cells pass through the above described system and are immediately characterized by previously established parameters. For sorting, the fluidic stream is broken into droplets, containing a cell each. These droplets then become charged by passing through an electric field and may be diverted into collection tubes by plates of opposite polarity.

3.14.3 Surface staining of mouse cells for flow cytometry

For flow cytometry cell staining of mouse cells usually $3-7 \times 10^6$ cells per sample of freshly isolated mouse cells were transferred into a well of a 96-well U-bottom plate and washed with the addition of 100 µl FACS buffer at 300 xg for 3 min at 4 °C. The supernatant was discarded by flicking the plate. In case of staining of myeloid cells FC block was added to prevent unspecific binding of antibodies. Prior surface staining cells were re-suspended in 50µl FC block diluted in FACS buffer and incubated in the dark for 15 min at room temperature. After incubation time an antibody mix was prepared in 50µl FACS buffer and added to the cells. The cells were re-suspended in the antibody mix and incubated for 15 min at room temperature or 20 min at 4 °C. After incubation, the cells were washed by addition of 100 µl FACS buffer per well and spun at 300 xg for 3 min. The cells were then

either re-suspended in FACS buffer for further processing or directly transferred into FACS tubes for measurement on the LSRII or fixed as described below.

3.14.4 Fixation of mouse cells

Depending on the performed intracellular stain, the cells were either fixed with Cytofix/Cytoperm from BD or with the Foxp3 staining set from eBioscience. If only cytoplasmic molecules were to be stained, the Cytofix/Cytoperm kit was used. For this the cells were re-suspended in 100 µl fixing buffer and incubated for 10 min at room temperature. Next the cells were washed with 100 µl of Cytofix/Cytoperm wash buffer, centrifuged at 540 xg for 4 min and stained for intracellular molecules. If nuclear molecules were to be stained, the Foxp3 staining set was used. The cells were re-suspended in 100 µL Foxp3 Fix/Perm fixing solution which was prepared according to the manufacturer's instructions (1:4 of Foxp3 Fix/Perm concentrate into diluent). The cells were left to fix for 2 to 4 hours at 4 °C. To stop the reaction 100 µl Foxp3 Fix/Perm wash buffer was added to each well and the cells were centrifuged at 540 xg for 4 min at 4°C and stained for intracellular molecules. The cells were then subsequently washed with the addition of FACS buffer and centrifuged at 540 xg for 4 min. Subsequently the cells were re-suspended in FACS buffer for this application and measured immediately on the LSRII.

3.14.5 Intracellular stain of mouse cells

For intracellular staining, an antibody mix was prepared in 50 µl of either Cytofix/Cytoperm wash buffer or Fix/Perm wash buffer (Foxp3 staining set). The cells were re-suspended in the antibody mix and stained for 30 min at 4 °C and, after addition of 100 µl of the appropriate buffer, centrifuged at 540 xg for 4 min. The cells were re-suspended in FACS buffer and transferred into FACS tubes for measurement on the LSRII.

3.14.6 Tetramer class I stain

A method to detect small populations of virus-specific CD8^{+} T cells is by the use of specific tetramers. T cell receptors (TCRs) recognize and bind to complexes which are expressed on APCs composed by MHC molecules and peptides with specific sequences processed by APC (MHC/peptide complexes). Monomeric MHC/peptide complexes were shown low affinity to the TCR and instability. To overthrow these difficulties MHC/peptide monomers are biotinylated and tetramerized with streptavidin to maintain stable binding to multiple TCR, enabling MHC/peptide tetramers to be used as a detection tool. MHC class I tetramers consist of four peptide- MHC class I complexes, which are linked by biotin-streptavidin. The complex may be detected via conjugated fluorophores in a flow cytometer. The peptide used to build the tetramer complex is only bound by the TCR of specific CD8^{+} T cells in combination with the MHC class I (2, 36). A schematic of the MHC class I are shown in Figure 3.2. The tetramer class I stain was done as described for the extracellular flow stain with a dilution of 1:200. The tetramer class I stain was also proof to fixation with Cytofix/Cytoperm.
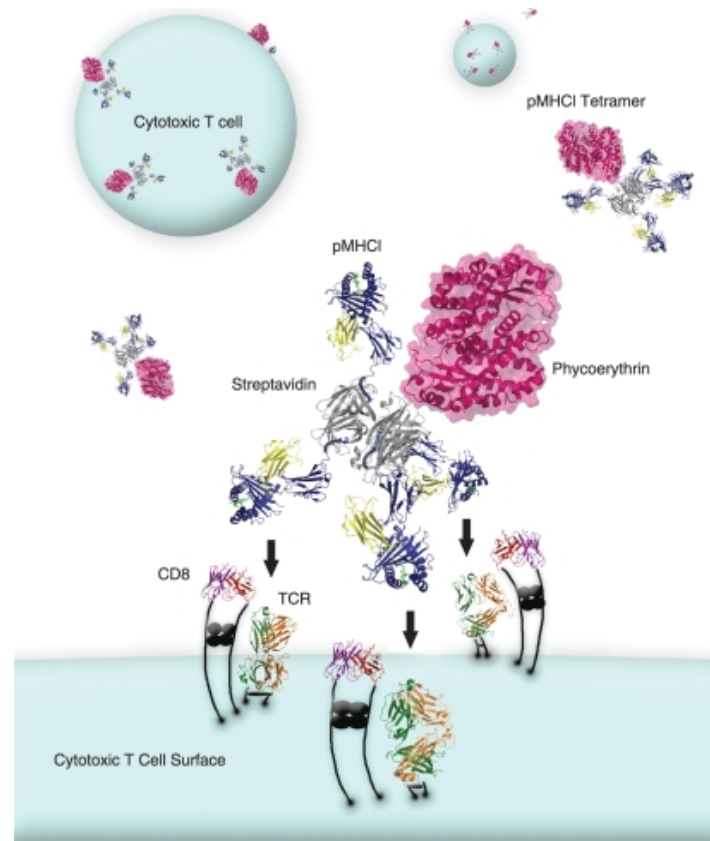
Figure 3.2 Schematic organization of MHC class I tetramer.

MHC class I tetramers consist of four MHC class I molecules, linked via biotin (B) to a streptavidin (SA) on the fluorophore (in this case PE). The MHC complexes are loaded with a specific peptide. (36)

3.14.7 Gating strategy for murine MDSCs

To gate murine MDSCs a special strategy was utilized. MDSCs share different markers with different cell populations, therefore careful gating is necessary. To guarantee that only MDSCs were considered the following gating strategies for flow cytometric analysis ware used.
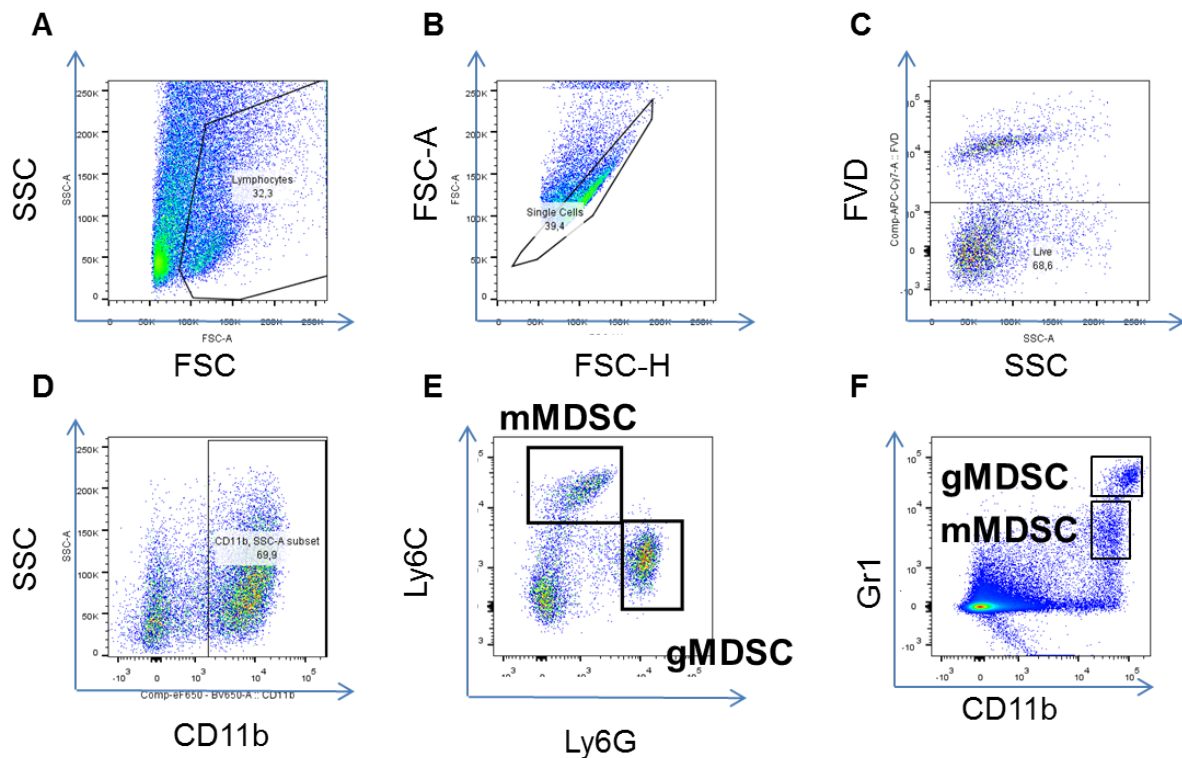
Figure 3.3 Gating strategy for murine MDSCs. To gate murine MDSCs firstly (A) lymphocytes, (B) singlets. Further dead and lineage (CD19, CD3, NK1.1) cells were excluded (C). CD11b⁺ cells were identified (D). MDSCs were characterized with help of Ly6C and Ly6G (E). In experiments with combinational therapy MDSCs were characterized as Gr1^{high} and Gr1^{low} cells and co-expression of CD11b⁺.

3.14.8 Exclusion of dead cells in flow cytometry

The exclusion of dead cells and cellular debris in flow cytometry was performed using the dye propidium iodide (PI) or fixable viability dye (FVD). In healthy cells, the cell membrane prevents access of PI to DNA. However, in damaged, apoptotic or dead cells, the membrane is not intact and unable to play its preventing function, allowing rapid PI access into the cell nucleus and DNA with which it interacts. This dye is useful for the DNA analysis and the dead cell exclusion during flow cytometric analysis. 0,5 µl of PI was added to the stained cells in 300 µl FACS buffer to the sample and immediately analyzed.

Discrimination of dead cells in intracellular staining was performed with help of Fixable Viability Dye (FVD). FVD is a viability dye that can be used to label dead cells prior to fixation and/or permeabilization procedures. FVD stain is based on the reaction of a fluorescent reactive dye with cellular proteins (amines). These dyes cannot penetrate live cell membranes, so only cell surface proteins are available to react with the dye, resulting in dim staining. The reactive dye can infuse the damaged membranes of dead cells and stain both the interior and exterior amines, resulting more intense staining. FVD eF780 was added in amount of 1 µl per 1 mL of cells together with the surface staining antibodies.

3.15 Cell isolation with the MACS technology

For the isolation of mouse CD8$^+$ T cells mouse CD8α (Ly-2) MicroBeads were used. (190) Using these beads CD8$^+$ T cells are directly labelled. In general, the cells were counted and re-suspended in MACS buffer (90 µL buffer per $1x10^7$ cells) and the CD8α MicroBeads were added (10 µl beads per $1x10^7$ cells). The mix was incubated for 20 min at 4 °C in the dark and subsequently re-suspended in 10-20 times the labelling volume of MACS buffer and centrifuged for 10 min at 300 xg. Finally, the supernatant was carefully discarded and the cells were re-suspended in up to 500 µL MACS buffer per $1x10^7$ cells. To protect from clogging the cells were passed through a 30 µm cell strainer before applying to the MACS columns. The cells were then applied on the column connected to magnetic field. After washing the column remained cells were flushed with 5 ml MACS buffer. After enrichment the cells were centrifuged, counted and processed for the further application.

For the isolation of mouse MDSCs mouse Myeloid Derived Suppressor Cells Isolation Kit was used (191) with a pre-isolation of CD19 cells (192). For pre-isolation of mouse CD19$^-$ T cells mouse CD19 MicroBeads were used. Using these beads CD19$^+$ T cells are directly labelled. In general, the cells were counted and re-suspended in MACS buffer (90 µL buffer per $1x10^7$ cells) and the CD19α

MicroBeads were added (10 µl beads per 1×10^7 cells). The mix was incubated for 15 min at 4 °C in the dark and subsequently re-suspended in 10-20 times the labelling volume of MACS buffer and centrifuged for 10 min at 300 xg. Finally, the supernatant was carefully discarded and the cells were re-suspended in up to 500 µL MACS buffer per 1×10^8 cells. To protect from clogging the cells were passed through a 30 µm cell strainer before applying to the MACS columns. The cells were then applied on the column connected to magnetic field. After washing the column, passed through cells were collected, centrifuged, counted and processed for the further MDSCs isolation.

In general, the cells then re-suspended in MACS buffer (350 µl buffer per 1×10^8) and the FC Block was added (50µl per 1×10^8). The mix was incubated for 10 minutes at 4°C. After incubation, 100µl of biotin-conjugated αLy6G antibody was added, and the cells incubated for a further 10 min at 4°C. Cells were washed by adding 10 ml of buffer and centrifuged at 300 xg for 10 min at 4°C. The cells were re-suspended in 800µl of buffer per 1×10^8 and 200µl of anti-biotin MicroBeads was added, mixed well, and incubated for 15 min at 4°C. Cells were washed by adding 10ml of buffer and centrifuged at 300 xg at 4°C. The cell pellet was re-suspended in 500µl of buffer, and magnetic separation was performed to positively isolate $Gr1^{high}$ $Ly6G^+$. To protect from clogging the cells were passed through a 30 µm cell strainer before applying to the MACS columns. The cells were then applied on the column connected to magnetic field. After washing the column remained cells were flushed with 5 ml MACS buffer. After enrichment the cells were centrifuged, counted and processed for the further application

Negatively isolated, $Ly6G^-$ cells were centrifuged 300 xg for 10 min at 4°C. The pellet was re-suspended in 400µl of buffer per 1×10^8 cells and 100µl of biotin-conjugated αGr1 antibody was added, mixed well and incubated for 10 minutes at 4°C. Cells were washed by adding 10ml of buffer and centrifuged at 300 xg at 4°C for 10 minutes. The cell pellet was re-suspended in 900µl of buffer per 1×10^8 and 100µl of streptavidin-conjugated MicroBeads was added, mixed well and incubated for 15 minutes at 4°C. Cells were washed by adding 10ml of buffer and centrifuged at 300 xg at 4°C. The cell pellet was re-suspended in 500µl of buffer and magnetic separation was performed to positively isolate $Gr1^{low}$ $Ly6G^-$. To

protect from clogging the cells were passed through a 30 µm cell strainer before applying to the MACS columns. Cells were then applied on the column connected to magnetic field. After washing the column remained cells were flushed with 5 ml MACS buffer. After the enrichment the cells were centrifuged, counted and processed for further application

3.16 *In vitro* suppression assay

Bead-isolated CD8$^+$ T cells from naïve TCRtg mice (55) were incubated for the different lengths of time with F-MuLV CD8$^+$ T cell peptide loaded onto mouse DCs in complete RPMI medium. The DCs were loaded with 5 µg peptide (AbuAbuLAbuLTVFL) for 1 hour at 37 °C. After loading, the DCs were washed, counted and seeded at a ratio of 1 DC to 5 CD8$^+$ T cells. Additionally, bead-isolated gMDSCs or mMDSCs from B6, PD-L1 KO or CD39 KO mice were isolated, stained with Violet Tracer dye for 20 min at 37°C followed by manufacturer's instructions, and added to this setup at different concentrations. The cells were incubated for 3 days at 37°C with 5 % CO$_2$. After 3 days the cells were harvest, stained for surface and intracellular molecules, and proliferation of live CD8$^+$ cells was analyzed. The cells were re-suspended in FACS buffer and transferred into FACS tubes for the measurement on the LSRII.

Additionally, for experiments that examined the effect of NO and arginase, described above assay was used for the characterization of gMDSCs functions in vitro with use of inhibitors. Besides bead-isolated CD8$^+$ T cells from naïve TCRtg mice, peptide loaded DCs and Violet Tracer stained gMDSCs an arginase inhibitor (0.5 mM) nor-NOHA (N^W-hydroxyl-nor-L-arginine) and NO inhibitor (0.5 mM) L-NMMA were added at the beginning of the culture (193).

3.17 Statistical analyses

Statistical analyses and graphical presentations were computed with Graph Pad Prism version 5. Statistical differences (p-value) between two groups were

performed using unpaired t test. Statistical differences (p-value) between the different parameters were performed testing with the one-way ANOVA analysis with Bonferroni multiple comparison post analysis. The p-value is a probability with a value ranging from zero to one.

4. Results

4.1 Myeloid derived suppressor cells expand during FV infection

Myeloid derived suppressor cells (MDSCs) were shown to play a role in the suppression of immune responses not only in cancer, but also in various infectious diseases, such as LCMV, HCV, HBV and HIV. However their exact role in retroviral infections is still elusive (45-47).

In order to characterize MDSCs during FV infection, B6 mice were infected and the kinetics of the MDSC response was determined. The numbers of both monocytic (mMDSC, Ly6G$^-$ Ly6C^{high}) and granulocytic (gMDSC, Ly6G^{high} Ly6C^{low}) MDSCs were analyzed at different time points in the spleen of FV infected mice (Figure 4.1). mMDSCs were detectible in naïve mice and their frequency was about three thousand mMDSCc per one million nucleated splenocytes. This number of MDSCs was stable during early FV infection until day 10. At day 12 and 14 after infection, the population of mMDSCs expanded significantly. The expansion of mMDSCs peaked on day 14 post infection in the spleen (Figure 4.1 A), and the frequency of these cells reached more than 6 000 per one million spleen cells. gMDSC numbers also peaked on day 14 post infection, reaching 6 000 per one million spleneocytes (Figure 4.1 B). During the chronic phase of FV infection, both numbers of granulocytic and monocytic MDSC were only slightly elevated in comparison to non-infected mice (Figure 4.1). These data indicate that the populations of mMDSCs and gMDSCs expanded at day 14 after FV infection, a time point that is concomitant with the reduction in virus-specific effector CD8$^+$ T cell responses (77).
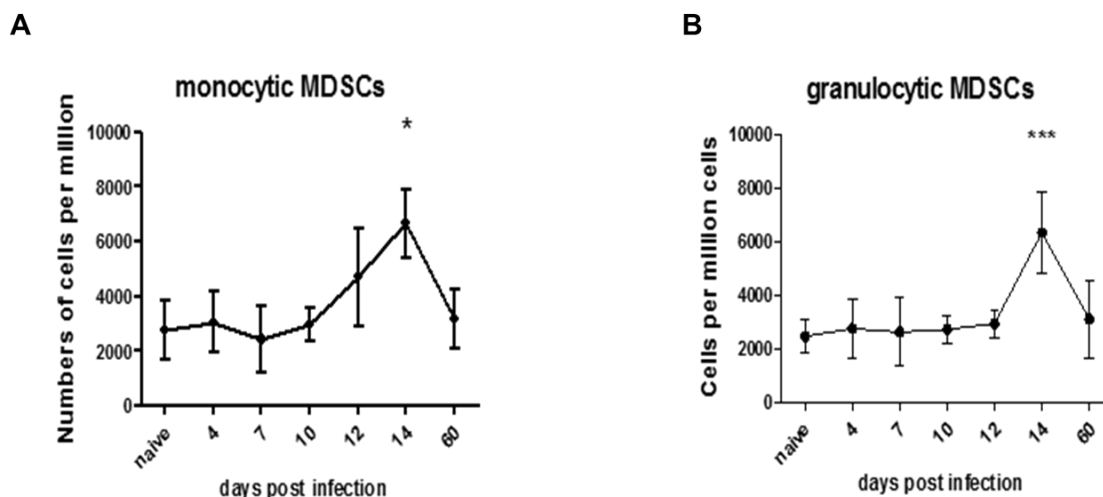
A

B

Figure 4.1 Kinetics of the mMDSC and gMDSC response during acute FV infection.
B6 mice were infected i.v. with 20 000 SFFU of FV or left un-infected, and MDSC numbers were measured using flow cytometry. Total spleen cells were analyzed at various time points post infection. **(A)** The numbers of Ly6G^{high} Ly6C^{low} and Ly6G^{-} Ly6C^{high} per 1x10^6 live splenocytes are displayed. At least 7 mice per group from five independent experiments were analyzed. Bars represent SEM of the mean. For statistical analysis an ANOVA multiple comparison test was carried out with the group of naïve mice as reference (* < 0.05, **, *** < 0.0005).

Next, it was of interest whether FV can infect MDSCs. During the course of infection, FV infects erythroblasts, B cells, and myeloid cells. To determine infected MDSCs, AK720, an antibody which binds to MuLV-*env gp70*, was used. gp70$^+$ MDSCs were found in both the monocytic and the granulocytic subpopulation of MDSCs at 7 days post infection (Figure 4.2 B). More mMDSCs than gMDSC were infected at this time point. However, while most infected mMDSCs subsequently disappeared from the spleen, infected gMDSCs were still detectable at 14 days post infection. Thus, MDSCs can be targets for FV infection.
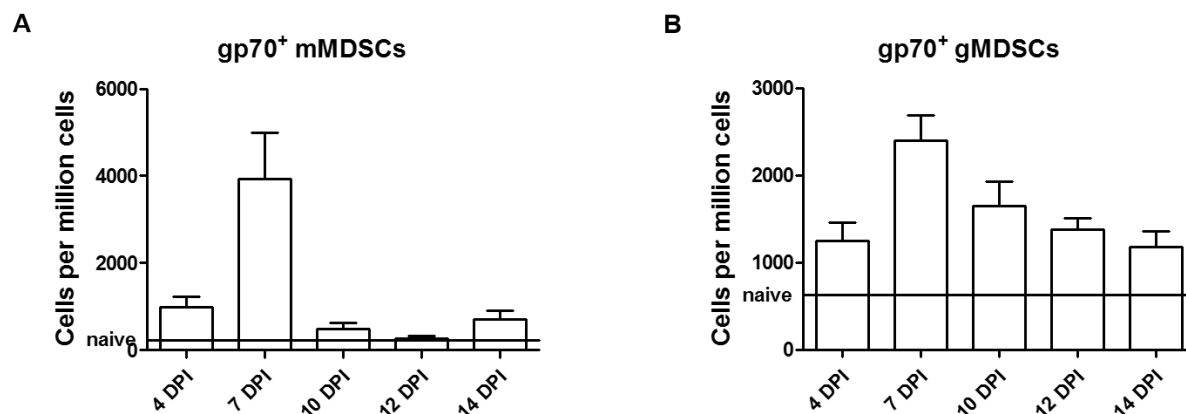
Figure 4.2 Kinetics of mMDSCs and gMDSCs infection during acute FV infection.
B6 mice were infected i.v. with 20 000 SFFU of FV or left un-infected, and MDSC numbers were measured in the spleen at various time points post infection using flow cytometry. **(A)** The numbers of gp70+ $Ly6G^{high}$ $Ly6C^{low}$ and $Ly6G^{-}$ $Ly6C^{high}$ per 1×10^{6} live cells in the spleen are displayed. At least five mice per group from 4 independent experiments were analysed. Bars represent the mean with SEM.

4.2 Upregulation of molecules associated with activation and effector functions on gMDSCs and mMDSCs during acute FV infection

It was previously shown that functional MDSCs express different molecules that were associated with the suppressive activity of these cells (45-47). PD-L1, CD80, NOS2 and Arg1 expression on both MDSCs populations were analyzed at the peak of MDSC expansion, which was day 14. PD-L1 (Program death–ligand 1) is a molecule expressed on a variety of cells, mostly antigen presenting cells. Through interaction with its receptor PD-1, PD-L1 suppresses responses of T lymphocytes. In various studies, PD-L1 was shown to be expressed on MDSC and was associated with MDSC activation (72).

CD80, which is also expressed on various cells, such as B cells and monocytes, is a member of the B7 family and is a co-stimulatory molecule of T cell activation. It is a ligand for two receptors: CTLA-4 and CD28. While CD28 induces T cell activation, CTLA-4 mediates T cell suppression (72).
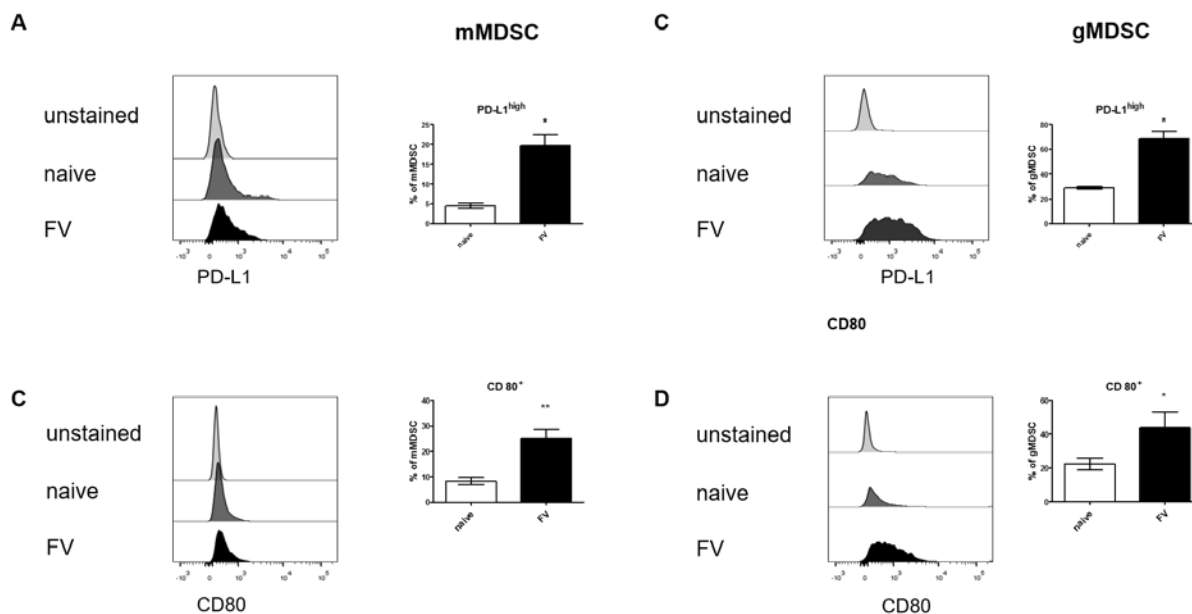
Figure 4.3 Expression of CD80 and PD-L1 molecules on the MDSCs during acute FV infection.

B6 mice were infected i.v. with 20 000 SFFU of FV or left un-infected, and the expression of PD-L1 and CD80 on the surface of MDSCs was measured using flow cytometry on day 14 post infection. **(A)** Representative histograms and **(B)** frequencies of CD80 and PD-L1^{high} expression on the surface of Ly6G^{high} Ly6C^{low} and Ly6G^{-} Ly6C^{high} cells in the spleen at 14 dpi are displayed. At least five mice per group from three independent experiments were analyzed. Bars represent the mean with SEM. For statistical analysis, a student t test was carried out with the group of naïve mice as a reference. (* < 0.05, ** < 0.005).

5% of the naïve mMDSCs were PD-L1^{high} (Figure 4.3 A), and up to 30% of the naïve gMDSCs (Figure 4.3 C) expressed high levels of this molecule (Figure 4.3 A and C). During FV infection, frequencies of the PD-L1^{high} gMDSCs increased four times up to 20% (Figure 4.3 C). 70% of mMDSC expressed PD-L1^{high} on the cell surface, increasing 2.5 times compared to naïve mice (Figure 4.3 A). Approximately 10% of the mMDSCs and 20% of the gMDSCs from naïve mice expressed CD80 (Figure 4.3 B and D). Upon infection a mean of 25% of the mMDSCs and 43% of the gMDSCs expressed CD80 (Figure 4.3 D). These data

demonstrate that the percentages of PD-L1^{high} and CD80^{+} of MDSCs increased during FV infection and suggest that MDSCs become active upon FV infection.

Adenosine metabolism was shown to play an important role in many processes involved in homeostasis and immune regulation of T cells. CD39 (Ectonucleoside triphosphate diphosphohydrolase-1) is an enzyme involved in the conversion of ATP (Adenosine triphosphate) to ADP (Adenosine diphosphate) and AMP (Adenosine monophosphate), which is further metabolized by CD73 (Ecto-5'nucleotidase) to adenosine. Both of these enzymes were shown to be involved in Treg mediated suppression of effector T cell responses (40).

To further characterize MDSCs during FV infection, the CD39 and CD73 expression, both involved in the adenosine metabolism, were analyzed. 15% of the naïve mMDSCs were positive for CD39, and upon infection this frequencies did not change. Percentages of CD39^{+} gMDSC from both naïve and FV infected mice reached 70% (Figure 4.4 A), with no difference between the distinct groups. Only 7% of the mMDSCs from naïve or infected mice expressed CD73, with no influence of the infection. 20-30% of the gMDSCs were positive for CD73 in both naïve and FV infected animals (Figure 4.4 B). According to this observation, the adenosine mechanism of immune regulation was not induced by FV infection.
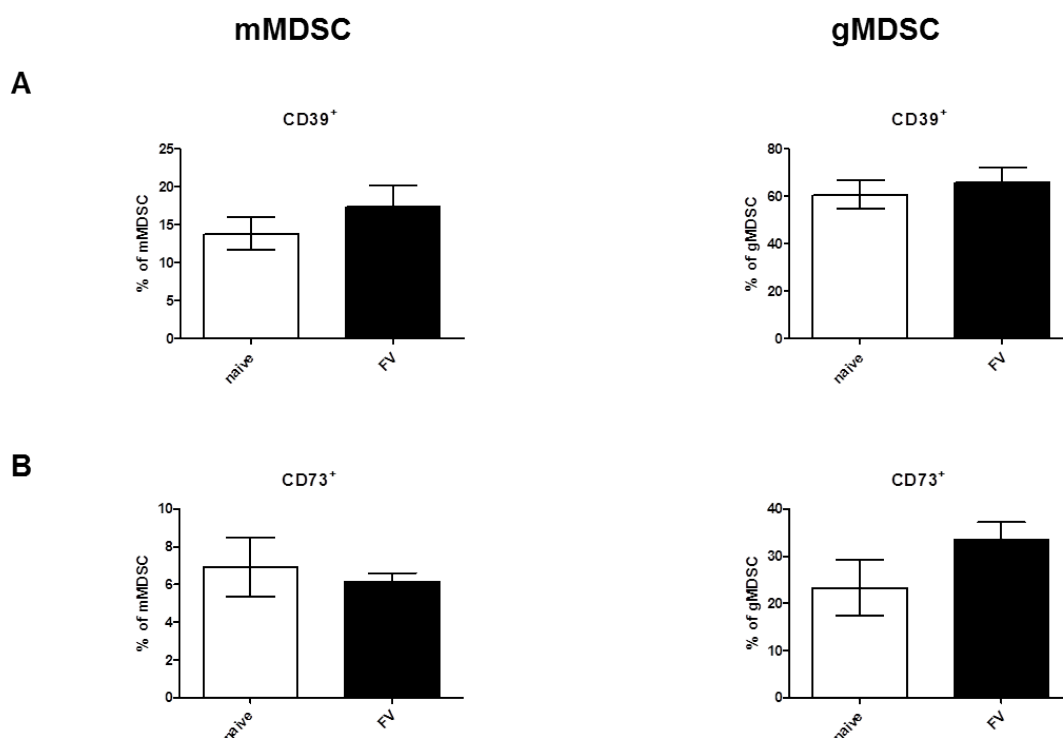
Figure 4.4 Expression levels of CD39 and CD73 on MDSCs during acute FV infection. B6 mice were infected i.v. with 20 000 SFFU of FV or left un-infected, and the expression of CD39 and CD73 on MDSCs was measured using flow cytometry at day 14 post infection. Frequencies of (A) CD39 and (B) CD73 expressing Ly6G^{high} Ly6C^{low} and Ly6G$^-$ Ly6C^{high} cells in the spleen are displayed. At least five mice per group from three independent experiments were analyzed. Bars represent the mean with SEM. For statistical analysis, a student t test was carried out.

In order to investigate the function of MDSCs, it was of interest to identify whether the main known mechanisms of MDSCs' mediated suppression were induced during acute FV infection. Arg1 was of special interest, which is an enzyme converting ɪ-arginine to urea and ɪ-ornithine, and NOS2, an enzyme further synthetizing nitric oxide (NO) and ɪ-citrulline (13).

Naïve animals did not express high levels of intracellular NOS2 on MDSCs. However, after infection up to 15% of all mMDSCs started to express NOS2. In the granulocytic subset, NOS2 expression was at the same frequency as in naïve animals (1-1.5%) (Figure 4.5 A). Arg1 was expressed in 2-5% of gMDSCs and mMDSCs from naïve mice but increase to around 10% post infection (Figure 4.5 B).

Summarizing the phenotypic data, it can be postulated that MDSCs become activated during FV infection. Elevated expression of PD-L1^{high} and CD80 may be associated with this activation. The expression of CD39 and CD73 on the cell surface of MDSCs did not change during infection. Possible mechanisms of mMDSC function may include nitric oxide metabolism and ɪ-arginine conversion by Arg1
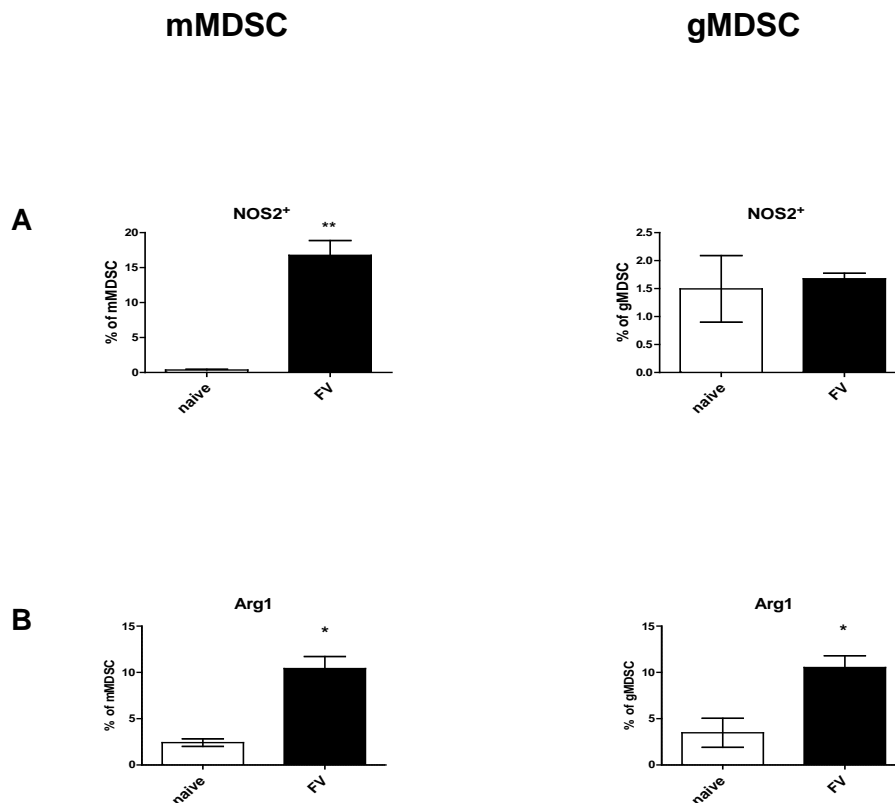
mMDSC   **gMDSC**

Figure 4.5 Expression levels of Arg1 and NOS2 in MDSCs are upregulated during acute FV infection.

B6 mice were infected i.v. with 20 000 SFFU of FV or left un-infected and the expression of Arg1 and NOS2 in the MDSCs was measured using flow cytometry for spleen cells at day 14 post infection. Frequencies of **(A)** NOS2 and **(B)** Arg1 expressing Ly6G^{high} Ly6C^{low} and Ly6G^{-} Ly6C^{high} cells in spleen are displayed. At least five mice per group from three independent experiments were analyzed. Bars represent the mean with SEM. For statistical analysis, a student t test was carried out with the group of naïve mice as a reference (* < 0.05, ** < 0.005).

4.3 5FU and αLy6G selectively deplete MDSCs

After characterizing the MDSC expansion and activation it was of interest to confirm the suppressive role of MDSCs *in vivo* during an ongoing FV infection.

Different methods to eliminate, block or suppress MDSCs have already been described, including antibody treatment (αGr1, αLy6G), directly acting drugs (5-Fluorouracil (5FU), Silendafil, doxorubicine) and drugs, which were described to maturate MDSCs (ATRA, CpG) (44, 50).

In order to investigate the role of MDSCs during FV infection in living mice either gMDSCs or both the gMDSC and mMDSC population were depleted. By single administration of 5FU four days prior to sacrificing the mice on day 14 post infection, both MDSC populations were depleted, with an efficacy of 91% (Figure 4.6 C). The pyrimidine analog 5FU is a cytostatic drug with MDSCs specific cytotoxicity.
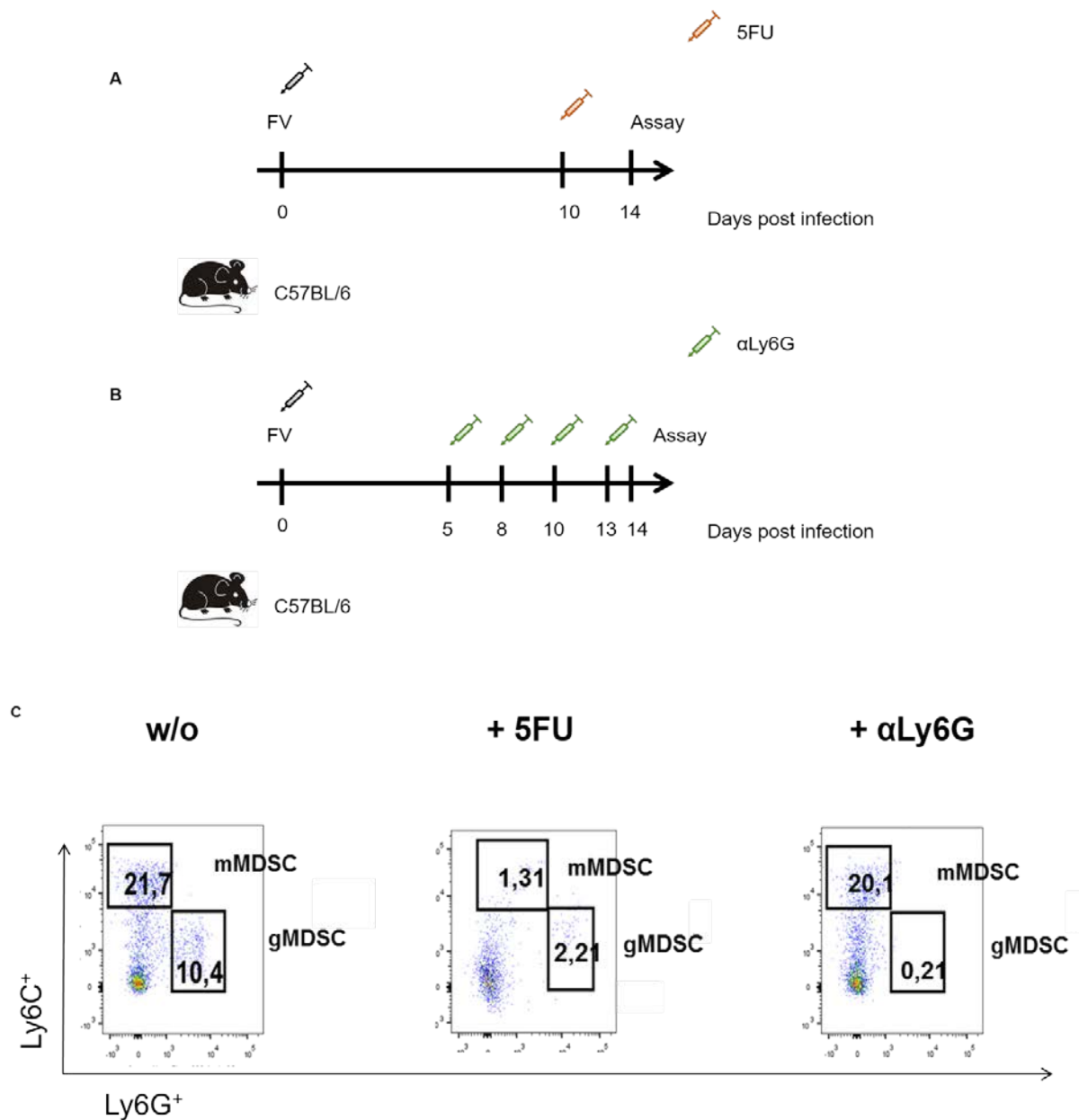
Figure 4.6 Schematic of the MDSC depletion during acute FV infection in the spleen.
B6 mice were infected i.v. with 20 000 SFFU of FV, and/or treated with 5FU or αLy6G.
Experimental design of the MDSC depletion by administration of (A) 5FU or (B) αLy6G.
(C) Representative dotplots of MDSC during FV infection after administration of 5FU,
αLy6G or untreated.

The second approach, the i.p. administration of αLy6G antibody, selectively
depleted only gMDSCs, with a depletion efficiency of 98% (Figure 4.6 C). αLy6G

antibody was administered four times every third day and organs were harvest at day 14 post infection.

4.3.1 Depletion of MDSCs leads to a reduction in FV loads and an increase of cytotoxic CD8$^+$ T cells

The depletion of MDSCs was first shown in cancer models and led to a reduction of tumor size and activation of different immune cell subsets, primarily T cells. Therefore, it was of interest to investigate the influence of MDSC depletion on acute retroviral infection.

The main question after the depletion of MDSCs appeared to be whether the reduction of these cells has an effect on viral loads and on different immune cell subsets. First, an Infectious center assay was performed in order to analyses the viral loads. After depletion of total MDSCs with 5FU (gMDSCs and mMDSCs), a up to 10 fold reduction in viral loads per million cells was observed. After the depletion of only gMDSCs a slight and not significant reduction of viral loads was observed (Figure 4.7 A). Replication of FV is normally associated with a mild splenomegaly in C57/Bl6 mice. The depletion of all MDSCs resulted in diminished spleen weights after administration of 5FU. The depletion of only gMDSCs with αLy6G antibodies likewise diminished spleen sizes (Figure 4.7B). These data suggest that MDSC influence numbers of FV-infected cells *in vivo*.
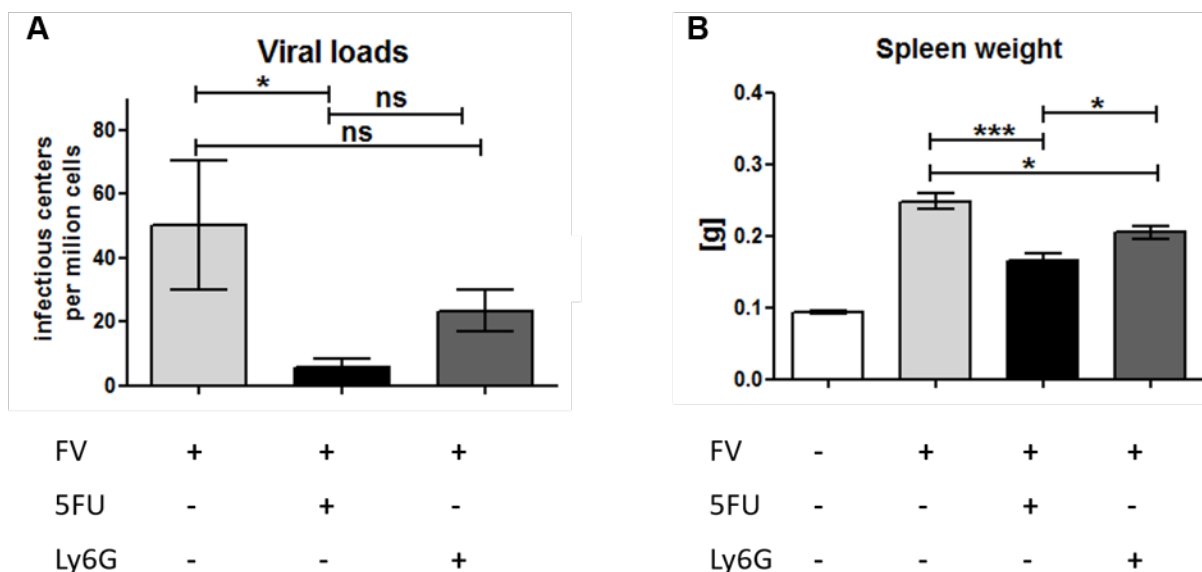
Figure 4.7 Depletion of MDSCs leads to a reduction in viral loads during acute FV infection.

B6 mice were infected i.v. with 20 000 SFFU of FV, and/or treated with 5FU and/or αLy6G, and viral loads as well as spleen weight were estimated at day 14 post infection. **(A)** The numbers of infected cells per 1×10^6 cells in spleen are displayed. (B) Spleen weights were assessed. At least five mice per group from three independent experiments were analyzed. Bars represent the mean with SEM. For statistical analysis an ANOVA multiple comparison test was carried out (* < 0.05, *** < 0.0005).

Previous data show that the elimination of MDSCs led to a reduced number of infected cells. CD8^{+} T cells were shown to play a major role in the control of acute FV infection and reduction of viral loads during the acute phase of FV Infection (82). Interestingly, the contraction phase of the CD8^{+} T cell response at day 12 post infection correlated with the expansion of MDSCs (77). Thus it was of interest whether the population of effector CD8^{+} T cells was influenced by MDSCs. CD43^{+}, a sialoglycoprotein, expressed on the cell surface of a variety of hematopoietically derived cells, including T lymphocytes, is a part of the receptor-ligand complex, required for T cell activation (52-53). Naïve CD8^{+} cells do not express CD43^{+}, but CD43^{+} becomes highly up-regulated on antigen specific effector CD8^{+} T cells (58). Interestingly, after the depletion of all MDSCs, the frequency of CD43^{+} CD8^{+} T cells increased significantly, reaching levels of 20 000 CD43^{+}CD8^{+} cells per one million spleen cells in comparison to 10 000 activated CD8^{+} cells per million in only

FV-infected mice (Figure 4.8A). After the depletion using αLy6G antibodies, higher frequencies of activated CD8^{+} T cells were observed, reaching 18 000 activated CD8^{+} T cells per one million cells. These results suggest that the depletion of MDSCs and the following reduction in viral loads during acute FV infection may be a result of an improved expansion CD8^{+} T cell response.
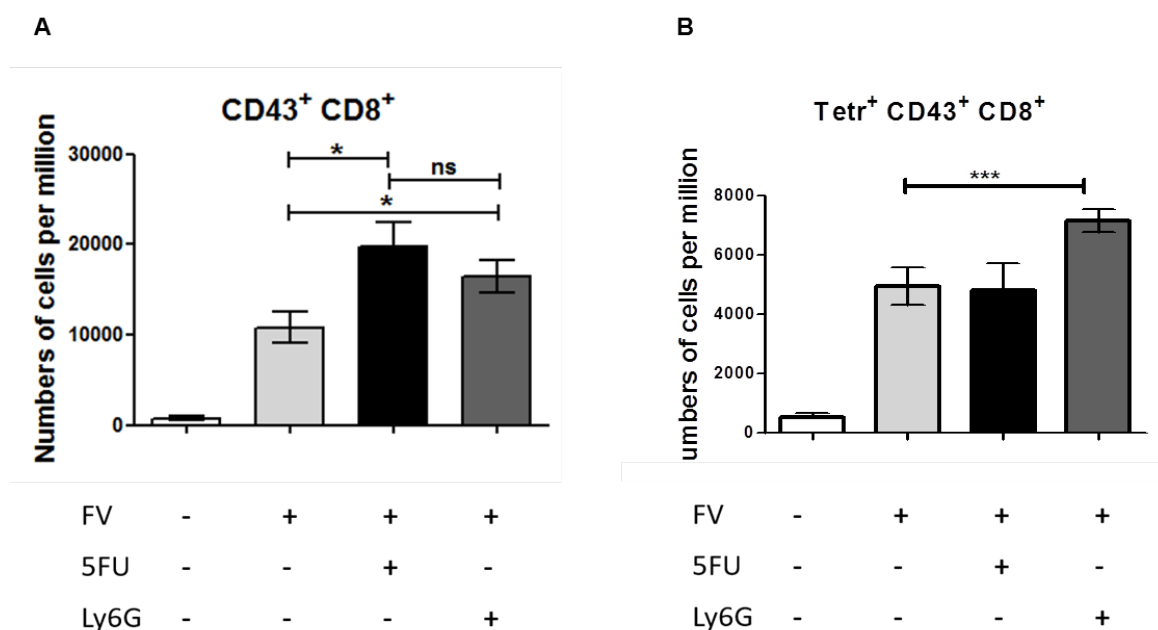

Figure 4.8 Depletion of MDSC leads to an expansion of effector CD8^{+} T cells during acute FV infection.

B6 mice were infected i.v. with 20 000 SFFU of FV and/or treated with 5FU and/or αLy6G or left un-infected and CD8^{+} numbers were measured using flow cytometry for spleen cells at 14 days post infection. **(A)** The numbers of CD43^{+} of live CD8^{+} per 1×10^6 live cells in spleen are displayed. **(B)** The numbers of FV-D[b]gagL class I tetramers of live CD8^{+}CD43^{+} cells in spleen are displayed. At least five mice per group from three independent experiments were analyzed. Bars represent the mean with SEM. For statistical analysis an ANOVA multiple comparison test was carried out (* < 0.05).

Next, it was of interest whether the expanded population of CD8^{+} T cells was specific for the immunodominant epitope of Friend virus. With the use of FV-D[b]gagL class I tetramers it was possible to assess that the administration of 5FU did not result in increased percentages of virus-specific effector CD8^{+} T cells. However, the depletion with αLy6G antibodies significantly increased the

frequency of tetramer^{+} CD8^{+} cells. These data imply that antibody mediated gMDSCs depletion leads to an expansion of virus-specific CD8^{+} T cells, but the administration of 5FU was more associated with polyclonal expansion of CD8^{+} effector cells.
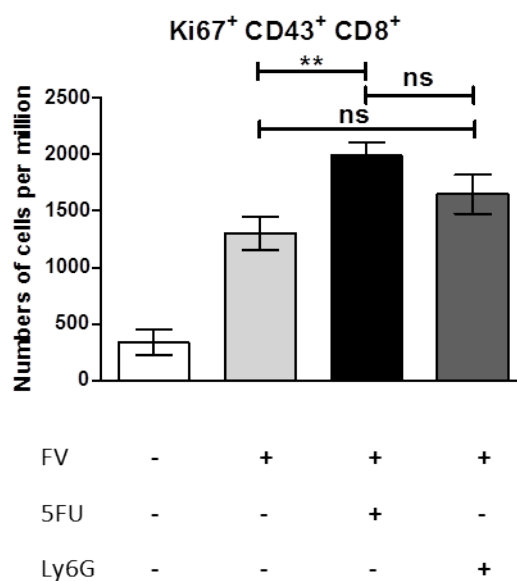

Figure 4.9 Increased proliferation of CD8^{+} T cells after MDSC depletion during acute FV infection.

B6 mice were infected i.v. with 20 000 SFFU of FV and/or treated with 5FU and/or αLy6G or left un-infected, and the CD8^{+} numbers were measured using flow cytometry for spleen cells at 14 days post infection. The numbers of Ki67^{+} of live CD43^{+}CD8^{+} per 1×10^6 live cells in spleen are displayed. At least five mice per group from three independent experiments were analyzed. Bars represent the mean with SEM. For statistical analysis an ANOVA multiple comparison test was carried out (*** < 0.0005).

Ki67 is a nuclear protein involved in cell proliferation (18). To characterize the proliferation of the CD8^{+} T cell population upon MDSC depletion, the intranuclear expression of Ki67 was analyzed. During the 5FU administration almost 2000 CD43^{+} CD8^{+} cells per million proliferated compared to the infected only group, in which 1300 cells were positive for Ki67^{+}. In gMDSC depleted mice, 1600 activated CD8^{+} T cells were proliferating, however this difference was not significant (Figure

4.9). Thus, the depletion of MDSCs may lead to an increased proliferation of CD8$^+$ cells.

IL-2, IFNγ and TNFα are three cytokines produced by activated functional CD8$^+$ T cells. Therefore, the cytokine profile of the CD8$^+$ T cell population was analyzed after MDSC depletion. IFNγ is a very important cytokine in both the innate and the adaptive immune response. The main functions are the activation of macrophages and induction of MHC class II expression. TNFα shows a strong pro-inflammatory capacity with direct lytic effects on tumor cells. IL-2 stimulates the T and B cell proliferation, induces cytotoxicity of macrophages, and induces cytokine production. Expression of TNFα, INFγ and IL-2 in activated CD8$^+$ cells after intracellular cytokine staining was analyzed. During FV infection around 15% of the CD8$^+$ T cells expressed TNFα or IFNγ. IL-2 expression was lower at around 8%. Depletion of total MDSCs (5FU) resulted in significant increases in the percentages of TNFα (up to 27%), IFNγ (up to 28%), and IL-2 (up to 15%) producing CD8+ T cells (Figure 4.10 A-B). In contrast, gMDSC depletion (αLy6G antibody) did not influence cytokine responses of CD8+ T cells. The depletion of total MDSCs but not gMDSCs resulted in an increased functionality of CD8$^+$ T cells in terms of cytokine production.
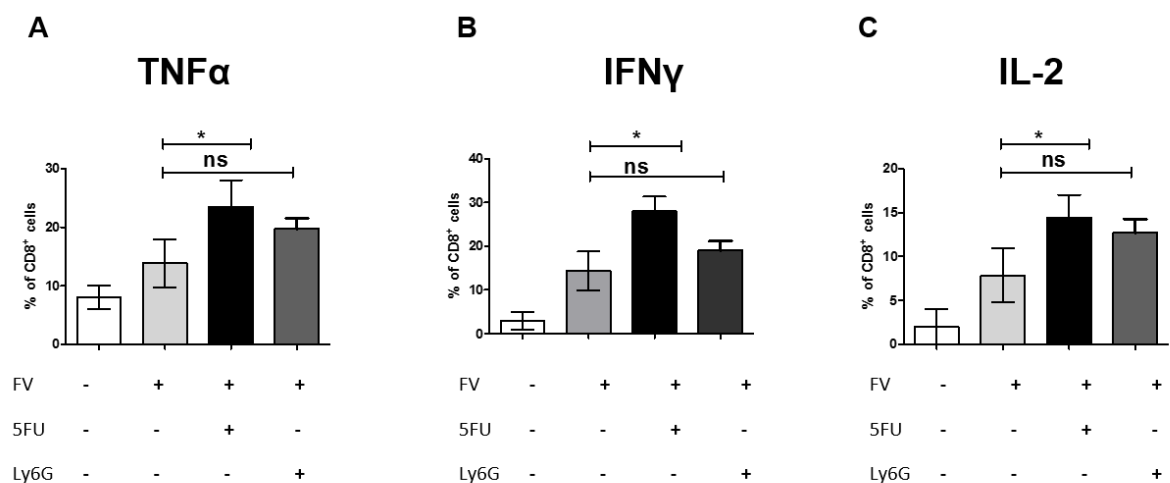
Figure 4.10 Upregulation of proinflammatory cytokine expression by CD8$^+$ T cells after MDSC depletion during acute FV infection.
B6 mice were infected i.v. with 20 000 SFFU of FV and/or treated with 5FU and/or αLy6G or left un-infected, and CD8+ numbers were measured using flow cytometry for spleen cells 14 days post infection. The frequencies of **(A)** TNFα, **(B)** IFNγ and **(B)** IL-2 of live CD8$^+$ in spleen are displayed. At least five mice per group from three independent experiments were analyzed. Bars represent the mean with SEM. For statistical analysis, an ANOVA multiple comparison test was carried out with a group of naïve mice as reference (* < 0.05).

Virus-specific CD8$^+$ T cells kill FV-infected cells by releasing cytotoxic granules. The main cytotoxic effector molecule stored in the granule of cytotoxic CD8$^+$ T cells is Granzyme B (GzmB). To further characterize effector CD8$^+$ T cells after MDSC depletion, a closer look was taken at the GzmB expression by these cells. After depletion of the total MDSC population, the frequency of GzmB$^+$ activated CD8$^+$ T cells was almost twice as high as in the infected only group. Specific gMDSC depletion showed a slight, however not significant, increase in GzmB$^+$ cells compared to the infected only group (Figure 4.11). Thus, only depletion of total MDSCs resulted in an increased cytotoxicity of CD8$^+$ T cells.
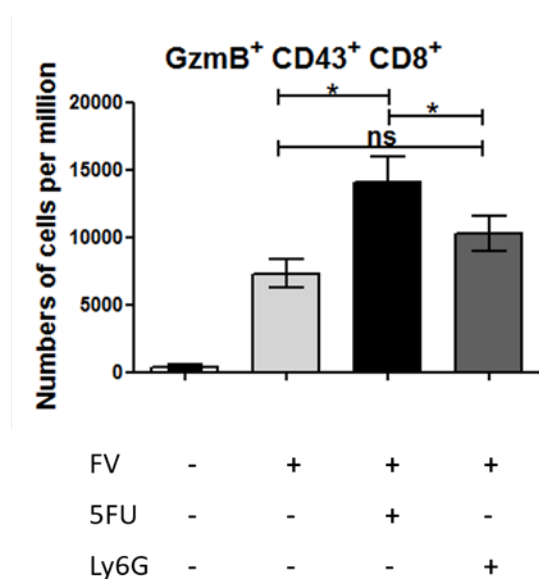
Figure 4.11 Increased production of granzyme B by CD8$^+$ T cells after MDSC depletion during acute FV infection.

B6 mice were infected i.v. with 20 000 SFFU of FV and/or treated with 5FU or αLy6G or left un-infected, and CD8$^+$ numbers were measured using flow cytometry for spleen cells at 14 days post infection. The numbers of GzmB$^+$ of live CD43$^+$CD8$^+$ cells in spleen are displayed. At least five mice per group from three independent experiments were analyzed. Bars represent the mean with SEM. For statistical analysis, an ANOVA multiple comparison test was carried out with the group of naïve mice as reference (*** < 0.0005).

To analyze whether MDSCs have an influence on CD8$^+$ T cell killing, an *in vivo* cytotoxicity assay was performed. B6 mice were infected with FV and depleted for MDSCs with 5FU. On day 14 post infection all groups of mice received lymphocytes from naïve donor mice that were loaded with a MHC class I-restricted, FV-specific CD8$^+$ T cell epitope peptide and labelled with CFSE. One hour after i.v. injection of target cells, mice were sacrificed and the *in vivo* killing activity was quantified. It was not possible to detect any differences in the *in vivo* killing between infected and the infected MDSC depleted mice in any of the analyzed organs. Thus, depletion of total MDSCs did not significantly improve CD8$^+$ T cells killing target cells during FV infection (Figure 4.12).
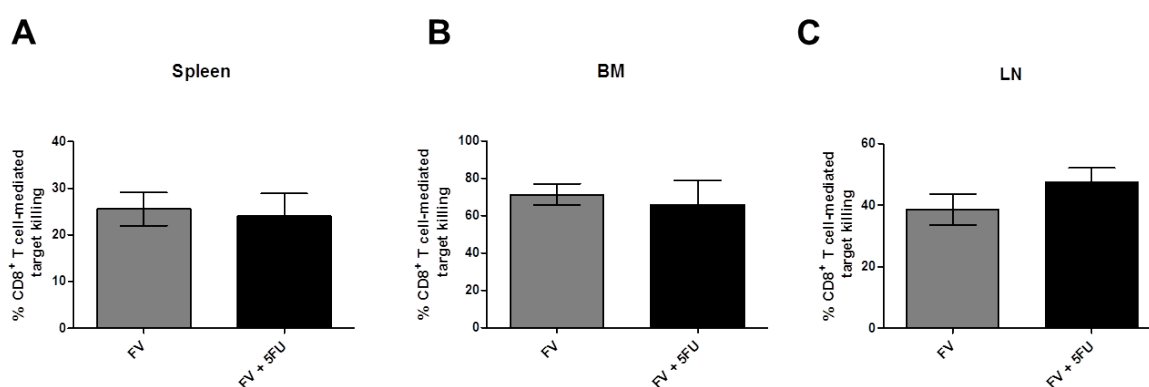

Figure 4.12 Depletion of total MDSCs did not affect *in vivo* cytotoxicity of CD8$^+$ T cells. Spleen cells from donor naïve mice were isolated and loaded with a MHC class I-restricted FV-specific CD8$^+$ T cell epitope peptide labelled with CFSE and injected i.v. into FV-infected B6 mice. Mice were treated with 5FU or left untreated One hour after i.v. injection of CFSE targets, mice were sacrificed and the *in vivo* killing activity was

quantified in single-cell suspensions from the spleen, lymph nodes and bone marrow. At least two independent experiments were analyzed.

4.4 gMDSC suppress CD8$^+$ T cell responses *in vitro*

After characterizing MDSCs during Friend Virus infection, it was of interest to analyze the suppressive activity and effector mechanisms of MDSCs in an *in vitro* model.

To achieve this goal, a CD8$^+$ T cell proliferation assay was performed. Bone marrow derived dendritic cells were incubated with Violet Cell tracer labeled virus-specific CD8$^+$ T cells isolated from DbGagL TCR transgenic mice, of which more than 90% of the CD8$^+$ T cells contained a TCR specific for the DbGagL FV epitope (73). The DCs were loaded with the DbGagL epitope peptide to induce virus-specific proliferation of the CD8$^+$ T cells. mMDSCs and gMDSCs were isolated from FV-infected mice and added in different cell numbers in order to determine the effect of these cells on the CD8$^+$ T cell response. After 3 days, CD8$^+$ T cell proliferation and GzmB expression was analyzed. At this time point an average of 90% of the CD8$^+$ T cells in the culture had undergone at least one cell division. Interestingly, this CD8$^+$ T cell proliferation was only suppressed by gMDSCs, but not by mMDSCs (Figure 4.13). The suppression by gMDSCs was cell number dependent and a 4.5 fold reduction of proliferation was found at an effector target ratio of 1:10. At this ratio no significant effect of mMDSCs on the proliferation of FV-specific CD8$^+$ T cell was found.
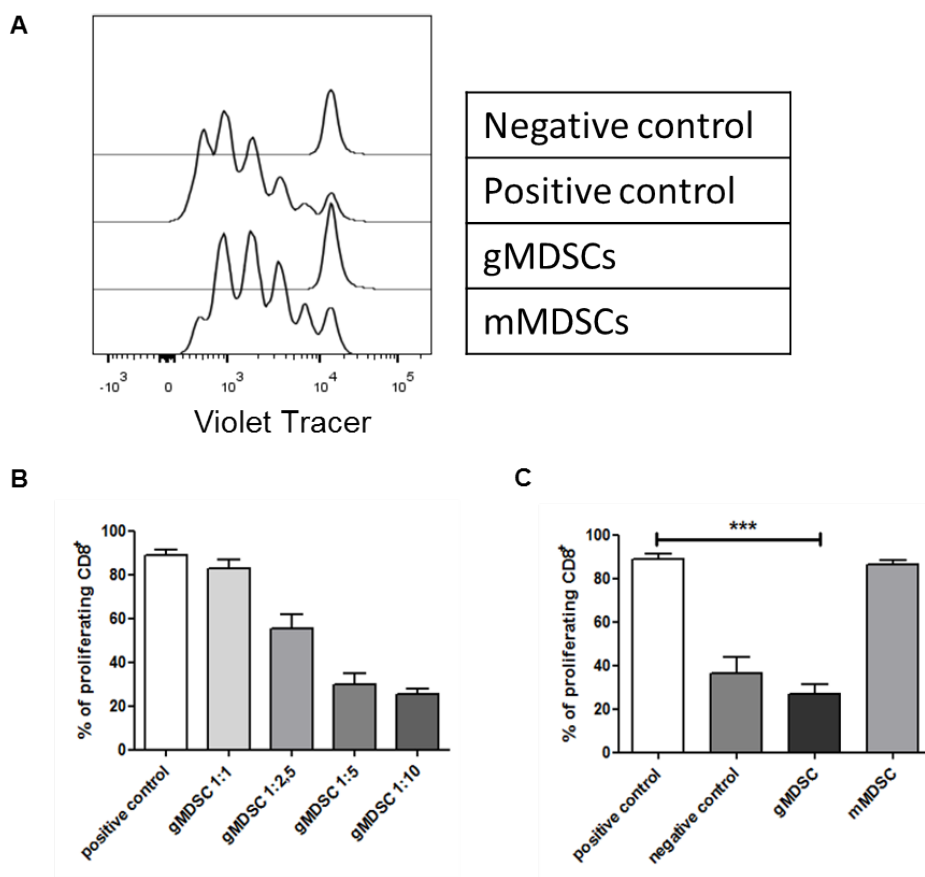
Figure 4.13 Granulocytic myeloid derived suppressor cells inhibited CD8$^+$ T cell proliferation.

CD8$^+$ T cells isolated from DbGagL TCR transgene mice were incubated with dendritic cells loaded with MHC class I-restricted FV-specific CD8$^+$ T cell epitope peptide and co-incubated with either gMDSCs or mMDSCs. (A) Representative histograms and (C) percentages of CD8$^+$ T cells after co-incubation with or without either gMDSC or mMDSCs from FV-infected mice are shown. (B) CD8$^+$ T cell proliferation was measured after co-incubation with different effector target rations of gMDSCs. CD8$^+$ T cells incubated with peptide loaded DC serve as a positive control, CD8$^+$ T cells incubated with non-loaded DC serve as negative control. At least three independent experiments were analyzed. Bars represent the mean with SEM. For statistical analysis, an ANOVA multiple comparison test was carried out with the group of naïve mice as a reference (** < 0.005).

Additionally, the GzmB expression of activated CD8$^+$ T cells was measured. An average of 90% of all CD8$^+$ T cells in the cultures produced GzmB. This expression of GzmB was also diminished by gMDSCs, but not by mMDSCs co-

incubation (Figure 4.14). An effector target ratio of 1:10 gMDSCs reduced the percentage of GzmB$^+$ CD8$^+$ T cells to a mean of below 20% which corresponds with the previously obtained results on the suppression of proliferation (Figure 4.12).
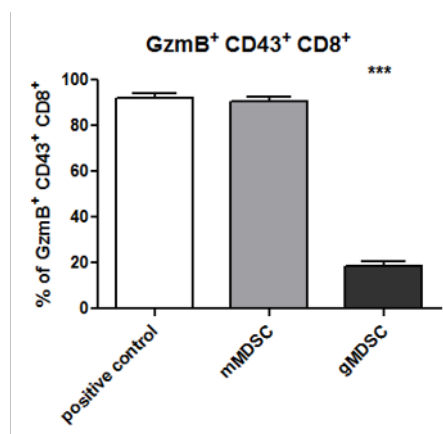

Figure 4.14 Granulocytic myeloid derived suppressor cells inhibited GzmB production by CD8$^+$ T cells.

CD8$^+$ T cells isolated from DbGagL TCR transgene mice were incubated with dendritic cells loaded with MHC class I-restricted FV-specific CD8$^+$ T cell epitope peptide and co-incubated with either gMDSCs or mMDSCs. Frequencies of GzmB expressing CD43$^+$CD8$^+$ cells after incubation of CD8$^+$ cells with gMDSCs or mMDSCs from FV-infected mice are shown. Bars represent the mean with SEM. For statistical analysis, an ANOVA multiple comparison test was carried out (*** < 0.0005). The experiment was repeated five times with comparable results.

These data suggest that gMDSC but not mMDSCs from FV-infected mice were able to suppress virus specific CD8$^+$ T cell responses *in vitro*.

4.4.1 gMDSC suppression of CD8$^+$ T cells was blocked by arginase or NO inhibition

Different mechanisms of MDSC suppression were described, among them the pathways of L-arginine metabolism. There are two enzymes essential for this process. Arg1 converts ʟ-arginine to urea and ʟ-ornithine. This is followed by NOS2, which metabolizes substrates to nitric oxide (NO) and ʟ-citrulline (13). These two enzymes play an important role in ʟ-arginine metabolism.. As shown above, during FV infection, the expression of Arg1 in gMDSCs increased but the expression of NOS2 on gMDSCs was not altered (Figure 4.4). mMDSC expression of both Arg1 and NOS2 was augmented during FV infection (Figure 4.4).

In order to investigate whether CD8$^+$ T cell suppression is arginase or NO dependent, the previously described proliferation assay was used. Additionally, nor-NOHA, which is a pan arginase inhibitor, or L-NMMA, a pan NO inhibitor, were used. After administration of the arginase inhibitor, we observed an approximately 2.5 times higher percentage of proliferating CD8$^+$ T cells in the presence of gMDSCs in comparison to the untreated control. Administration of the NO inhibitor led to an almost 3 times higher percentage of proliferating CD8$^+$ T cells compared to the untreated group.(Figure 4.15). These data suggest that ʟ-arginine metabolism is at least one mechanism of gMDSCs mediated suppression of T cell proliferation *in vitro*.
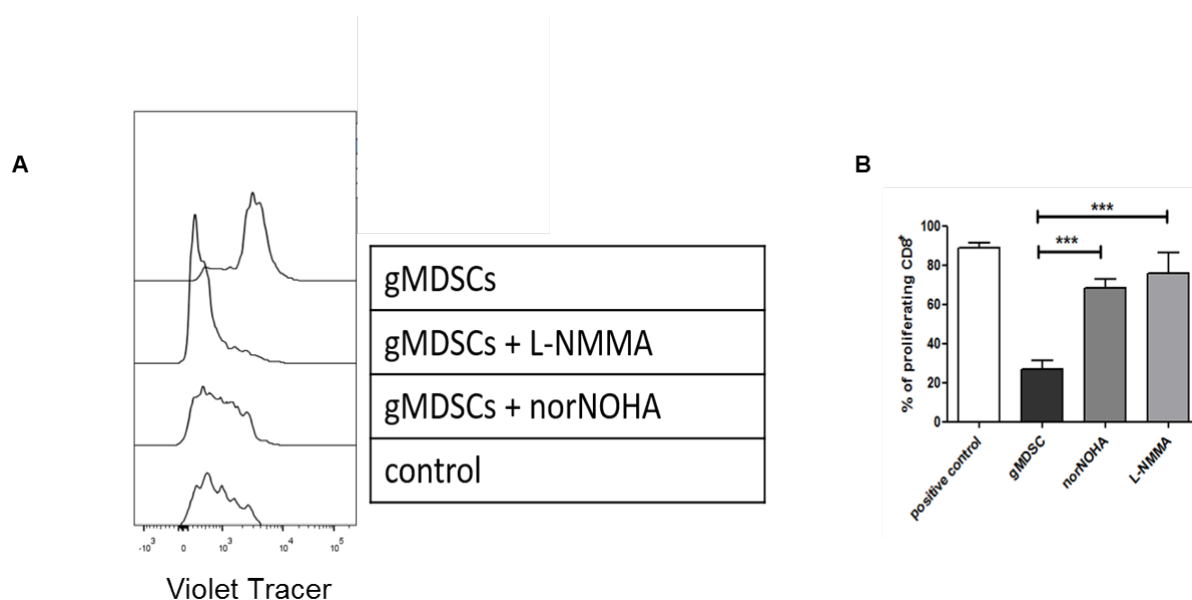
Figure 4.15 Suppression of nitric oxide and arginase partially restored CD8$^+$ T cell proliferation.

CD8$^+$ T cells isolated from DbGagL TCR transgenic mice were incubated with dendritic cells loaded with MHC class I-restricted FV-specific CD8$^+$ T cell epitope peptide and co-incubated with gMDSCs with or without addition of L-NMMA or nor-NOHA. (A) Representative histograms and (B) percentages of CD8$^+$ T cell proliferation after co-incubation with or without gMDSCs in the presence or absence of L-NMMA/nor-NOHA are shown. At least three independent experiments were analyzed. Bars represent the mean with SEM. For statistical analysis, an ANOVA multiple comparison test was carried out (*** < 0.0005).

4.4.2 gMDSC suppression of CD8 T cells was partially abrogated when MDSC lacked PD-L1

PD-1 (Programmed cell death receptor-1) is a well-characterized receptor involved in the suppression of immune response of virus-specific T cells (42). By binding with its ligand, PD-L1, PD-1 expressing T cells become dysfunctional or "exhausted". PD-L1 is expressed on a variety of cells, including MDSCs (25). As shown above, the expression of PD-L1 on MDSCs increased during FV infection (Figure 4.3). Therefore, it is of interest to analyze whether PD-L1 plays a role in MDSC mediated suppression.

To analyze the role of PD-L1 during the T cell suppression by gMDSCs, the previously described proliferation assay was used. For this experiment, gMDSCs were isolated from FV-infected PD-L1 knockout mice.
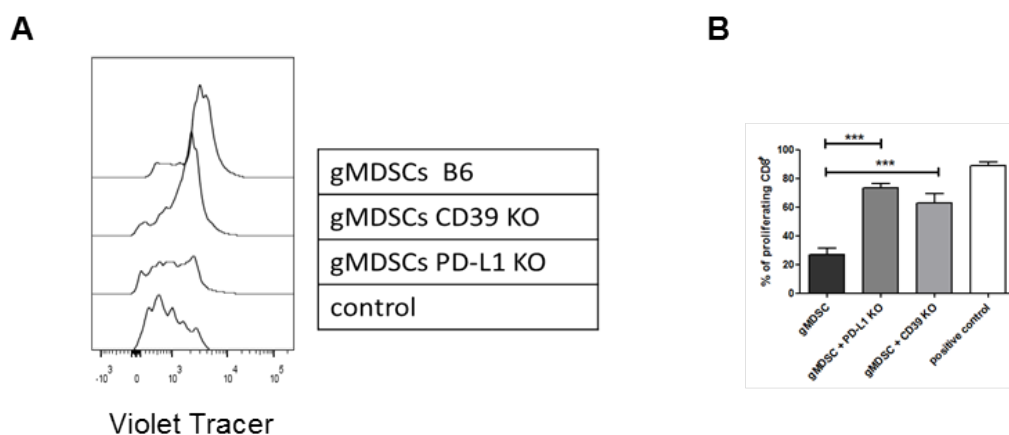
Figure 4.16 Lack of PD-L1 or CD39 partly restored CD8$^+$ T cell proliferation

CD8$^+$ T cells isolated from DbGagL TCR transgenic mice were incubated with dendritic cells loaded with MHC class I-restricted FV-specific CD8$^+$ T cell epitope peptide and co-incubated with gMDSCs isolated from PD-L1 KO or CD39 KO mice. (A) Representative histograms and (B) percentages of CD8$^+$ T cells after co-incubation with or without gMDSCs isolated from B6, PD-L1 KO or CD39 KO FV infected mice are shown. At least three independent experiments were analyzed. The bars represent the mean with SEM. For statistical analysis, an ANOVA multiple comparison test was carried out (*** < 0.0005).

Interestingly, gMDSCs lacking PD-L1 were not able to efficiently suppress CD8$^+$ T cell proliferation *in vitro* (76% of all CD8+ T cell proliferated) in contrast to PD-L1 expressing gMDSCs (25% proliferation rate) (Figure 4.16). This suggests the importance of PD-L1 in gMDSC mediated CD8$^+$ T cell suppression.

Adenosine metabolism plays an important role in maintaining immune homeostasis. CD39 (Ectonucleoside triphosphate diphosphohydrolase-1), an enzyme involved in the conversion of ATP to ADP and AMP, was shown to have a role in the effector T cell suppression mediated by regulatory T cells. Therefore, it was of interest to investigate whether adenosine metabolism may also be involved in MDSC mediated immune suppression.

The previously described CD8$^+$ T cell proliferation assay was again used to answer this question. After incubation of gMDSCs isolated from CD39 KO mice with CD8$^+$ T cells, 64% of the CD8$^+$ T cells had undergone cell division, which was

almost 2.5 higher as in the control group with gMDSCs from wild type mice (Figure 4.16). These data suggest a significant role of adenosine metabolism in gMDSC mediated suppression.

The first part of this thesis concentrated on MDSCs and their function during acute FV infection. We observed an expansion of both gMDSCs and mMDSCs at day 14 post infection and they also showed a higher expression of PD-L1^{high}, CD80, Arg1 compared to naïve mice. Further, we were able to show that mainly FV-activated gMDSCs but not mMDSCs were able to suppress virus-specific CD8$^+$ T cell responses *in vitro*. Moreover, *in vivo* depletion of MDSCs resulted in a reduction of viral loads and in augmented cytotoxic CD8$^+$ T cell responses. As mechanisms of gMDSC mediated suppression of virus-specific T cell proliferation in vitro NO or arginase metabolism as well as PD-L1 and CD39 expression were identified. These data demonstrate the importance of MDSCs in the regulation of CD8$^+$ T cell responses during acute retroviral infection and identify mechanisms involved in the suppressive function of these cells.

5 The interaction of inhibitory mechanisms: MDSCs, T regulatory cells (Tregs) and inhibitory receptors.

The immune response to acute viral infection is restrained by different mechanisms such as MDSCs, Tregs or inhibitory receptors to prevent severe immunopathology by overshooting T cell responses. All of these mechanisms were shown to work independently. Recently, immune therapies involving immune checkpoint blockers are gaining increasing attention. However, the interactions between the different suppressor mechanisms are not very well studied. Therefore, the question arises what influence the depletion or blockage of one of these mechanisms may have on the quality and quantity of the other inhibitory mechanisms.

5.1 Regulatory T cell responses during MDSC depletion

Another important mechanism of suppressing immune responses is the activity of Tregs. Previous work showed the importance of the Treg mediated inhibition of T cells in acute and chronic FV infection (137).

During the depletion of MDSCs in FV-infected mice, an increase of Tregs was observed. In naïve mice approximately 10% of $CD4^+$ cells are $Foxp3^+$. In FV-infected mice approximately 17% of the $CD4^+$ T cells are $Foxp3^+$ Tregs, whereas animals depleted for total MDSCs (5FU) had up to 25% of Tregs and αLy6G treated mice 22% (Figure 5.1 A). After MDSC depletion we found a slight increase in Treg proliferation ($Ki67^+$), but this was not statistically significant (Figure 5.1B). This result shows that indeed different immune checkpoints influence each other and the question arose how the MDSC response is altered during FV infection if Tregs are depleted and/or inhibitory receptors are blocked.
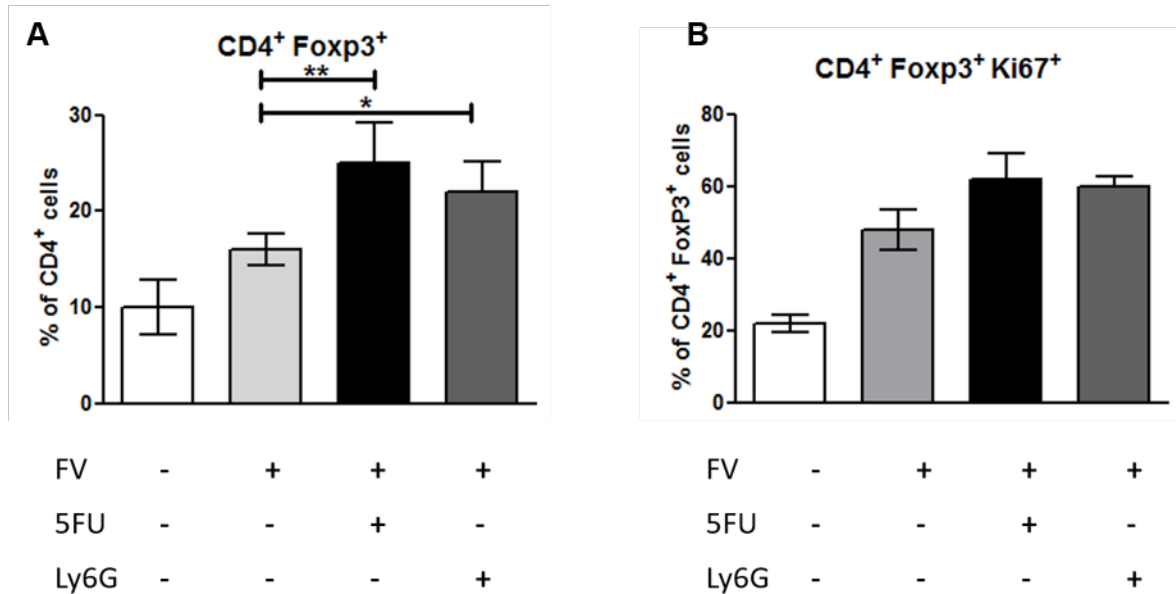
Figure 5.1 Tregs expand upon MDSCs depletion in FV-infected mice

B6 mice were infected i.v. with 20 000 SFFU of FV or left un-infected, and Tregs frequencies were measured using flow cytometry for spleen cells at 14 days post infection. **(A)** The frequencies of FoxP3$^+$ of live CD4$^+$ in spleen are displayed. **(B)** The frequencies of Ki67$^+$ of live FoxP3$^+$CD4$^+$ in spleen at 14 dpi are displayed. At least five mice per group from three independent experiments were analyzed. Bars represent the mean and SEM. For statistical analysis, an ANOVA multiple comparison test was carried out (* < 0.05, ** < 0.005,).

To answer this question, a DEREG mouse model was used for the selective depletion of Tregs, and MDSC numbers were assessed. After Treg depletion, almost 4-times higher frequencies of mMDSCs (Figure 5.2 A) and 2-times of gMDSCs, compared with infected non-depleted mice, were observed (Figure 5.2 B). The expanded populations of gMDSCs also showed slightly increased percentages of CD80+ and PD-L1^{high} cells (Figure 5.3 A). This increase in CD80 and PD-L1 expressing cells was even more pronounced in the mMDSC population after Treg depletion (Figure 5.3 B).
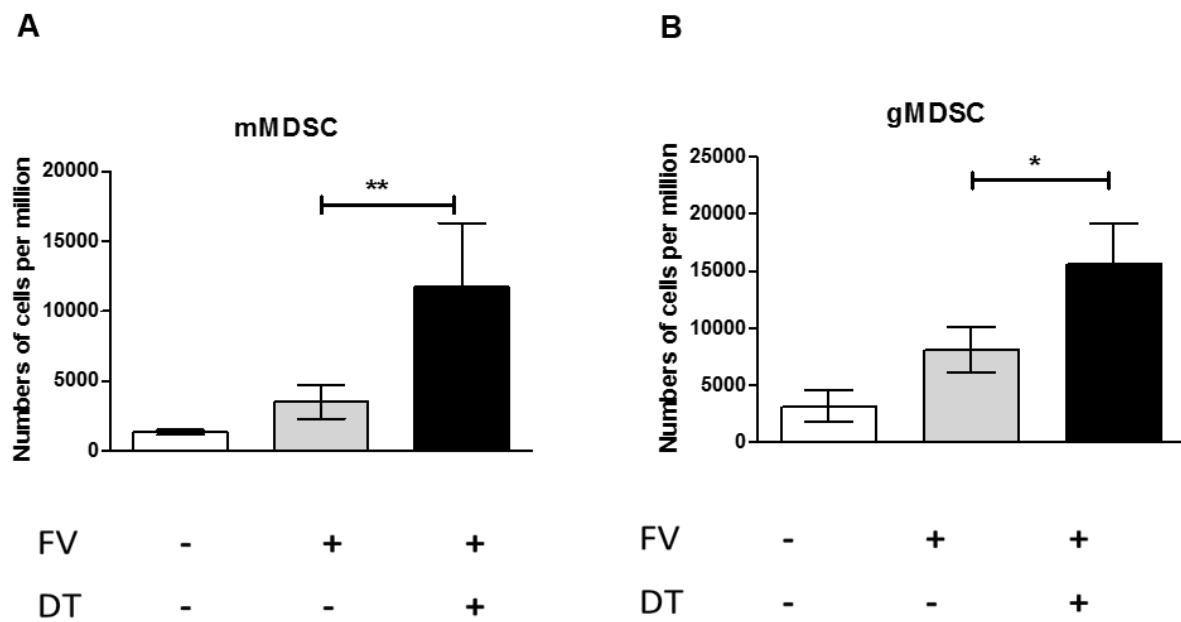
A

B

Figure 5.2 Depletion of Tregs led to MDSC expansion in FV-infected mice

DEREG mice were infected with 20 000 SFFU of FV and depleted for Tregsand MDSC numbers were measured using flow cytometry for spleen cells at 14 days post infection. The numbers of **(A)** mMDSCs and **(B) g**MDSCs per 10^6 living cells in spleen at 14 dpi are displayed. At least five mice per group from three independent experiments were analyzed. Bars represent the mean and SEM. For statistical analysis, an ANOVA multiple comparison test was carried out (* < 0.05, ** < 0.005).

Notably, the loss of one suppressive mechanism led to a compensatory mechanism for another inhibitor. Depletion of MDSCs resulted in the expansion of Tregs during acute FV infection. Similarly, the depletion of Tregs resulted in an activation of MDSCs.
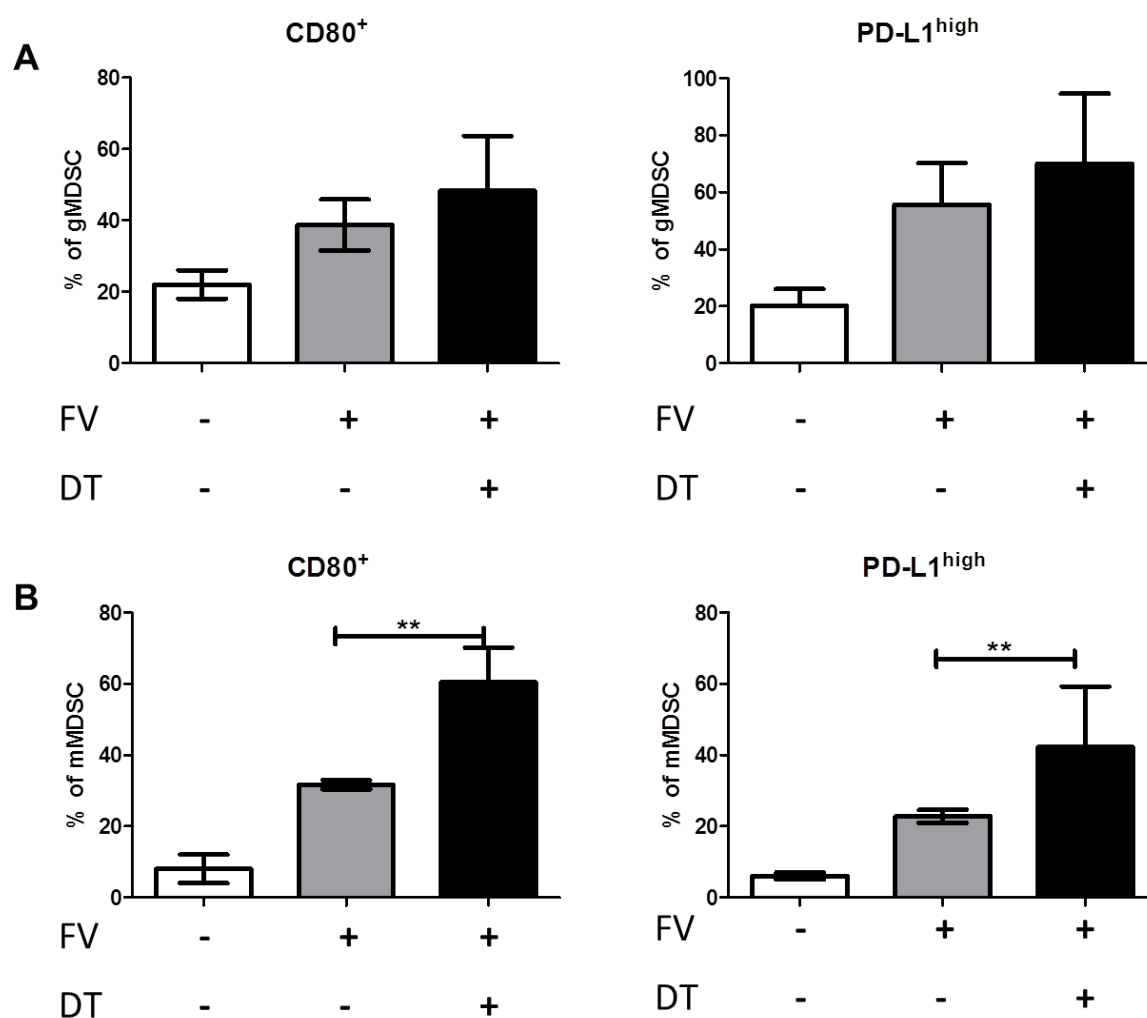
Figure 5.3 Characterization of MDSCs after Treg depletion during acute FV infection.

DEREG mice were infected with 20 000 SFFU of FV, treated with diphtheria toxin or left un-treated, and the expression of PD-L1^{high} and CD80 on the surface of MDSCs was measured using flow cytometry. **(A)** Frequencies of CD80 and PD-L1 expression on the surface of Ly6G^{high} Ly6C^{low} and Ly6G^{-} Ly6C^{high} cells in spleen at 14 dpi are displayed. At least five mice per group from three independent experiments were analyzed. Bars represent the mean with SEM. For statistical analysis, an ANOVA multiple comparison test was carried out with the group of naïve mice as reference (* < 0.05, ** < 0.005, *** < 0.0005).

5.2 Combination of MDSC and Treg depletion

As shown in the previous chapter, the depletion of one inhibitory cell population led to compensatory mechanisms. The question arises whether the simultaneous depletion of different inhibitory cell populations may lead to a stronger activation of effector mechanisms as well as a reduction of viral loads. In order to answer this question, both gMDSC and Tregs were simultaneously depleted during FV infection and mice were analyzed on day 14 post infection. Interestingly, the reduction in viral loads was higher in Treg plus gMDSC depleted animals than in only Treg or gMDSC depleted mice, however this difference was not significant (Figure 5.4 A). Moreover, after the depletion of the two regulatory cell populations, the frequencies of activated, virus specific CD8$^+$ T cells significantly increased compared to mice depleted for Tregs. (Figure 5.4 B).
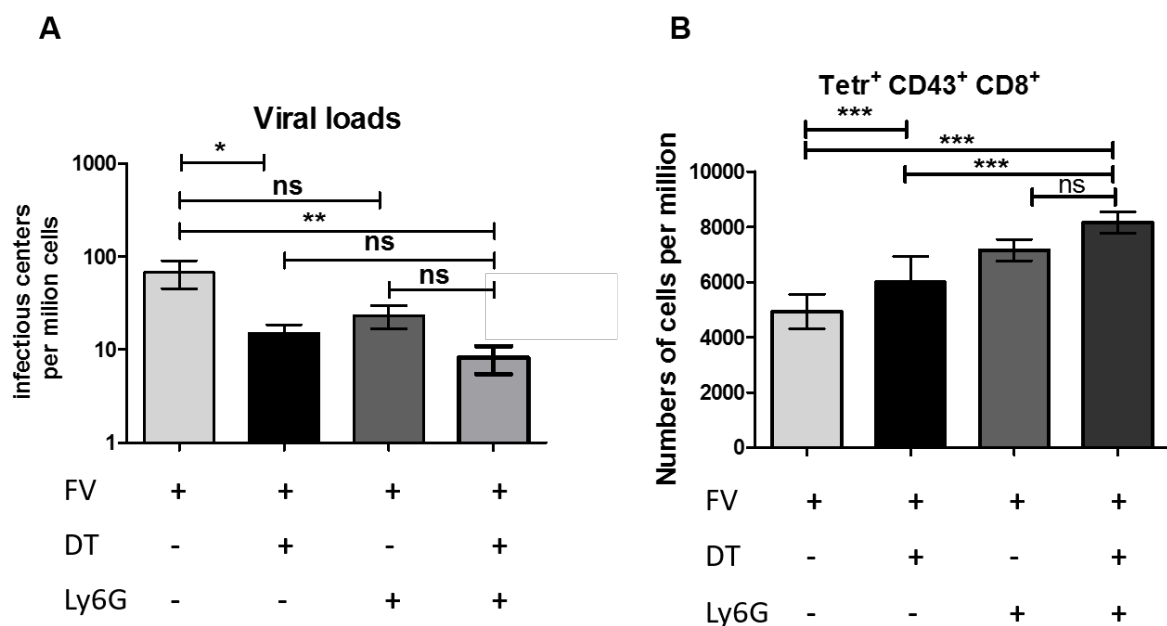

Figure 5.4 Combination of gMDSCs and Tregs depletion leads to a reduction in viral loads and increased numbers of activated virus specific CD8$^+$ T cells.

DEREG mice were infected with FV, and/or treated with DT and/or αLy6G, and an IC assay was performed and CD8$^+$ T cell numbers were analyzed. **(A)** The numbers of infected cells per 1x10^6 cells in the spleen are displayed. The numbers of (B) Tetr$^+$ or (C) GzmB$^+$ of live CD43$^+$CD8$^+$ in the spleen at 14 dpi are displayed. Bars represent the mean with SEM. For statistical analysis, an ANOVA multiple comparison test was carried out with the group of naïve mice as reference (* < 0.05, ** < 0.005, *** < 0.0005).

However, it is important to notice that on the last day of the experiment, animals were starting to experience light health disturbance, their fur was slightly unpolished and matt, and the movements were slower compared to animals treated with DT or αLy6G. Therefore, it is of importance to further investigate the combination treatment of gMDSCs and Tregs depletion, with regard to the development of immunopathology. These results suggest that combination therapy with depletion of gMDSCs and Tregs might improve immune responses and be may considered as immunotherapy for retroviral infection. However, it is crucial to further investigate this topic.

5.3 Combined blockage of inhibitory receptors with Treg depletion

We have previously shown that a combination therapy which blocks the inhibitory receptors PD-1 and Tim-3 reduces viral loads and restores CD8$^+$ T cell responses in chronic FV infection (137).
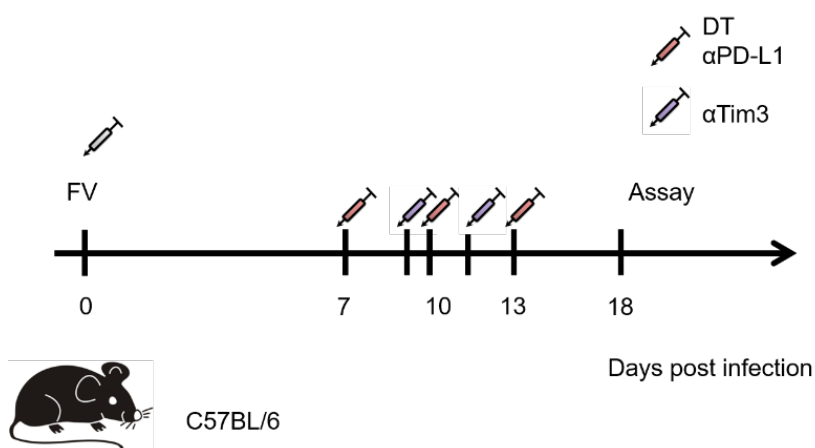
Figure 5.5 Treatment of acute FV infection with αPD-L1, αTim3 and depletion of Tregs. Schematic representation of the experiment. Shortly, DEREG mice were infected with 20 000 SFFV FV + LDV, treated with DT and αPD-L1, αTim3 in combination or alone or left untreated. On day 18 post infection spleen, bone marrow, peripheral lymph nodes, and intestinal lymph nodes were harvest for further analysis.

It was of interest weather a combination therapy targeting two checkpoint blockers (inhibitory receptors and Tregs) would affect the MDSC and T cell response in acutely FV infected mice. First, viral loads were analyzed after combination therapy. At day 14 post infection an average of 5000 cells per million splenocytes were infected in mice inoculated with FV. Treg depletion or antibody therapy reduced this viral load to 50 to 100 infected cells per million. Interestingly, combination treatment resulted in a further reduction of viral loads to around 20 infected cells per million (Figure 5.6). These results suggest that the simultaneous blocking of different inhibitory mechanisms may further reduce viral loads and improve the therapy outcome.
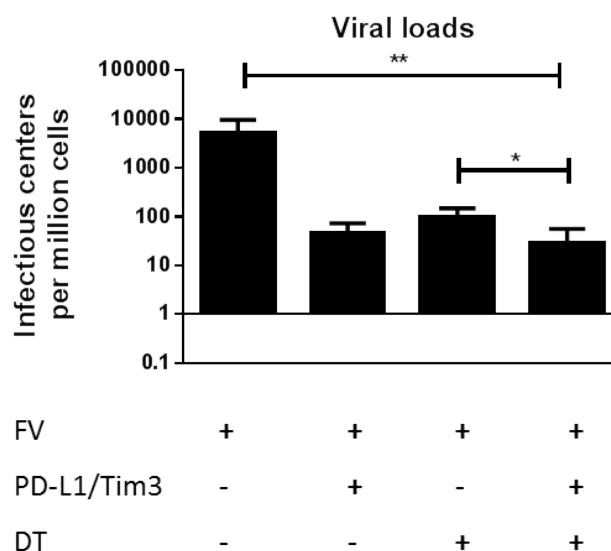

Figure 5.6 Depletion of Tregs combined with blocking inhibitory receptors leads to reduction of viral loads during acute FV infection.
Shortly, DEREG mice were infected with FV + LDV and treated with DT, αPD-L1, αTim3 in combination or alone, or left untreated, and infectious center assay was performed on day 14 post infection. The numbers of infected cells per 1×10^6 cells in spleen are displayed. At

least five mice per group from three independent experiments were analyzed. Bars represent the mean with SEM. For statistical analysis, an ANOVA multiple comparison test was carried out (* < 0.05, ** < 0.005).
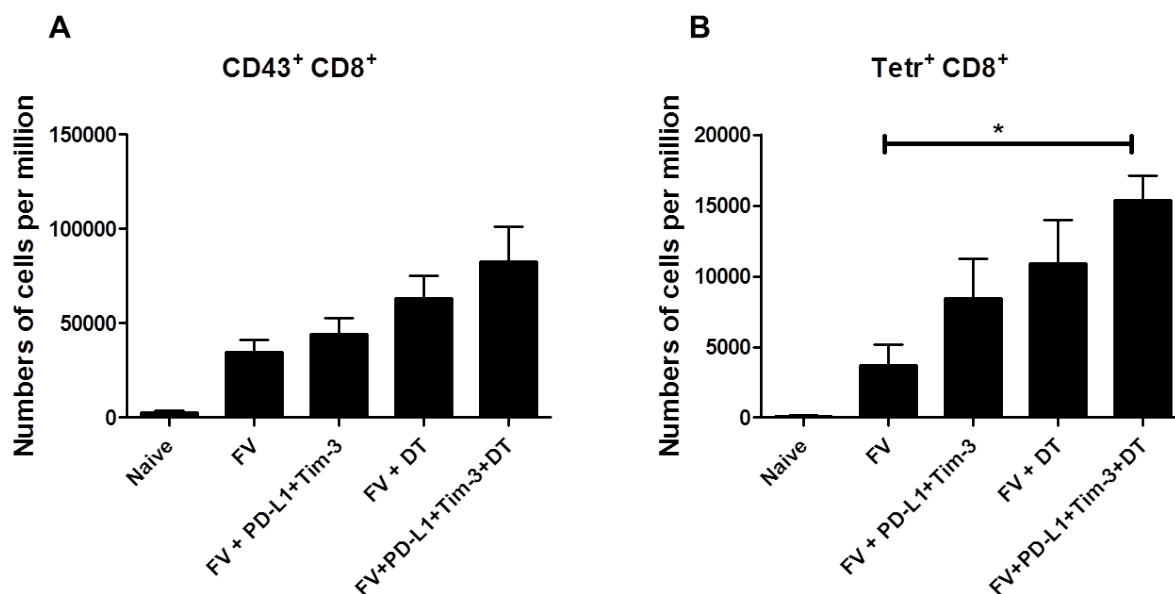
Figure 5.7 CD8$^+$ T cell responses during acute FV infection after Treg depletion combined with αPD-L1 and αTim3 treatment.

DEREG mice were infected with FV + LDV, treated with DT, αPD-L1, αTim3 in combination or alone, or left untreated. Numbers of (A) CD43$^+$ CD8$^+$ and (B) CD8$^+$Tetramer$^+$ of one million spleen cells at 14 dpi are displayed. At least five mice per group from three independent experiments were analyzed. Bars represent the mean and SEM. For statistical analysis, an ANOVA multiple comparison test was carried out (* < 0.05, ** < 0.005).

To investigate the immune response during combinatorial treatment, we had a closer look at different populations of T cells. Frequencies of activated CD8$^+$ T cells increased upon treatment, reaching the highest values during combination treatment at more than 80 000 CD43$^+$ CD8$^+$ cells per million, however, the difference to only FV infected mice was not significant (Figure 5.7 B). After combination treatment, we were also able to observe increased frequencies of virus-specific CD8$^+$ T cells in comparison to the group of only infected mice. Even

though the results for the combination therapy group were not significantly different compared to the groups with single treatment they always had the highest values (Figure 5.7 A). Further, the cytotoxic effector function of T cells was of interest. Combination therapy significantly increased the percentage of GzmB$^+$ CD8$^+$ T cells in comparison to all other groups, reaching up to 40% of all CD8$^+$ spleen cells. Similarly, we observed a very strong increase in the percentage of GzmB$^+$ CD4$^+$ T cells after combination treatment during acute FV infection. Thus, the combination treatment resulted in augmented cytotoxic CD8$^+$ and CD4$^+$ T cell response.
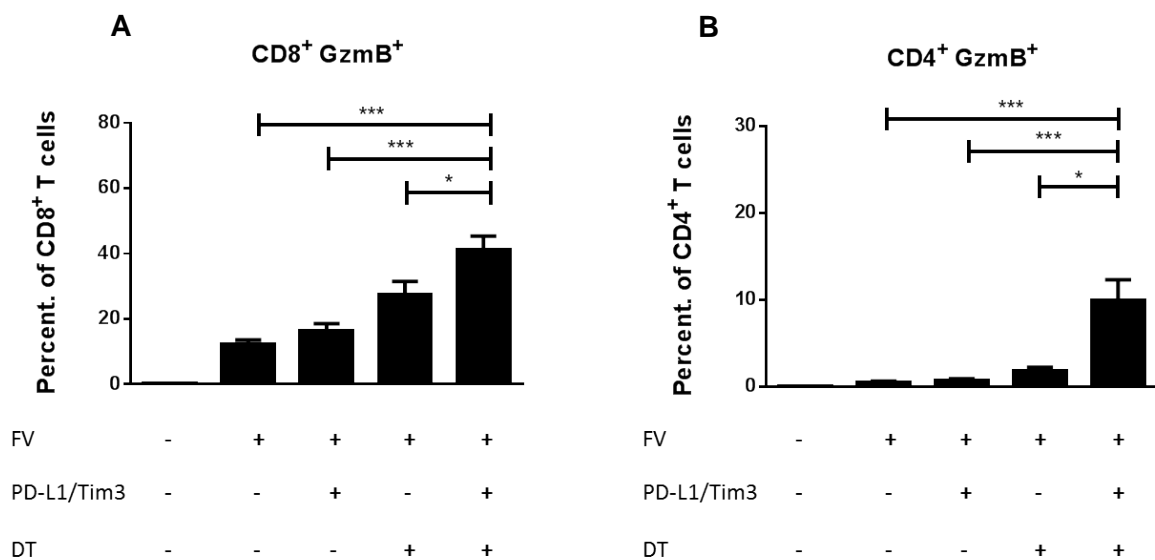

Figure 5.8 Percentage of CD8$^+$GzmB$^+$ and CD4$^+$GzmB$^+$ T cells after Treg depletion combined with αPD-L1 and αTim3 treatment during FV infection.

DEREG mice were infected with FV + LDV, treated with DT, αPD-L1, αTim3 in combination or alone, or left untreated. The frequencies of (A) GzmB$^+$ CD8$^+$ and (B) GzmB$^+$ CD4$^+$ from spleen cells at 14 dpi are displayed. At least five mice per group from three independent experiments were analyzed. Bars represent the mean and SEM. For statistical analysis, an ANOVA multiple comparison test was carried out (* < 0.05, ** < 0.005).

5.4 Combined depletion of Tregs and PD-L1 and Tim3 blocking leads to massive expansion of MDSC

During combination treatment for depletion of Tregs and blocking of PD-L1 and Tim3 during acute FV infection an expansion of potentially cytotoxic CD8$^+$ and CD4$^+$ T cells was observed. As MDSC may try to counter-regulate these T cell responses MDSC populations were analyzed in the spleen and small intestine after combination therapy. On day 18 post FV + LDV infection, an expansion of mMDSCs and gMDSCs was observed which was most predominant after combination treatment. Only for mMDSC in the spleen the expansion was similar between mice that received combination therapy and those that were only Treg depleted (Figure 5.9 A and B). In the small intestine the expansion of both MDSC populations after combinatorial treatment was most dramatic (Figure 5.9 C).
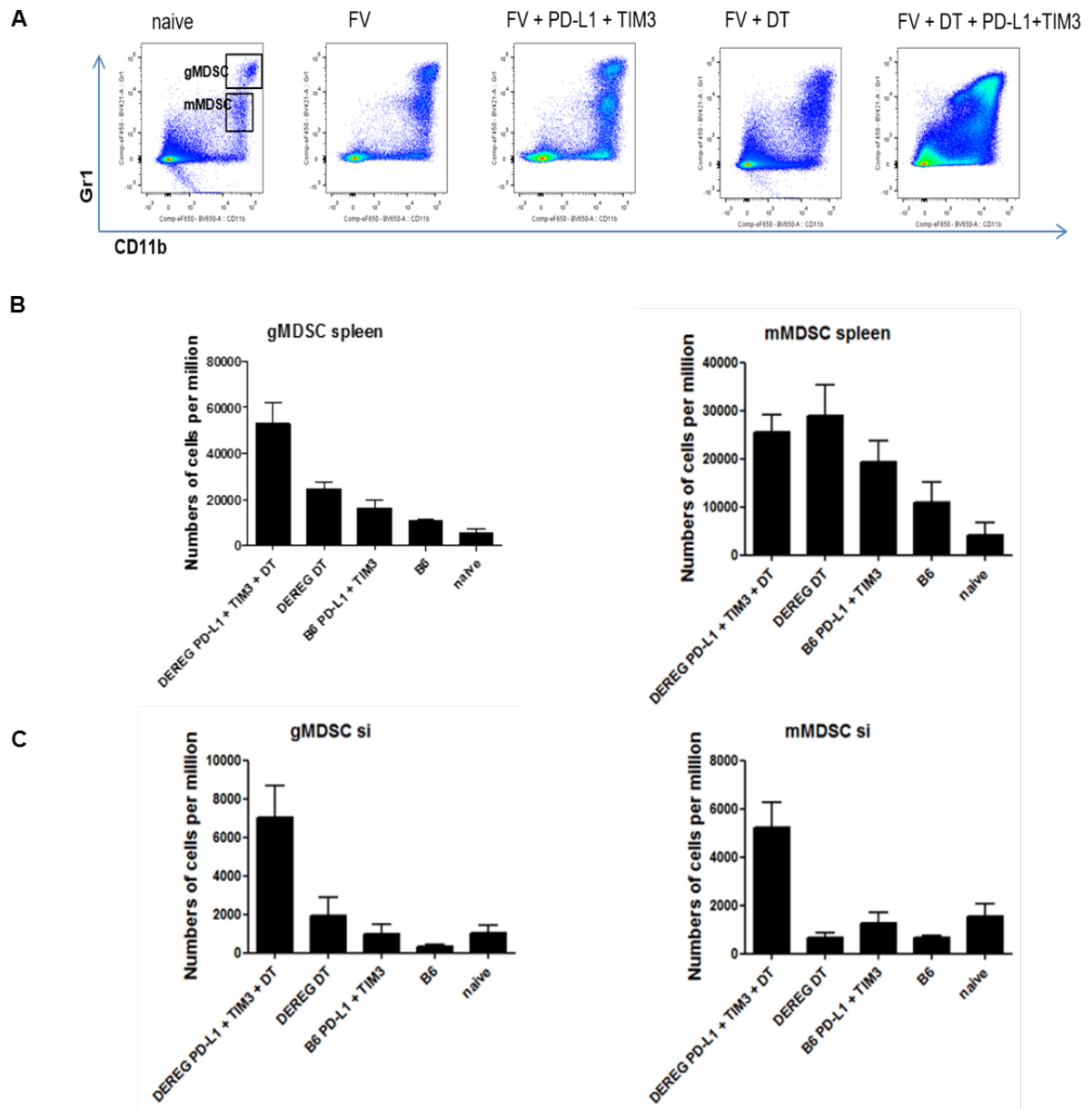
Figure 5.9 MDSC expansion after Treg depletion combined with αPD-L1 and αTim3 treatment.

DEREG mice were infected with FV + LDV, treated with DT, αPD-L1, αTim3 in combination or alone, or left non-treated. (A) Representative dot plots of splenic gMDSCs and mMDSCs are displayed. The numbers of gMDSCs and mMDSCs of (B) spleen and (C) small intestine are displayed. At least five mice per group from three independent experiments were analyzed. Bars represent the mean with SEM. For statistical analysis, an ANOVA multiple comparison test was carried out with the group of naïve mice as a reference (* < 0.05, ** < 0.005).

The gMDSCs that expanded during combination treatment were further analyzed for activation and functional markers. The percentages of CD80^{+} gMDSC after combination treatment were significantly higher compared to FV-infected mice, reaching over 60% of all MDSCs. No significant difference was found for PD-L1[high] and Arg1 expression of gMDSCs between the groups (Figure 5.10).

Treatment by depletion of Treg and blocking of αPD-L1 and αTim3 may result in the expansion of MDSCs, as a compensatory mechanism to counter-regulate T cell responses
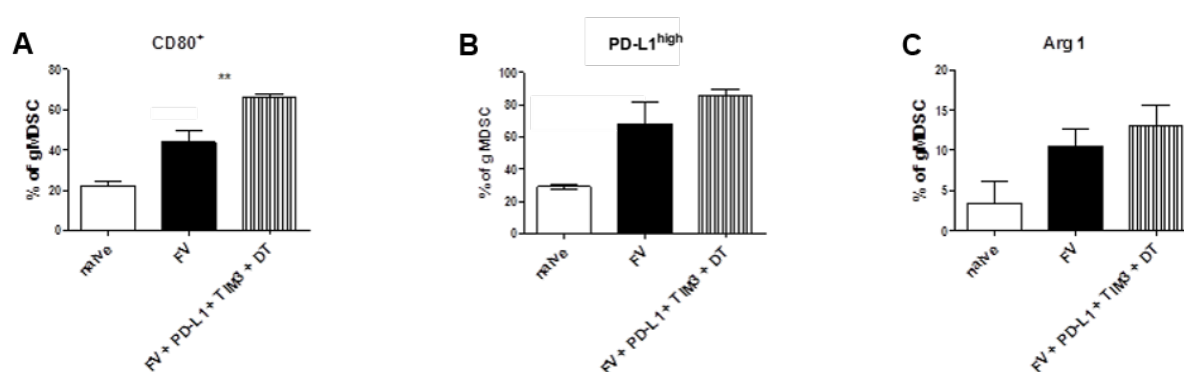

Figure 5.10 Characterization of gMDSCs after Tregs depletion combined with αPD-L1 and αTim3 treatment.
DEREG mice were infected with FV + LDV, treated with DT, αPD-L1, and αTim3 in combination or left untreated. Bars represent mean frequencies (with SEM) of CD80, PD-L1[high] and Arg1 expression of gMDSCs from spleen. For statistical analysis, an ANOVA multiple comparison test was carried out with the naïve group as a reference (** < 0.005).

5.5 Newly expanded population of MDSCs suppresses CD8 T cell responses

Interestingly, after combination treatment a new population of MDSCs was observed, expressing low levels of CD11b and Gr1 (Figure 5.11 A). For this experiment the spleen cells were pre-isolated with Cd19^{+} B cells (MACS technology) from mice treated with DT, αPD-L1 and Tim3. The cells were sorted on the basis of FITC and APC fluorescence. The separation of the Gr1^{high} CD11b^{+}

and Gr1$^+$ CD11b^{dim} cells was performed on a FACSDiVa cell-sorter (Becton Dickinson, San Jose, CA). Gr1 was excited with a 488 nm laser wavelength and fluorescence was measured through a 585/42 nm bandpass filter. CD11b was excited with a 650nm laser wavelength and fluorescence was measured through a 694/42 nm bandpass filter For each experiment 200.000–330.000 cells were sorted by flow cytometry.

After the separation of the cells the purity of the separated cell populations was always analyzed again by flow cytometric analysis of 10.000 cells. To >95% pure populations of Gr1^{high} CD11b$^+$ or Gr1$^+$ CD11b^{dim} cells was achieved. The cells were then and co-incubated with CD8$^+$ T cells in the previously described suppression assay in different effector target ratios. Interestingly, we observed that CD8$^+$ T cell proliferation was already suppressed by a lower ratio of the CD11b^{dim} population in comparison to gMDSCs (Figure 5.11 B). This may suggest that the absence of other inhibitory mechanisms results in the compensatory appearance of a new CD11b^{dim} population of MDSCs with higher suppressor functions.
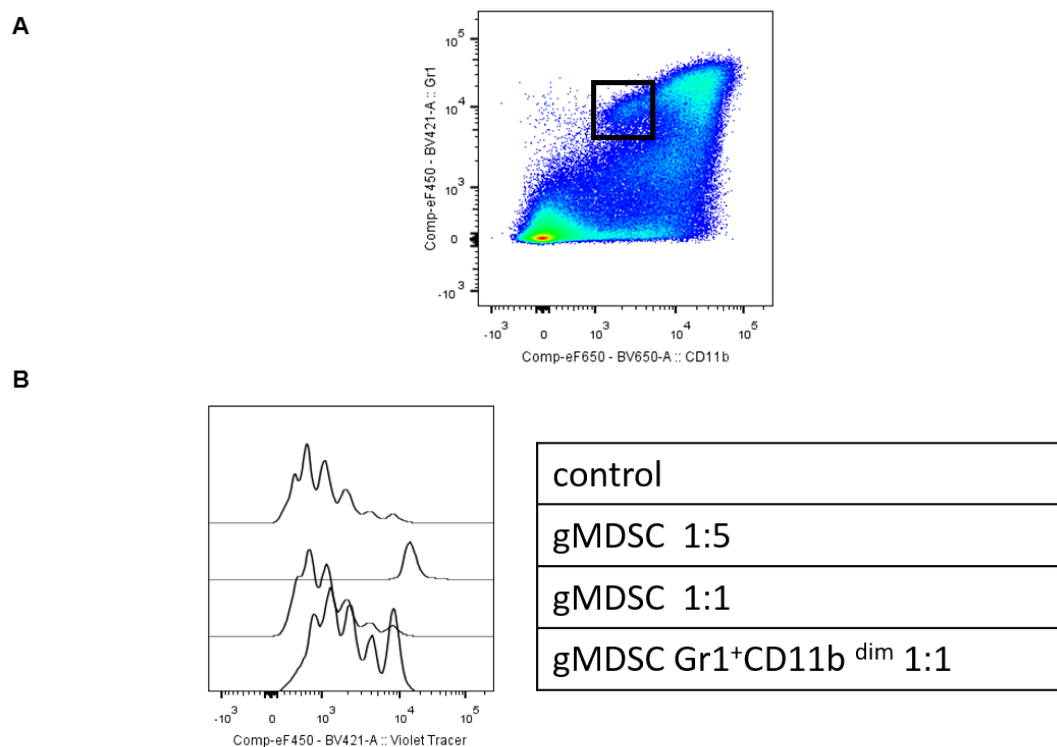
A

B

| control |
| gMDSC 1:5 |
| gMDSC 1:1 |
| gMDSC Gr1$^+$CD11b ^{dim} 1:1 |

Figure 5.11 Newly expanded Gr1$^+$ CD11b^{dim} population suppressed CD8$^+$ T cell proliferation.

CD8$^+$ T cells isolated from TCRtg mice were incubated with dendritic cells loaded with MHC class I-restricted FV-specific CD8$^+$ T cell epitope peptide and co-incubated with Gr1$^+$ CD11b^{dim} or gMDSCs isolated from DEREG mice infected with FV + LDV, treated with DT, αPD-L1, and αTim3 in combination. (A) A representative dotplot of Gr1$^+$ CD11b^{dim} after treatment with DT, αPD-L1 and αTim3 isolated at day 18 post FV infection. (B) Representative histograms for CD8$^+$ T cell proliferation after co-incubation with Gr1$^+$ CD11b^{dim} or gMDSCs at different ratios to CD8$^+$ T cells. As a control group CD8$^+$ cells without gMDSCs were used.

In current work we show a compensatory response of different inhibitory mechanisms during an acute retroviral infection. The depletion of one of inhibitory mechanism resulted in the expansion and increased activation of different inhibitory mechanism. Results presented in this thesis show the importance of inhibitory mechanisms in the immune response against retroviral infection.

6. Discussion

Myeloid derived suppressor cells play an important role in regulating the immune response. Their influence may be beneficial, as they limit immune responses in order to prevent tissue damage via cell cytotoxicity. On the other hand, they may be suppressing immune responses against retroviral infections, which results in inability to completely eliminate the virus and, consequently, establishment of chronicity (40). The exact mechanisms controlling the impact of MDSCs on different cell types are not fully understood. Therefore, it is of immense importance to define the mechanisms and functions of MDSCs in order to find a better way to modulate immune responses, and to further develop immunotherapies for retroviral infections.

The work presented in this thesis demonstrates the influence of MDSCs on cytotoxic CD8^{+} T cells during an acute FV infection. MDSCs expanded during the late phase of acute FV infection (Figure 4.1), which was correlated with CD8^{+} T cell dysfunction (27). Additionally, we found suppression of FV-specific, cytotoxic CD8^{+} T cells by the gMDSC subpopulation (Figure 4.12). We also showed the important role of PD-L1 and arginase in the suppression process. Finally, we observed interplays between different inhibitory mechanisms, such as Tregs and inhibitory receptors and their ligands. Moreover, blocking of these two mechanisms resulted in the expansion of MDSCs with a new CD11b^{dim} phenotype, which showed strong suppressive activity against CD8^{+} T cell proliferation.

Under normal conditions, common precursors of myeloid cells develop into mature myeloid cells. Under pathological conditions, these cells may not fully mature and start to develop inhibitory functions. This population of immature myeloid cells showing robust suppressive activity is known as MDSCs (41, 45,). Since MDSC is a recently discovered population, studies upon these cells are controversially discussed and various aspects, including phenotypic and functional characterization differ depending on experimental models (39, 47, 52). The commonly used gating strategy for murine MDSCs is based on co-expression of the markers CD11b and Gr1. The subpopulations of MDSCs, monocytic and granulocytic, are distinguished by high or dim expression of the Gr1 marker. Initially, identification by these two markers was useful. However, exact

characterization of mMDSCs and gMDSCs may encounter obstacles due to the blurred line between high and low expression of Gr1 in these two populations. In order to more precisely distinguish the gMDSC and mMDSC population, use of two Gr1 epitopes: Ly6C and Ly6G was proposed: gMDSCs are defined as $CD11b^+$ $Ly6G^+$ and $Ly6C^-$, and mMDSCs are characterize as $CD11b^+$ $Ly6G^-$ $Ly6C^+$. The Gr1 marker was used by several groups together with Ly6C and Ly6G in one panel. However, simultaneous use of the Gr1 and Ly6G may lead to incorrect MDSCs numbers due to competition of specific antibodies for Gr1 epitopes (121). One difficulty is the correct characterization of MDSCs, since they share many markers with other cell types, especially myeloid precursor cells and neutrophils (45, 46). gMDSCs share an important marker with neutrophils, which is Ly6G. This may cause difficulties in distinguishing both populations (46). Neutrophils are classically described as a short-lived, homogenous cell type and their role is restricted to the elimination of pathogens during the innate immune response. In numerous publications, gMDSC populations are called neutrophil like MDSCs (21) or MDSCs like neutrophils (20, 21), indicating their similar, if not identical characteristics.

In this study we characterize MDSCs by using antibodies against $CD11b^+$, $Ly6G^+$ and $Ly6C^+$. It was also of importance to distinguish MDSC subpopulations, since it has been shown that they possess distinct functions. MDSCs were also characterized by PD-L1, CD80, as well as functional markers Arg1 and NOS2. The described strategy allows to precisely distinguish the MDSC subtypes in mice. Only in experiments with combination therapy, due to appearance of $CD11b^{dim}$ population, the $Gr1^+CD11b^+$ strategy was used. Additionally, to correctly define the MDSC populations it is important to assess their suppressive activity, as well as biochemical and molecular markers described for MDSCs. Thanks to this attempt one may be sure the correct population of MDSCs is characterized.

Expansion of MDSCs was previously observed in various experimental models. Recent studies suggest that MDSC may serve as a prognostic marker for disease progression in various cancer models as well as during viral infections. The main aim of this thesis was to characterize MDSC during an acute retroviral infection of mice. In this study we could show an expansion of gMDSCs on day 14 post

infection and of mMDSCs between day 12-14 post infection (Figure 4.1). Elevation of MDSC numbers was also observed in blood of chronic HCV patients (54, 87, 105, 159), as well as during human (53, 104, 143) and murine HBV infection (29). The total MDSC population as well as only gMDSCs was shown to be increased in numbers in HIV infection (5, 110, 142).

Chronic infections expand MDSCs with immune suppressive activity, as T cell responses were found to be suppressed by MDSC in HIV, HBV and HCV infection (47-49). Most studies conducted in viral infections evaluated the whole $Gr1^+CD11b^+$ MDSCs population, without distinguishing between different subpopulations (5, 142). However, the effects of MDSC subpopulations on immune responses may vary significantly. The question remained which subpopulation of the MDSCs is mainly involved in restricting T cell responses in retroviral infections. Our current study demonstrates the suppressive impact of gMDSCs on $CD8^+$ T cells in acute Friend virus infection, whereas mMDSCs were less effective. In contrary to our findings, mMDSCs were able to suppress the T and B cell response in a model of murine LP-BM5 retrovirus infection (63,64). The different results might be explained by technical differences in the T cell proliferation assay used in both studies. While we stimulated virus-specific T cells with its cognate antigen presented by DCs, a physiological way of inducing T cell proliferation and differentiation, Robertson et al., used a non-specific stimulation of T cells with CD3 and CD28. It was already reported that mMDSCs mainly suppress polyclonally activated T cells, as shown in tumor models (184) and in different infections such as LP-BM5, LCMV, HBV, HCV (46-49). On the other hand antigen-specific suppression of T cells was associated with gMDSCs function (183). Thus, gMDSCs may have a significant influence on disease progression in various cancer diseases, including multiple melanoma (149), hepatic inflammation and fibrosis (155), and in HIV infection (142).

An activation of MDSCs has been associated with expression of different molecules. CD80, PD-L1, CD73, CD39, CD270, CD62L are just a few markers which were shown to be expressed on the cell surface of MDSCs and were linked to an activation of these cells (45-52). In the current study we analyzed the

expression of PD-L1 and CD80 as markers associated with the activation of MDSCs. An upregulated PD-1 expression on virus-specific CD8$^+$ T cells in chronically infected mice was shown to be involved in the development of CD8$^+$ T cell dysfunction. It has previously been shown that the ligand PD-L1 is expressed on the cell surface of activated MDSCs and might be associated with their suppressive potential (20). Both gMDSCs and mMDSCs showed an increased expression of PD-L1 upon FV infection (Figure 4.3). These results may be associated with the suggested role of the PD-1/PD-L1 pathway in MDSC-mediated immunosuppression. This possibility was proposed in various diseases, e.g. multiple melanoma (116) as well as in HIV (140). Vollbrecht et al. illustrated the role of PD-1/PD-L1 signaling in suppression mediated through HIV expanded gMDSC (43). The functional role of PD-L1 in MDSCs mediated CD8$^+$ T cell suppression was determined in an in an *in vitro* analysis of CD8$^+$ T cell proliferation. MDSCs used for this study lacked PD-L1, and were not able to suppress CD8+ proliferation as efficiently as gMDSCs expressing PD-L1 control group (Figure 4.15). However, more studies are required to determine the exact role of PD-L1 in MDSC mediated immunosuppression.

CD80 was analyzed as an additional marker associated with MDSC activation and suppression. Expression of CD80 on MDSCs increased during FV infection (Figure 4.3). There are two different receptors for CD80, which differ in functionality. Binding of CD80 to the co-stimulatory receptor CD28, together with the T cell receptor (TCR)-CD3 complex, may generate cell-activating signal. CD28 is expressed predominantly on naïve and early activated T cells. On the other hand, the binding of CD80 to CTLA-4 may deliver inhibitory signals. CTLA-4 is expressed by subset of late- and post-activated T lymphocytes (93, 147). CD80 was shown to be a possible inhibitory mechanism involved in T cell suppression, e.g. in Cutaneous T cell Lymphoma (172). The importance of CD80 in MDSC function was suggested in 2008 in melanoma studies (153) and was confirmed in the following years (58-59). In our study we found increased frequencies of CD80 expressed on mMDSC and gMDSC, however the exact role of CD80 in MDSC mediated immunosuppression should be closer characterized.

The phenotypic characterization of MDSCs can be challenging, therefore their functional properties should be the focus of attention. In the current work, MDSCs were functionally characterized by the expression of NOS2 and Arg1, as well as by the use of a virus-specific T cell proliferation assay. Expression of NOS2 increased only in mMDSCs, but not in gMDSCs. Arg1 expression increased in both gMDSCs and mMDSCs upon FV infection (Figure 4.3). These two important mechanisms of MDSC mediated immunosuppression are connected to ʟ-arginine metabolism. Both arginase and NO inhibitors were used in the current study in order to confirm the mechanism of gMDSC mediated immunosuppression of CD8$^+$ T cells. Both, L-NMMA, as well as nor-NOHA, partially restored the CD8$^+$ T cell proliferation in vitro. Although the NO inhibitor was able to partially restore the gMDSC mediated suppression of CD8$^+$ T cell proliferation, our previous results showed no expression of NOS2 on gMDSCs (Figure 4.4). However, it is important to note the existence of two different enzymes involved in to nitric oxide metabolism: NOS1 and NOS3 (173). The expression and activity of NOS3 was reported to play a role in gMDSC function in the murine model of malignant tumors (174). Thus, NOS3 might also be involved in suppression by virus induced gMDSCs, which has not been studied so far.

Adenosine metabolism with the two cell-surface enzymes CD39 and CD73 is involved in the regulation of T cell responses (18). Their significance in Treg mediated immunosuppression (17) has been demonstrated. During FV infection both CD39 and CD73 were expressed on the cell surface of MDSCs. However, the level of expression did not differ between MDSCs from infected and uninfected mice (Figure 4.4). It has been shown that the activity of CD39, but not of CD73, has been important in MDSCs-mediated immunosuppression of T cells *in vitro* in the murine melanoma model (38). However, this has not been investigated in viral infections so far. In this study, we were able to demonstrate that CD39 contributed to the MDSC mediated suppression of CD8$^+$ T cell proliferation *in vitro* in retroviral infection (Figure 4.15).

Different attempts to study the function of MDSCs *in vivo* have been presented. First, transfer experiments were performed, in which freshly isolated,

lipopolisaccharid (LPS) or IFNγ induced MDSCs were transferred into recipient mice. This attempt was shown to inhibit inflammation (147) and reduce CD8+ T cell responses in a melanoma model (128). Another approach to study the function of MDSCs *in vivo* is a specific depletion of these cells. There are different ways to modulate MDSC by reduction of numbers or blockade of the function of MDSCs *in vivo*. The most commonly used way of depletion is by administrating αLy6G or αGr1 antibodies into mice. This procedure allows the efficient depletion of all MDSCs (αGr1 antibody) or of granulocytic MDSCs only (αLy6G antibody). Nevertheless, as lately shown, long term administration of either αGr1 or αLy6G antibody leads to reappearance of immature Ly6G$^+$ cells (45).

The modulation of immune responses offers promising results for the therapy of different diseases, including cancer and viral infections. As a recently observed population, MDSCs give encouraging prospects for future treatments of viral infections. Different methods were described to deactivate or deplete MDSCs, as well as differentiate them into mature cells or block their development (44-50). Many of these agents, like 5-Fluorouracil (5FU), ATRA, PDE-5 inhibitors, NO-aspirins, CSF-1R inhibitors, Zoledronic Acid, JAK/STAT3 inhibitors and Multi-Kinase inhibitors, as well as VEGF inhibitors, are already under clinical investigation in cancer treatment (46). Nonetheless, it is important to note the influence of these immunomodulatory methods on different immune cells. Moreover, different therapeutic drugs already used in the clinic for treatment of various diseases, such as cytotoxic agents, vitamins or modulators of the cell signaling, are shown to regulate MDSCs (46). Similarly, different medicaments were described to interfere with different immune cells and have an influence on the immune response (161). Therefore, it is of immense importance to carefully plan and apply a combination of different therapies in order to achieve possible therapeutic success without overstimulating and burdening the immune system .

In the current study, MDSC function was investigated by using αLy6G antibody, which selectively depletes gMDSC, and the use of 5FU, an anti-cancer drug known for selectively depleting all MDSCs. Both αLy6G and 5FU administration resulted in the depletion of MDSCs and led to an expansion of activated CD8$^+$ T cells and Tregs. Although both depletion attempts have proven to be MDSC

specific, it is important to note that αLy6G is also used for the depletion of neutrophils, and that 5FU appears to be cytotoxic in higher concentration. Therefore, further studies and different immunomodulation attempts are necessary to precisely investigate MDSCs *in vivo*.

The current study shows the interaction between MDSCs and Tregs during acute retroviral infection. Depletion of MDSCs resulted in an increased Treg expression, whereas Treg depletion led to growth of MDSCs numbers (Figure 5.2). Interaction between MDSCs and Tregs was first suggested by Yang et al in 2006 in an ovarian cancer model (152). Two years later, Borello and colleagues observed that MDSCs may induce Treg expansion, and MDSC depletion led to a suppressed Treg proliferation in the B cell lymphoma model (153). Since then several of studies have been investigating the interactions between MDSCs and Tregs. Most of them confirm the expansion of Tregs, as well as their *de novo* generation by MDSCs, through TGFβ dependent and independent mechanisms. (154-158). In viral infections the interaction between MDSCs and Tregs was observed so far in HCV (161), HBV (142) and murine retrovirus induced immunodeficiency (162). HCV induced mMDSCs from PBMCs led to the expansion of Tregs *in vitro* and the depletion of mMDSCs resulted in the reduction of Tregs in PBMCs *(*107).

Inhibitory mechanisms are used by our organisms to maintain immune homeostasis. Without them, over-activation of cytotoxic cells may appear, causing tissue damage and organ failure. However, cancer and chronic infections may benefit from different suppressive mechanisms. One of the approaches used in this study is the combination treatment blocking different inhibitory mechanisms: inhibitory receptors and their ligands, as well as Tregs. The depletion of PD-L1, Tim3 and Tregs resulted in reduced viral loads (Figure 5.6) and an increased production of cytotoxic granula in T cells (Figure 5.7). Distinct studies involving combinational treatment by blocking different inhibitory mechanisms exhibit beneficial influence on the disease (19). It has been shown that the immune checkpoint blockade is a possible, effective way of treating cancer (61-65). Combination treatment blocking different checkpoint inhibitors resulted in a reduction of tumor size and an enhanced immune response in cancer patients (93). Inhibitors of PD-1 and CTLA-4 as a combination treatment were used in a

phase 3 clinical trial of melanoma therapy (138), as well as of metastatic renal cell carcinoma (160) with promising results. Further promising findings came e.g. from the cancer field, where combining radiation therapy with dual checkpoint blockade of melanoma (138) resulted in an enhanced T cell response and reversed CD8$^+$ T cell exhaustion. Surprisingly, the model of combination therapy by Treg depletion combined with dual blockade of inhibitory receptors presented in this work was shown to reduce viral loads and restore CD8$^+$ T cell cytotoxicity during chronic FV infection (138). It is worth mentioning that in both of these studies blocking of αPD-L1 was used as one of the immune checkpoint treatments. Interestingly, the level of PD-L1 on the cell surface had an influence on therapy outcome during αCTLA-4 treatment. When the level of PD-L1 on the cell surface during αCTLA-4 treatment combined with radiation of melanoma tumor was high, CD8$^+$ T cell functionality was not recovered. However, by addition of αPD-L1 antibody, its CD8$^+$ T cell function was further restored (138).

Finally, for the first time to our knowledge, we were able to show that the population of Gr1$^+$ CD11b^{dim}, isolated from mice treated with DT, αPD-L1, αTim3 expanded during FV infection (Figure 5.11). Proliferation of CD8$^+$ was suppressed by a lower number of Gr1$^+$ CD11b^{dim} cells compared to gMDSCs. Thus, these data suggest the appearance of a new Gr1$^+$ CD11b^{dim} MDSC subset, and the expansion of MDSCs during combination treatment may be a compensatory mechanism for blocking other inhibitory mechanisms to prevent tissue damage during acute retroviral infection. The newly described Gr1$^+$ CD11b^{dim} population will be further characterized.

The FV infection of mice used in the current study is a good model to analyze retroviral infections in general. HIV infection of humans still presents a major threat to the world population. Even though current therapies of retroviral infections are effective in controlling viral replication, the virus cannot be completely eliminated. Therefore, it is important to develop possible immunotherapies of retroviral infections. The approach used in this study was focused on one of the inhibitory mechanisms that restrict retrovirus-specific immunity: MDSC. It has already been shown that MDSCs expand during HIV infection (127, 142). Enhanced numbers of MDSCs in patient blood were associated with a chronic progressive phase of HIV

infection (110). mMDSCs have been reported to expand in PBMCs from healthy volunteers incubated with HIV-1 proteins (gp120 or Tat) or the TLR4 ligand LPS in vitro (142). Targeting different subtypes of myeloid cells, including MDSCs, was suggested to be a new, promising approach for immunotherapy of HIV (142).

Consequently, the results of this thesis suggest that MDSCs might be a possible target for the future treatment of retroviral infections, providing new important information about the interaction between different regulatory mechanisms and MDSCs.

7. Summary

A recently observed population of myeloid-derived suppressor cells (MDSCs) restrains the T cell immune response by showing robust suppressive activity. The inhibitory influence of MDSCs was observed in different tumor diseases. First attempts to describe MDSCs in infectious diseases were conducted. Nonetheless, the role of these cells during viral infection is not fully understood.

Friend virus is a good model to study both acute and chronic retroviral infections. In the FV model, similar to the Human Immunodeficiency Virus (HIV) or Hepatitis C Virus (HCV) infections, cytotoxic virus-specific $CD8^+$ T Lymphocytes (CTLs) efficiently control acute virus infections but become exhausted when a chronic infection develops.

The data presented in this thesis evidences the influence of myeloid derived suppressor cells on cytotoxic $CD8^+$ T cells during acute Friend Virus infection. Two populations of MDSCs, granulocytic MDSCs (gMDSCs) and monocytic MDSCs (mMDSCs), are expanding during the late phase of acute FV infection, which may be correlated with the $CD8^+$ T cell contraction. Additionally, the *in vivo* elimination of the expanded population of granulocytic MDSCs shows the suppressive influence of these cells on $CD8^+$ T cell proliferation and their production of cytotoxic granules. This effect may be mediated by several mechanisms, as proven *in vitro*, such as PD-L1, arginase, nitric oxide and CD39. Furthermore, possible compensatory interactions between different inhibitory mechanisms, such as myeloid derived suppressor cells, T regulatory cells, and inhibitory receptors/ligands were observed. Finally, the elimination of two important immune regulatory mechanisms after the depletion of T regulatory cells, and blocking of PD-L1 and Tim3 resulted in an expansion of myeloid derived suppressor cells with appearance of the new $CD11b^{dim}$ population of cells. The newly revealed population was showing strong suppressive activity against $CD8^+$ T cells during acute retroviral infection.

Myeloid derived suppressor cells play an important role in the regulation of the immune response. Thus, the results presented in this thesis show the inhibitory

role of myeloid derived suppressor cells in the Friend virus infection and may be a possible target for the immune therapy of retroviral infections.

8. Zusammenfassung

Myeloide Suppressorzellen (MDSCs) wurden vor kurzem auf Grund ihrer Suppression von T-Zellen identifiziert. Der inhibitorische Einfluss von MDSCs wurde in verschiedenen Tumorerkrankungen beobachtet. Die Funktion dieser Zellen während der viralen Infektion ist jedoch bis heute nicht vollständig verstanden.

Das Friend Virus Mausmodell eignet sich sowohl für die Untersuchung der akuten als auch der chronischen retroviralen Infektion. Ähnlich wie bei Infektionen mit dem Humanen Immundefizienz-Virus (HIV) oder Hepatitis-C-Virus (HCV), bekämpfen zytotoxische virus-spezifische $CD8^+$ T-Lymphozyten (CTLs) die akute Virusinfektion, wohingegen sie während der chronischen Infektion dysfunktional sind.

Insgesamt wurde in dieser Doktorarbeit der Einfluss von Myeloiden Suppressorzellen auf zytotoxische $CD8^+$ T-Zellen während der akuten Friend Virus Infektion untersucht. Zwei Populationen von MDSCs, granulozytäre MDSCs (gMDSCs) und monocytäre MDSCs (mMDSCs) werden während der späten Phase der akuten FV Infektion expandiert, was mit einer $CD8^+$ T-Zell-Kontraktion korreliert. Eine Population der MDSCs, die Granulozytären MDSCs, zeigen einen suppressiven Einfluss auf die $CD8^+$ T-Zell-Proliferation und die Produktion von zytotoxischen Granula *in vivo*. Dieser Effekt kann durch verschiedene Mechanismen modelliert werden, wie beispielsweise PD-L1, Arginase, Stickstoffmonoxid oder CD39. Die Interaktion zwischen verschiedenen hemmenden Mechanismen, wie Myeloide Suppressorzellen, regulatorischen T-Zellen und inhibitorischen Rezeptoren und Liganden während der akuten FV Infektion wurde beobachtet. Die Elimination von zwei wichtigen immunregulatorischen Mechanismen führte nach Depletion der regulatorischen T-Zellen und der Blockierung von PD-L1 und TIM3 zur Expansion der Myeloiden Suppressorzellen und einer neuen, durch $CD11b^{dim}$ charakterisierten Population, die starke supprimierende Effekte gegenüber $CD8^+$ T-Zellen zeigt.

Myeloide Suppressorzellen spielen eine wichtige Rolle bei der Regulation der Immunantwort. Die in dieser Arbeit vorgestellten Ergebnisse, d. h. die hemmende

Rolle von Myeloide Suppressorzellen während der akuten Friend Virus Infektion, können als Ansatz für eine Immuntherapie retroviraler Infektionen verwendet werden.

References:

1.   **Akhmetzyanova I, Drabczyk M, Neff CP, Gibbert K, Dietze KK, Werner T, Liu J, Chen L, Lang KS, Palmer BE, Dittmer U, and Zelinskyy G**. PD-L1 Expression on Retrovirus-Infected Cells Mediates Immune Escape from CD8+ T Cell Killing. *PLoS Pathog* 11: e1005224, 2015.
2.   **Akkina RK, Walton RM, Chen ML, Li QX, Planelles V, and Chen IS**. High-efficiency gene transfer into CD34+ cells with a human immunodeficiency virus type 1-based retroviral vector pseudotyped with vesicular stomatitis virus envelope glycoprotein G. *J Virol* 70: 2581-2585, 1996.
3.   **Altman JD, Moss PA, Goulder PJ, Barouch DH, McHeyzer-Williams MG, Bell JI, McMichael AJ, and Davis MM**. Phenotypic analysis of antigen-specific T lymphocytes. *Science* 274: 94-96, 1996.
4.   **Anthony DD, Umbleja T, Aberg JA, Kang M, Medvik K, Lederman MM, Peters MG, Koziel MJ, and Overton ET**. Lower peripheral blood CD14+ monocyte frequency and higher CD34+ progenitor cell frequency are associated with HBV vaccine induced response in HIV infected individuals. *Vaccine* 29: 3558-3563, 2011.
5.   **Anthony DD, Yonkers NL, Post AB, Asaad R, Heinzel FP, Lederman MM, Lehmann PV, and Valdez H**. Selective impairments in dendritic cell-associated function distinguish hepatitis C virus and HIV infection. *J Immunol* 172: 4907-4916, 2004.
7.   **Antunes I, Tolaini M, Kissenpfennig A, Iwashiro M, Kuribayashi K, Malissen B, Hasenkrug K, and Kassiotis G**. Retrovirus-specificity of regulatory T cells is neither present nor required in preventing retrovirus-induced bone marrow immune pathology. *Immunity* 29: 782-794, 2008.
8.   **Arina A, and Bronte V**. Myeloid-derived suppressor cell impact on endogenous and adoptively transferred T cells. *Curr Opin Immunol* 33: 120-125, 2015.
9.   **Arina A, Corrales L, and Bronte V**. Enhancing T cell therapy by overcoming the immunosuppressive tumor microenvironment. *Semin Immunol* 28: 54-63, 2016.
10.   **Balu DT, Hodes GE, Hill TE, Ho N, Rahman Z, Bender CN, Ring RH, Dwyer JM, Rosenzweig-Lipson S, Hughes ZA, Schechter LE, and Lucki I**. Flow cytometric analysis of BrdU incorporation as a high-throughput method for measuring adult neurogenesis in the mouse. *J Pharmacol Toxicol Methods* 59: 100-107, 2009.
11.   **Banchereau J, Briere F, Caux C, Davoust J, Lebecque S, Liu YJ, Pulendran B, and Palucka K**. Immunobiology of dendritic cells. *Annu Rev Immunol* 18: 767-811, 2000.
12.   **Barber DL, Wherry EJ, Masopust D, Zhu B, Allison JP, Sharpe AH, Freeman GJ, and Ahmed R**. Restoring function in exhausted CD8 T cells during chronic viral infection. *Nature* 439: 682-687, 2006.
13.   **Bazhin AV, von Ahn K, Maier C, Soltek S, Serba S, Diehl L, Werner J, and Karakhanova S**. Immunological in vivo effects of B7-H1 deficiency. *Immunol Lett* 162: 273-286, 2014.
14.   **Bengsch B, and Wherry EJ**. The importance of cooperation: partnerless NFAT induces T cell exhaustion. *Immunity* 42: 203-205, 2015.
15.   **Bergenfelz C, Larsson AM, von Stedingk K, Gruvberger-Saal S, Aaltonen K, Jansson S, Jernstrom H, Janols H, Wullt M, Bredberg A, Ryden L, and Leandersson K**. Systemic Monocytic-MDSCs Are Generated from Monocytes and Correlate with Disease Progression in Breast Cancer Patients. *PLoS One* 10: e0127028, 2015.

16.   **Bila C, Oberhauser V, Ammann CG, Ejaz A, Huber G, Schimmer S, Messer R, Pekna M, von Laer D, Dittmer U, Hasenkrug KJ, Stoiber H, and Banki Z**. Complement opsonization enhances friend virus infection of B cells and thereby amplifies the virus-specific CD8+ T cell response. *J Virol* 85: 1151-1155, 2011.

17.   **Bjoern J, Juul Nitschke N, Zeeberg Iversen T, Schmidt H, Fode K, and Svane IM**. Immunological correlates of treatment and response in stage IV malignant melanoma patients treated with Ipilimumab. *Oncoimmunology* 5: e1100788, 2016.

18.   **Bodogai M, Moritoh K, Lee-Chang C, Hollander CM, Sherman-Baust CA, Wersto RP, Araki Y, Miyoshi I, Yang L, Trinchieri G, and Biragyn A**. Immunosuppressive and Prometastatic Functions of Myeloid-Derived Suppressive Cells Rely upon Education from Tumor-Associated B Cells. *Cancer Res* 75: 3456-3465, 2015.

19.   **Bopp T, Becker C, Klein M, Klein-Hessling S, Palmetshofer A, Serfling E, Heib V, Becker M, Kubach J, Schmitt S, Stoll S, Schild H, Staege MS, Stassen M, Jonuleit H, and Schmitt E**. Cyclic adenosine monophosphate is a key component of regulatory T cell-mediated suppression. *J Exp Med* 204: 1303-1310, 2007.

20.   **Borsellino G, Kleinewietfeld M, Di Mitri D, Sternjak A, Diamantini A, Giometto R, Hopner S, Centonze D, Bernardi G, Dell'Acqua ML, Rossini PM, Battistini L, Rotzschke O, and Falk K**. Expression of ectonucleotidase CD39 by Foxp3+ Treg cells: hydrolysis of extracellular ATP and immune suppression. *Blood* 110: 1225-1232, 2007.

21.   **Bowers NL, Helton ES, Huijbregts RP, Goepfert PA, Heath SL, and Hel Z**. Immune suppression by neutrophils in HIV-1 infection: role of PD-L1/PD-1 pathway. *PLoS Pathog* 10: e1003993, 2014.

22.   **Bronte V, Brandau S, Chen SH, Colombo MP, Frey AB, Greten TF, Mandruzzato S, Murray PJ, Ochoa A, Ostrand-Rosenberg S, Rodriguez PC, Sica A, Umansky V, Vonderheide RH, and Gabrilovich DI**. Recommendations for myeloid-derived suppressor cell nomenclature and characterization standards. *Nat Commun* 7: 12150, 2016.

23.   **Buessow SC, Paul RD, and Lopez DM**. Influence of mammary tumor progression on phenotype and function of spleen and in situ lymphocytes in mice. *J Natl Cancer Inst* 73: 249-255, 1984.

24.   **Buonerba C, Di Lorenzo G, and Sonpavde G**. Combination therapy for metastatic renal cell carcinoma. *Ann Transl Med* 4: 100, 2016.

25.   **Burga RA, Thorn M, Point GR, Guha P, Nguyen CT, Licata LA, DeMatteo RP, Ayala A, Joseph Espat N, Junghans RP, and Katz SC**. Liver myeloid-derived suppressor cells expand in response to liver metastases in mice and inhibit the anti-tumor efficacy of anti-CEA CAR-T. *Cancer Immunol Immunother* 64: 817-829, 2015.

26.   **Cai W, Qin A, Guo P, Yan D, Hu F, Yang Q, Xu M, Fu Y, Zhou J, and Tang X**. Clinical significance and functional studies of myeloid-derived suppressor cells in chronic hepatitis C patients. *J Clin Immunol* 33: 798-808, 2013.

27.   **Cao Y, Feng Y, Zhang Y, Zhu X, and Jin F**. L-Arginine supplementation inhibits the growth of breast cancer by enhancing innate and adaptive immune responses mediated by suppression of MDSCs in vivo. *BMC Cancer* 16: 343, 2016.

28.   **Chae M, Peterson TE, Balgeman A, Chen S, Zhang L, Renner DN, Johnson AJ, and Parney IF**. Increasing glioma-associated monocytes leads to increased intratumoral and systemic myeloid-derived suppressor cells in a murine model. *Neuro Oncol* 17: 978-991, 2015.

29.   **Chen HM, Ma G, Gildener-Leapman N, Eisenstein S, Coakley BA, Ozao J, Mandeli J, Divino C, Schwartz M, Sung M, Ferris R, Kao J, Wang LH, Pan PY, Ko EC, and Chen SH**. Myeloid-Derived Suppressor Cells as an Immune Parameter in

Patients with Concurrent Sunitinib and Stereotactic Body Radiotherapy. *Clin Cancer Res* 21: 4073-4085, 2015.

30. **Chen S, Akbar SM, Abe M, Hiasa Y, and Onji M**. Immunosuppressive functions of hepatic myeloid-derived suppressor cells of normal mice and in a murine model of chronic hepatitis B virus. *Clin Exp Immunol* 166: 134-142, 2011.

31. **Chen W, Qin H, Chesebro B, and Cheever MA**. Identification of a gag-encoded cytotoxic T-lymphocyte epitope from FBL-3 leukemia shared by Friend, Moloney, and Rauscher murine leukemia virus-induced tumors. *J Virol* 70: 7773-7782, 1996.

32. **Chesebro B, Miyazawa M, and Britt WJ**. Host genetic control of spontaneous and induced immunity to Friend murine retrovirus infection. *Annu Rev Immunol* 8: 477-499, 1990.

33. **Cmarik J, and Ruscetti S**. Friend Spleen Focus-Forming Virus Activates the Tyrosine Kinase sf-Stk and the Transcription Factor PU.1 to Cause a Multi-Stage Erythroleukemia in Mice. *Viruses* 2: 2235-2257, 2010.

34. **Cullen JN, Yuan C, Totton S, Dzikamunhenga R, Coetzee JF, da Silva N, Wang C, and O'Connor AM**. A systematic review and meta-analysis of the antibiotic treatment for infectious bovine keratoconjunctivitis: an update. *Anim Health Res Rev* 17: 60-75, 2016.

35. **Darcy CJ, Minigo G, Piera KA, Davis JS, McNeil YR, Chen Y, Volkheimer AD, Weinberg JB, Anstey NM, and Woodberry T**. Neutrophils with myeloid derived suppressor function deplete arginine and constrain T cell function in septic shock patients. *Crit Care* 18: R163, 2014.

36. **De Sanctis F, Bronte V, and Ugel S**. Tumor-Induced Myeloid-Derived Suppressor Cells. *Microbiol Spectr* 4: 2016.

37. **De Sanctis F, Solito S, Ugel S, Molon B, Bronte V, and Marigo I**. MDSCs in cancer: Conceiving new prognostic and therapeutic targets. *Biochim Biophys Acta* 1865: 35-48, 2016.

38. **De Veirman K, Van Ginderachter JA, Lub S, De Beule N, Thielemans K, Bautmans I, Oyajobi BO, De Bruyne E, Menu E, Lemaire M, Van Riet I, Vanderkerken K, and Van Valckenborgh E**. Multiple myeloma induces Mcl-1 expression and survival of myeloid-derived suppressor cells. *Oncotarget* 6: 10532-10547, 2015.

39. **Deaglio S, Dwyer KM, Gao W, Friedman D, Usheva A, Erat A, Chen JF, Enjyoji K, Linden J, Oukka M, Kuchroo VK, Strom TB, and Robson SC**. Adenosine generation catalyzed by CD39 and CD73 expressed on regulatory T cells mediates immune suppression. *J Exp Med* 204: 1257-1265, 2007.

40. **Di Mitri D, Toso A, and Alimonti A**. Molecular Pathways: Targeting Tumor-Infiltrating Myeloid-Derived Suppressor Cells for Cancer Therapy. *Clin Cancer Res* 21: 3108-3112, 2015.

41. **Dietze KK, Zelinskyy G, Liu J, Kretzmer F, Schimmer S, and Dittmer U**. Combining regulatory T cell depletion and inhibitory receptor blockade improves reactivation of exhausted virus-specific CD8+ T cells and efficiently reduces chronic retroviral loads. *PLoS Pathog* 9: e1003798, 2013.

42. **Dittmer U, and Hasenkrug KJ**. Different immunological requirements for protection against acute versus persistent Friend retrovirus infections. *Virology* 272: 177-182, 2000.

43. **Dittmer U, He H, Messer RJ, Schimmer S, Olbrich AR, Ohlen C, Greenberg PD, Stromnes IM, Iwashiro M, Sakaguchi S, Evans LH, Peterson KE, Yang G, and Hasenkrug KJ**. Functional impairment of CD8(+) T cells by regulatory T cells during persistent retroviral infection. *Immunity* 20: 293-303, 2004.

44.   **Dittmer U, Race B, Peterson KE, Stromnes IM, Messer RJ, and Hasenkrug KJ**. Essential roles for CD8+ T cells and gamma interferon in protection of mice against retrovirus-induced immunosuppression. *J Virol* 76: 450-454, 2002.

45.   **Dolen Y, Gunaydin G, Esendagli G, and Guc D**. Granulocytic subset of myeloid derived suppressor cells in rats with mammary carcinoma. *Cell Immunol* 295: 29-35, 2015.

46.   **Draghiciu O, Boerma A, Hoogeboom BN, Nijman HW, and Daemen T**. A rationally designed combined treatment with an alphavirus-based cancer vaccine, sunitinib and low-dose tumor irradiation completely blocks tumor development. *Oncoimmunology* 4: e1029699, 2015.

47.   **Draghiciu O, Lubbers J, Nijman HW, and Daemen T**. Myeloid derived suppressor cells-An overview of combat strategies to increase immunotherapy efficacy. *Oncoimmunology* 4: e954829, 2015.

48.   **Draghiciu O, Nijman HW, Hoogeboom BN, Meijerhof T, and Daemen T**. Sunitinib depletes myeloid-derived suppressor cells and synergizes with a cancer vaccine to enhance antigen-specific immune responses and tumor eradication. *Oncoimmunology* 4: e989764, 2015.

49.   **Drake K**. Quality of life for cancer patients: From diagnosis to treatment and beyond. *Nurs Manage* 2012.

50.   **Dwyer KM, Deaglio S, Gao W, Friedman D, Strom TB, and Robson SC**. CD39 and control of cellular immune responses. *Purinergic Signal* 3: 171-180, 2007.

51.   **Enjyoji K, Sevigny J, Lin Y, Frenette PS, Christie PD, Esch JS, 2nd, Imai M, Edelberg JM, Rayburn H, Lech M, Beeler DL, Csizmadia E, Wagner DD, Robson SC, and Rosenberg RD**. Targeted disruption of cd39/ATP diphosphohydrolase results in disordered hemostasis and thromboregulation. *Nat Med* 5: 1010-1017, 1999.

52.   **Failli A, Legitimo A, Mazzoni A, Urbani L, Scatena F, Mosca F, and Consolini R**. The combination of immunosuppressive drugs with 8-methoxypsoralen and ultraviolet a light modulates the myeloid-derived dendritic cell function. *Int J Immunopathol Pharmacol* 24: 89-99, 2011.

53.   **Fan HZ, Yu HP, Yu R, Zhang Y, Deng HJ, and Chen X**. Passive transfer of lipopolysaccharide-derived myeloid-derived suppressor cells inhibits asthma-related airway inflammation. *Eur Rev Med Pharmacol Sci* 19: 4171-4181, 2015.

54.   **Fang Z, Li J, Yu X, Zhang D, Ren G, Shi B, Wang C, Kosinska AD, Wang S, Zhou X, Kozlowski M, Hu Y, and Yuan Z**. Polarization of Monocytic Myeloid-Derived Suppressor Cells by Hepatitis B Surface Antigen Is Mediated via ERK/IL-6/STAT3 Signaling Feedback and Restrains the Activation of T Cells in Chronic Hepatitis B Virus Infection. *J Immunol* 195: 4873-4883, 2015.

55.   **Fang Z, Zhu K, Guo N, Zhang N, Guan M, Yang C, Pan Q, Wei R, Deng C, Liu X, Zhao P, and Leng Q**. HCV J6/JFH1 tilts the capability of myeloid-derived dendritic cells to favor the induction of immunosuppression and Th17-related inflammatory cytokines. *Pharm Res* 32: 741-748, 2015.

56.   **Fletcher M, Ramirez ME, Sierra RA, Raber P, Thevenot P, Al-Khami AA, Sanchez-Pino D, Hernandez C, Wyczechowska DD, Ochoa AC, and Rodriguez PC**. l-Arginine depletion blunts antitumor T-cell responses by inducing myeloid-derived suppressor cells. *Cancer Res* 75: 275-283, 2015.

57.   **Foster JR**. The functions of cytokines and their uses in toxicology. *Int J Exp Pathol* 82: 171-192, 2001.

58.   **Frank MM, and Fries LF**. The role of complement in inflammation and phagocytosis. *Immunol Today* 12: 322-326, 1991.

59.   **Friend C**. Cell-free transmission in adult Swiss mice of a disease having the character of a leukemia. *J Exp Med* 105: 307-318, 1957.

60.   **Gabrilovich DI, and Nagaraj S**. Myeloid-derived suppressor cells as regulators of the immune system. *Nat Rev Immunol* 9: 162-174, 2009.

61.   **Galluzzi L, Vacchelli E, Bravo-San Pedro JM, Buque A, Senovilla L, Baracco EE, Bloy N, Castoldi F, Abastado JP, Agostinis P, Apte RN, Aranda F, Ayyoub M, Beckhove P, Blay JY, Bracci L, Caignard A, Castelli C, Cavallo F, Celis E, Cerundolo V, Clayton A, Colombo MP, Coussens L, Dhodapkar MV, Eggermont AM, Fearon DT, Fridman WH, Fucikova J, Gabrilovich DI, Galon J, Garg A, Ghiringhelli F, Giaccone G, Gilboa E, Gnjatic S, Hoos A, Hosmalin A, Jager D, Kalinski P, Karre K, Kepp O, Kiessling R, Kirkwood JM, Klein E, Knuth A, Lewis CE, Liblau R, Lotze MT, Lugli E, Mach JP, Mattei F, Mavilio D, Melero I, Melief CJ, Mittendorf EA, Moretta L, Odunsi A, Okada H, Palucka AK, Peter ME, Pienta KJ, Porgador A, Prendergast GC, Rabinovich GA, Restifo NP, Rizvi N, Sautes-Fridman C, Schreiber H, Seliger B, Shiku H, Silva-Santos B, Smyth MJ, Speiser DE, Spisek R, Srivastava PK, Talmadge JE, Tartour E, Van Der Burg SH, Van Den Eynde BJ, Vile R, Wagner H, Weber JS, Whiteside TL, Wolchok JD, Zitvogel L, Zou W, and Kroemer G**. Classification of current anticancer immunotherapies. *Oncotarget* 5: 12472-12508, 2014.

62.   **Gato-Canas M, Martinez de Morentin X, Blanco-Luquin I, Fernandez-Irigoyen J, Zudaire I, Liechtenstein T, Arasanz H, Lozano T, Casares N, Chaikuad A, Knapp S, Guerrero-Setas D, Escors D, Kochan G, and Santamaria E**. A core of kinase-regulated interactomes defines the neoplastic MDSC lineage. *Oncotarget* 6: 27160-27175, 2015.

63.   **Green KA, Cook WJ, and Green WR**. Myeloid-derived suppressor cells in murine retrovirus-induced AIDS inhibit T- and B-cell responses in vitro that are used to define the immunodeficiency. *J Virol* 87: 2058-2071, 2013.

64.   **Green KA, Wang L, Noelle RJ, and Green WR**. Selective Involvement of the Checkpoint Regulator VISTA in Suppression of B-Cell, but Not T-Cell, Responsiveness by Monocytic Myeloid-Derived Suppressor Cells from Mice Infected with an Immunodeficiency-Causing Retrovirus. *J Virol* 89: 9693-9698, 2015.

65.   **Guan Q, Blankstein AR, Anjos K, Synova O, Tulloch M, Giftakis A, Yang B, Lambert P, Peng Z, Cuvelier GD, and Wall DA**. Functional Myeloid-Derived Suppressor Cell Subsets Recover Rapidly after Allogeneic Hematopoietic Stem/Progenitor Cell Transplantation. *Biol Blood Marrow Transplant* 21: 1205-1214, 2015.

66.   **Gupta PK, Godec J, Wolski D, Adland E, Yates K, Pauken KE, Cosgrove C, Ledderose C, Junger WG, Robson SC, Wherry EJ, Alter G, Goulder PJ, Klenerman P, Sharpe AH, Lauer GM, and Haining WN**. CD39 Expression Identifies Terminally Exhausted CD8+ T Cells. *PLoS Pathog* 11: e1005177, 2015.

67.   **Hammerich L, and Tacke F**. Emerging roles of myeloid derived suppressor cells in hepatic inflammation and fibrosis. *World J Gastrointest Pathophysiol* 6: 43-50, 2015.

68.   **Hasenkrug KJ**. The leptin connection: regulatory T cells and autoimmunity. *Immunity* 26: 143-145, 2007.

69.   **Hasenkrug KJ**. Lymphocyte deficiencies increase susceptibility to friend virus-induced erythroleukemia in Fv-2 genetically resistant mice. *J Virol* 73: 6468-6473, 1999.

70.   **Hasenkrug KJ, Brooks DM, Nishio J, and Chesebro B**. Differing T-cell requirements for recombinant retrovirus vaccines. *J Virol* 70: 368-372, 1996.

71.   **Hasenkrug KJ, Brooks DM, Robertson MN, Srinivas RV, and Chesebro B**. Immunoprotective determinants in friend murine leukemia virus envelope protein. *Virology* 248: 66-73, 1998.

72.   **Hasenkrug KJ, and Chesebro B**. Immunity to retroviral infection: the Friend virus model. *Proc Natl Acad Sci U S A* 94: 7811-7816, 1997.

73.   **Hasenkrug KJ, and Dittmer U**. Immune control and prevention of chronic Friend retrovirus infection. *Front Biosci* 12: 1544-1551, 2007.

74.   **Hodi FS, Corless CL, Giobbie-Hurder A, Fletcher JA, Zhu M, Marino-Enriquez A, Friedlander P, Gonzalez R, Weber JS, Gajewski TF, O'Day SJ, Kim KB, Lawrence D, Flaherty KT, Luke JJ, Collichio FA, Ernstoff MS, Heinrich MC, Beadling C, Zukotynski KA, Yap JT, Van den Abbeele AD, Demetri GD, and Fisher DE**. Imatinib for melanomas harboring mutationally activated or amplified KIT arising on mucosal, acral, and chronically sun-damaged skin. *J Clin Oncol* 31: 3182-3190, 2013.

75.   **Ito H, Ando T, and Seishima M**. Inhibition of iNOS activity enhances the anti-tumor effects of alpha-galactosylceramide in established murine cancer model. *Oncotarget* 6: 41863-41874, 2015.

76.   **Joedicke JJ, Dietze KK, Zelinskyy G, and Dittmer U**. The phenotype and activation status of regulatory T cells during Friend retrovirus infection. *Virol Sin* 29: 48-60, 2014.

77.   **Joedicke JJ, Zelinskyy G, Dittmer U, and Hasenkrug KJ**. CD8+ T cells are essential for controlling acute friend retrovirus infection in C57BL/6 mice. *J Virol* 88: 5200-5201, 2014.

78.   **Kahan SM, Wherry EJ, and Zajac AJ**. T cell exhaustion during persistent viral infections. *Virology* 479-480: 180-193, 2015.

79.   **Kang X, Zhang X, Liu Z, Xu H, Wang T, He L, and Zhao A**. CXCR2-Mediated Granulocytic Myeloid-Derived Suppressor Cells' Functional Characterization and Their Role in Maternal Fetal Interface. *DNA Cell Biol* 35: 358-365, 2016.

80.   **Kang X, Zhang X, Liu Z, Xu H, Wang T, He L, and Zhao A**. Granulocytic myeloid-derived suppressor cells maintain feto-maternal tolerance by inducing Foxp3 expression in CD4+CD25-T cells by activation of the TGF-beta/beta-catenin pathway. *Mol Hum Reprod* 22: 499-511, 2016.

81.   **Karakhanova S, Link J, Heinrich M, Shevchenko I, Yang Y, Hassenpflug M, Bunge H, von Ahn K, Brecht R, Mathes A, Maier C, Umansky V, Werner J, and Bazhin AV**. Characterization of myeloid leukocytes and soluble mediators in pancreatic cancer: importance of myeloid-derived suppressor cells. *Oncoimmunology* 4: e998519, 2015.

82.   **Kawano M, Mabuchi S, Matsumoto Y, Sasano T, Takahashi R, Kuroda H, Kozasa K, Hashimoto K, Isobe A, Sawada K, Hamasaki T, Morii E, and Kimura T**. The significance of G-CSF expression and myeloid-derived suppressor cells in the chemoresistance of uterine cervical cancer. *Sci Rep* 5: 18217, 2015.

83.   **Kobie JJ, Shah PR, Yang L, Rebhahn JA, Fowell DJ, and Mosmann TR**. T regulatory and primed uncommitted CD4 T cells express CD73, which suppresses effector CD4 T cells by converting 5'-adenosine monophosphate to adenosine. *J Immunol* 177: 6780-6786, 2006.

84.   **Kong X, Sun R, Chen Y, Wei H, and Tian Z**. gammadeltaT cells drive myeloid-derived suppressor cell-mediated CD8+ T cell exhaustion in hepatitis B virus-induced immunotolerance. *J Immunol* 193: 1645-1653, 2014.

85.   **Kumar V, Patel S, Tcyganov E, and Gabrilovich DI**. The Nature of Myeloid-Derived Suppressor Cells in the Tumor Microenvironment. *Trends Immunol* 37: 208-220, 2016.

86.   **Lahl K, Loddenkemper C, Drouin C, Freyer J, Arnason J, Eberl G, Hamann A, Wagner H, Huehn J, and Sparwasser T**. Selective depletion of Foxp3+ regulatory T cells induces a scurfy-like disease. *J Exp Med* 204: 57-63, 2007.

87.   **Lander MR, and Chattopadhyay SK**. A Mus dunni cell line that lacks sequences closely related to endogenous murine leukemia viruses and can be infected by ectropic, amphotropic, xenotropic, and mink cell focus-forming viruses. *J Virol* 52: 695-698, 1984.

88.   **Lee JE, Walsh MC, Hoehn KL, James DE, Wherry EJ, and Choi Y**. Acetyl CoA Carboxylase 2 Is Dispensable for CD8+ T Cell Responses. *PLoS One* 10: e0137776, 2015.

89.   **Lei AH, Yang Q, Cai WP, Liu YF, Lan Y, Qin AP, Hu FY, and Zhou J**. Clinical Significance of Myeloid-Derived Suppressor Cells in Human Immunodeficiency Virus-1/ Hepatitis C Virus-coinfected Patients. *Scand J Immunol* 83: 438-444, 2016.

90.   **Lindau D, Gielen P, Kroesen M, Wesseling P, and Adema GJ**. The immunosuppressive tumour network: myeloid-derived suppressor cells, regulatory T cells and natural killer T cells. *Immunology* 138: 105-115, 2013.

91.   **Luke JJ, and Hodi FS**. Ipilimumab, vemurafenib, dabrafenib, and trametinib: synergistic competitors in the clinical management of BRAF mutant malignant melanoma. *Oncologist* 18: 717-725, 2013.

92.   **Mairhofer DG, Ortner D, Tripp CH, Schaffenrath S, Fleming V, Heger L, Komenda K, Reider D, Dudziak D, Chen S, Becker JC, Flacher V, and Stoitzner P**. Impaired gp100-Specific CD8(+) T-Cell Responses in the Presence of Myeloid-Derived Suppressor Cells in a Spontaneous Mouse Melanoma Model. *J Invest Dermatol* 135: 2785-2793, 2015.

93.   **Markowitz J, Wesolowski R, Papenfuss T, Brooks TR, and Carson WE, 3rd**. Myeloid-derived suppressor cells in breast cancer. *Breast Cancer Res Treat* 140: 13-21, 2013.

94.   **McCoy JP, Jr., and Overton WR**. Quality control in flow cytometry for diagnostic pathology: II. A conspectus of reference ranges for lymphocyte immunophenotyping. *Cytometry* 18: 129-139, 1994.

95.   **McCoy KD, and Le Gros G**. The role of CTLA-4 in the regulation of T cell immune responses. *Immunol Cell Biol* 77: 1-10, 1999.

96.   **Mills KH**. Regulatory T cells: friend or foe in immunity to infection? *Nat Rev Immunol* 4: 841-855, 2004.

97.   **Mills KH, and McGuirk P**. Antigen-specific regulatory T cells--their induction and role in infection. *Semin Immunol* 16: 107-117, 2004.

98.   **Mills KR, Reginato M, Debnath J, Queenan B, and Brugge JS**. Tumor necrosis factor-related apoptosis-inducing ligand (TRAIL) is required for induction of autophagy during lumen formation in vitro. *Proc Natl Acad Sci U S A* 101: 3438-3443, 2004.

99.   **Moreau-Gachelin F**. Multi-stage Friend murine erythroleukemia: molecular insights into oncogenic cooperation. *Retrovirology* 5: 99, 2008.

100.   **Moses K, and Brandau S**. Human neutrophils: Their role in cancer and relation to myeloid-derived suppressor cells. *Semin Immunol* 28: 187-196, 2016.

101.   **Moses K, Klein JC, Mann L, Klingberg A, Gunzer M, and Brandau S**. Survival of residual neutrophils and accelerated myelopoiesis limit the efficacy of antibody-mediated depletion of Ly-6G+ cells in tumor-bearing mice. *J Leukoc Biol* 99: 811-823, 2016.

102.   **Munn DH, and Bronte V**. Immune suppressive mechanisms in the tumor microenvironment. *Curr Opin Immunol* 39: 1-6, 2016.

103.   **Murphy K, Travers P, Walport M, and Janeway C**. *Janeway's immunobiology*. New York: Garland Science, 2012, p. xix, 868 p.

104.   **Myers L, and Hasenkrug KJ**. Retroviral immunology: lessons from a mouse model. *Immunol Res* 43: 160-166, 2009.

105. **Ning G, She L, Lu L, Liu Y, Zeng Y, Yan Y, and Lin C**. Analysis of monocytic and granulocytic myeloid-derived suppressor cells subsets in patients with hepatitis C virus infection and their clinical significance. *Biomed Res Int* 2015: 385378, 2015.

106. **O'Connor MA, Fu WW, Green KA, and Green WR**. Subpopulations of M-MDSCs from mice infected by an immunodeficiency-causing retrovirus and their differential suppression of T- vs B-cell responses. *Virology* 485: 263-273, 2015.

107. **Odorizzi PM, Pauken KE, Paley MA, Sharpe A, and Wherry EJ**. Genetic absence of PD-1 promotes accumulation of terminally differentiated exhausted CD8+ T cells. *J Exp Med* 212: 1125-1137, 2015.

108. **Pallett LJ, Gill US, Quaglia A, Sinclair LV, Jover-Cobos M, Schurich A, Singh KP, Thomas N, Das A, Chen A, Fusai G, Bertoletti A, Cantrell DA, Kennedy PT, Davies NA, Haniffa M, and Maini MK**. Metabolic regulation of hepatitis B immunopathology by myeloid-derived suppressor cells. *Nat Med* 21: 591-600, 2015.

109. **Pang X, Song H, Zhang Q, Tu Z, and Niu J**. Hepatitis C virus regulates the production of monocytic myeloid-derived suppressor cells from peripheral blood mononuclear cells through PI3K pathway and autocrine signaling. *Clin Immunol* 164: 57-64, 2016.

110. **Passiglia F, Bronte G, Bazan V, Natoli C, Rizzo S, Galvano A, Listi A, Cicero G, Rolfo C, Santini D, and Russo A**. PD-L1 expression as predictive biomarker in patients with NSCLC: a pooled analysis. *Oncotarget* 7: 19738-19747, 2016.

111. **Pauken KE, and Wherry EJ**. Overcoming T cell exhaustion in infection and cancer. *Trends Immunol* 36: 265-276, 2015.

112. **Pauken KE, and Wherry EJ**. SnapShot: T Cell Exhaustion. *Cell* 163: 1038-1038 e1031, 2015.

113. **Pinton L, Solito S, Damuzzo V, Francescato S, Pozzuoli A, Berizzi A, Mocellin S, Rossi CR, Bronte V, and Mandruzzato S**. Activated T cells sustain myeloid-derived suppressor cell-mediated immune suppression. *Oncotarget* 7: 1168-1184, 2016.

114. **Qin A, Cai W, Pan T, Wu K, Yang Q, Wang N, Liu Y, Yan D, Hu F, Guo P, Chen X, Chen L, Zhang H, Tang X, and Zhou J**. Expansion of monocytic myeloid-derived suppressor cells dampens T cell function in HIV-1-seropositive individuals. *J Virol* 87: 1477-1490, 2013.

115. **Raber PL, Thevenot P, Sierra R, Wyczechowska D, Halle D, Ramirez ME, Ochoa AC, Fletcher M, Velasco C, Wilk A, Reiss K, and Rodriguez PC**. Subpopulations of myeloid-derived suppressor cells impair T cell responses through independent nitric oxide-related pathways. *International journal of cancer* 134: 2853-2864, 2014.

116. **Ren JP, Zhao J, Dai J, Griffin JW, Wang L, Wu XY, Morrison ZD, Li GY, El Gazzar M, Ning SB, Moorman JP, and Yao ZQ**. Hepatitis C virus-induced myeloid-derived suppressor cells regulate T-cell differentiation and function via the signal transducer and activator of transcription 3 pathway. *Immunology* 148: 377-386, 2016.

117. **Robertson MN, Miyazawa M, Mori S, Caughey B, Evans LH, Hayes SF, and Chesebro B**. Production of monoclonal antibodies reactive with a denatured form of the Friend murine leukemia virus gp70 envelope protein: use in a focal infectivity assay, immunohistochemical studies, electron microscopy and western blotting. *J Virol Methods* 34: 255-271, 1991.

118. **Robertson MN, Spangrude GJ, Hasenkrug K, Perry L, Nishio J, Wehrly K, and Chesebro B**. Role and specificity of T-cell subsets in spontaneous recovery from Friend virus-induced leukemia in mice. *J Virol* 66: 3271-3277, 1992.

119. **Robertson SJ, Ammann CG, Messer RJ, Carmody AB, Myers L, Dittmer U, Nair S, Gerlach N, Evans LH, Cafruny WA, and Hasenkrug KJ**. Suppression of

acute anti-friend virus CD8+ T-cell responses by coinfection with lactate dehydrogenase-elevating virus. *J Virol* 82: 408-418, 2008.

120. **Robertson SJ, and Hasenkrug KJ**. The role of virus-induced regulatory T cells in immunopathology. *Springer Semin Immunopathol* 28: 51-62, 2006.

121. **Robertson SJ, Messer RJ, Carmody AB, and Hasenkrug KJ**. In vitro suppression of CD8+ T cell function by Friend virus-induced regulatory T cells. *J Immunol* 176: 3342-3349, 2006.

122. **Robertson SJ, Messer RJ, Carmody AB, Mittler RS, Burlak C, and Hasenkrug KJ**. CD137 costimulation of CD8+ T cells confers resistance to suppression by virus-induced regulatory T cells. *J Immunol* 180: 5267-5274, 2008.

123. **Rodriguez PC, Quiceno DG, and Ochoa AC**. L-arginine availability regulates T-lymphocyte cell-cycle progression. *Blood* 109: 1568-1573, 2007.

124. **Rood JE, Rao S, Paessler M, Kreiger PA, Chu N, Stelekati E, Wherry EJ, and Behrens EM**. ST2 contributes to T-cell hyperactivation and fatal hemophagocytic lymphohistiocytosis in mice. *Blood* 127: 426-435, 2016.

125. **Saha A, O'Connor RS, Thangavelu G, Lovitch SB, Dandamudi DB, Wilson CB, Vincent BG, Tkachev V, Pawlicki JM, Furlan SN, Kean LS, Aoyama K, Taylor PA, Panoskaltsis-Mortari A, Foncea R, Ranganathan P, Devine SM, Burrill JS, Guo L, Sacristan C, Snyder NW, Blair IA, Milone MC, Dustin ML, Riley JL, Bernlohr DA, Murphy WJ, Fife BT, Munn DH, Miller JS, Serody JS, Freeman GJ, Sharpe AH, Turka LA, and Blazar BR**. Programmed death ligand-1 expression on donor T cells drives graft-versus-host disease lethality. *J Clin Invest* 126: 2642-2660, 2016.

126. **Santiago ML, Montano M, Benitez R, Messer RJ, Yonemoto W, Chesebro B, Hasenkrug KJ, and Greene WC**. Apobec3 encodes Rfv3, a gene influencing neutralizing antibody control of retrovirus infection. *Science* 321: 1343-1346, 2008.

127. **Sasso MS, Lollo G, Pitorre M, Solito S, Pinton L, Valpione S, Bastiat G, Mandruzzato S, Bronte V, Marigo I, and Benoit JP**. Low dose gemcitabine-loaded lipid nanocapsules target monocytic myeloid-derived suppressor cells and potentiate cancer immunotherapy. *Biomaterials* 96: 47-62, 2016.

128. **Schepers K, Toebes M, Sotthewes G, Vyth-Dreese FA, Dellemijn TA, Melief CJ, Ossendorp F, and Schumacher TN**. Differential kinetics of antigen-specific CD4+ and CD8+ T cell responses in the regression of retrovirus-induced sarcomas. *J Immunol* 169: 3191-3199, 2002.

129. **Schlie K, Westerback A, DeVorkin L, Hughson LR, Brandon JM, MacPherson S, Gadawski I, Townsend KN, Poon VI, Elrick MA, Cote HC, Abraham N, Wherry EJ, Mizushima N, and Lum JJ**. Survival of effector CD8+ T cells during influenza infection is dependent on autophagy. *J Immunol* 194: 4277-4286, 2015.

130. **Schuler PJ, Westerkamp AM, Kansy BA, Bruderek K, Dissmann PA, Dumitru CA, Lang S, Jackson EK, and Brandau S**. Adenosine metabolism of human mesenchymal stromal cells isolated from patients with head and neck squamous cell carcinoma. *Immunobiology* 2016.

131. **Seddiki N, Brezar V, and Draenert R**. Cell exhaustion in HIV-1 infection: role of suppressor cells. *Curr Opin HIV AIDS* 9: 452-458, 2014.

132. **Serafini P, Mgebroff S, Noonan K, and Borrello I**. Myeloid-derived suppressor cells promote cross-tolerance in B-cell lymphoma by expanding regulatory T cells. *Cancer Res* 68: 5439-5449, 2008.

133. **Shen L, Sundstedt A, Ciesielski M, Miles KM, Celander M, Adelaiye R, Orillion A, Ciamporcero E, Ramakrishnan S, Ellis L, Fenstermaker R, Abrams SI, Eriksson H, Leanderson T, Olsson A, and Pili R**. Tasquinimod modulates

suppressive myeloid cells and enhances cancer immunotherapies in murine models. *Cancer Immunol Res* 3: 136-148, 2015.

134. **Shi G, Wang H, and Zhuang X**. Myeloid-derived suppressor cells enhance the expression of melanoma-associated antigen A4 in a Lewis lung cancer murine model. *Oncol Lett* 11: 809-816, 2016.

135. **Smith LL, Wherry SJ, Larkey LK, Ainsworth BE, and Swan PD**. Energy expenditure and cardiovascular responses to Tai Chi Easy. *Complement Ther Med* 23: 802-805, 2015.

136. **Starborg M, Gell K, Brundell E, and Hoog C**. The murine Ki-67 cell proliferation antigen accumulates in the nucleolar and heterochromatic regions of interphase cells and at the periphery of the mitotic chromosomes in a process essential for cell cycle progression. *J Cell Sci* 109 (Pt 1): 143-153, 1996.

137. **Stoye JP**. Studies of endogenous retroviruses reveal a continuing evolutionary saga. *Nat Rev Microbiol* 10: 395-406, 2012.

138. **Stromnes IM, Dittmer U, Schumacher TN, Schepers K, Messer RJ, Evans LH, Peterson KE, Race B, and Hasenkrug KJ**. Temporal effects of gamma interferon deficiency on the course of Friend retrovirus infection in mice. *J Virol* 76: 2225-2232, 2002.

139. **Sui Y, Hogg A, Wang Y, Frey B, Yu H, Xia Z, Venzon D, McKinnon K, Smedley J, Gathuka M, Klinman D, Keele BF, Langermann S, Liu L, Franchini G, and Berzofsky JA**. Vaccine-induced myeloid cell population dampens protective immunity to SIV. *J Clin Invest* 124: 2538-2549, 2014.

140. **Tacke RS, Lee HC, Goh C, Courtney J, Polyak SJ, Rosen HR, and Hahn YS**. Myeloid suppressor cells induced by hepatitis C virus suppress T-cell responses through the production of reactive oxygen species. *Hepatology* 55: 343-353, 2012.

141. **Takenaka MC, Robson S, and Quintana FJ**. Regulation of the T Cell Response by CD39. *Trends Immunol* 37: 427-439, 2016.

142. **Twyman-Saint Victor C, Rech AJ, Maity A, Rengan R, Pauken KE, Stelekati E, Benci JL, Xu B, Dada H, Odorizzi PM, Herati RS, Mansfield KD, Patsch D, Amaravadi RK, Schuchter LM, Ishwaran H, Mick R, Pryma DA, Xu X, Feldman MD, Gangadhar TC, Hahn SM, Wherry EJ, Vonderheide RH, and Minn AJ**. Radiation and dual checkpoint blockade activate non-redundant immune mechanisms in cancer. *Nature* 520: 373-377, 2015.

143. **Vincent J, Mignot G, Chalmin F, Ladoire S, Bruchard M, Chevriaux A, Martin F, Apetoh L, Rebe C, and Ghiringhelli F**. 5-Fluorouracil selectively kills tumor-associated myeloid-derived suppressor cells resulting in enhanced T cell-dependent antitumor immunity. *Cancer Res* 70: 3052-3061, 2010.

144. **Vollbrecht T, Stirner R, Tufman A, Roider J, Huber RM, Bogner JR, Lechner A, Bourquin C, and Draenert R**. Chronic progressive HIV-1 infection is associated with elevated levels of myeloid-derived suppressor cells. *Aids* 26: F31-37, 2012.

145. **Waldron TJ, Quatromoni JG, Karakasheva TA, Singhal S, and Rustgi AK**. Myeloid derived suppressor cells: Targets for therapy. *Oncoimmunology* 2: e24117, 2013.

146. **Wang L, Zhao J, Ren JP, Wu XY, Morrison ZD, El Gazzar M, Ning SB, Moorman JP, and Yao ZQ**. Expansion of myeloid-derived suppressor cells promotes differentiation of regulatory T cells in HIV-1+ individuals. *Aids* 30: 1521-1531, 2016.

147. **Weber C**. Hepatitis: Myeloid-derived suppressor cells in HBV infection. *Nat Rev Gastroenterol Hepatol* 12: 370, 2015.

148. **Wesolowski R, Markowitz J, and Carson WE, 3rd**. Myeloid derived suppressor cells - a new therapeutic target in the treatment of cancer. *J Immunother Cancer* 1: 10, 2013.

149. **Wherry EJ, and Kurachi M**. Molecular and cellular insights into T cell exhaustion. *Nat Rev Immunol* 15: 486-499, 2015.

150. **Wherry JN, Huffhines LP, and Walisky DN**. A Short Form of the Trauma Symptom Checklist for Children. *Child Maltreat* 21: 37-46, 2016.

151. **Winograd R, Byrne KT, Evans RA, Odorizzi PM, Meyer AR, Bajor DL, Clendenin C, Stanger BZ, Furth EE, Wherry EJ, and Vonderheide RH**. Induction of T-cell Immunity Overcomes Complete Resistance to PD-1 and CTLA-4 Blockade and Improves Survival in Pancreatic Carcinoma. *Cancer Immunol Res* 3: 399-411, 2015.

152. **Wu J, Zhang R, Tang N, Gong Z, Zhou J, Chen Y, Chen K, and Cai W**. Dopamine inhibits the function of Gr-1+CD115+ myeloid-derived suppressor cells through D1-like receptors and enhances anti-tumor immunity. *J Leukoc Biol* 97: 191-200, 2015.

153. **Youn JI, Collazo M, Shalova IN, Biswas SK, and Gabrilovich DI**. Characterization of the nature of granulocytic myeloid-derived suppressor cells in tumor-bearing mice. *J Leukoc Biol* 91: 167-181, 2012.

154. **Young MR, Newby M, and Wepsic HT**. Hematopoiesis and suppressor bone marrow cells in mice bearing large metastatic Lewis lung carcinoma tumors. *Cancer Res* 47: 100-105, 1987.

155. **Yu Z, Tan Z, Lee BK, Tang J, Wu X, Cheung KW, Lo NT, Man K, Liu L, and Chen Z**. Antigen spreading-induced CD8+T cells confer protection against the lethal challenge of wild-type malignant mesothelioma by eliminating myeloid-derived suppressor cells. *Oncotarget* 6: 32426-32438, 2015.

156. **Zaunders JJ, Ip S, Munier ML, Kaufmann DE, Suzuki K, Brereton C, Sasson SC, Seddiki N, Koelsch K, Landay A, Grey P, Finlayson R, Kaldor J, Rosenberg ES, Walker BD, Fazekas de St Groth B, Cooper DA, and Kelleher AD**. Infection of CD127+ (interleukin-7 receptor+) CD4+ cells and overexpression of CTLA-4 are linked to loss of antigen-specific CD4 T cells during primary human immunodeficiency virus type 1 infection. *J Virol* 80: 10162-10172, 2006.

157. **Zehn D, and Wherry EJ**. Immune Memory and Exhaustion: Clinically Relevant Lessons from the LCMV Model. *Adv Exp Med Biol* 850: 137-152, 2015.

158. **Zelinskyy G, Balkow S, Schimmer S, Schepers K, Simon MM, and Dittmer U**. Independent roles of perforin, granzymes, and Fas in the control of Friend retrovirus infection. *Virology* 330: 365-374, 2004.

159. **Zelinskyy G, Balkow S, Schimmer S, Werner T, Simon MM, and Dittmer U**. The level of friend retrovirus replication determines the cytolytic pathway of CD8+ T-cell-mediated pathogen control. *J Virol* 81: 11881-11890, 2007.

160. **Zelinskyy G, Kraft AR, Schimmer S, Arndt T, and Dittmer U**. Kinetics of CD8+ effector T cell responses and induced CD4+ regulatory T cell responses during Friend retrovirus infection. *Eur J Immunol* 36: 2658-2670, 2006.

161. **Zelinskyy G, Robertson SJ, Schimmer S, Messer RJ, Hasenkrug KJ, and Dittmer U**. CD8+ T-cell dysfunction due to cytolytic granule deficiency in persistent Friend retrovirus infection. *J Virol* 79: 10619-10626, 2005.

162. **Zelinskyy G, Werner T, and Dittmer U**. Natural regulatory T cells inhibit production of cytotoxic molecules in CD8(+) T cells during low-level Friend retrovirus infection. *Retrovirology* 10: 109, 2013.

163. **Zeng QL, Yang B, Sun HQ, Feng GH, Jin L, Zou ZS, Zhang Z, Zhang JY, and Wang FS**. Myeloid-derived suppressor cells are associated with viral persistence and downregulation of TCR zeta chain expression on CD8(+) T cells in chronic hepatitis C patients. *Mol Cells* 37: 66-73, 2014.

164. **Zippelius A, Batard P, Rubio-Godoy V, Bioley G, Lienard D, Lejeune F, Rimoldi D, Guillaume P, Meidenbauer N, Mackensen A, Rufer N, Lubenow N, Speiser D, Cerottini JC, Romero P, and Pittet MJ**. Effector function of human

tumor-specific CD8 T cells in melanoma lesions: a state of local functional tolerance. *Cancer Res* 64: 2865-2873, 2004.

10 Appendix

10.1 List of Abbreviations

Abbreviations	Full name
5FU	5-Fluorouracil
˚C	Degree Celsius
µl	Microlitre
ADCC	Antibody dependent cell mediated cytotoxicity
AF 700	Alexa Fluor 700
AF 488	Alexa Fluor 488
AF 647	Alexa Fluor 647
AIDS	Acquired Immune Deficiency Syndrome
APC	Antigen presenting cells
APC	Allophycocyanin
APC-Cy7	APC-cyanine 7
Arg	Arginase
B7RP1	B7-Related protein1
BCL-6	B cell lymphoma 6
BM	Bone marrow
BSA	Bovine Serum Albumin
BV421	Brilliant violet 421

BV605	Brilliant violet 605
CAD	Caspase-activated deoxyribonuclease
cAMP	Cyclic adenosine monophosphate
CD	Cluster of differentiation
CFSE	Carboxyfluorescein succinimidyl ester
CTL	Cytotoxic T cells
CTLA-4	Cytotoxic T Lymphocyte Antigen 4
DC	Dendritic cell
DEREG	Depletion of regulatory T cells
DMSO	Dimethyl sulfoxide
DNA	Deoxyribonucleic acid
DT	Diphtheria toxin
DTR	Diphtheria toxin receptor
EDTA	Etylenadiaminetetraacetic acid
eF650	eFluor 650
eF780	eFluor 780
eF450	eFluor 450
Env	Envelope protein
FACS	Fluorescence Activated Cells Scanner (Flow cytometer)
FASL	FAS ligand

FCS	Fetal Calf Serum
FITC	Fluorescein isothiocyanate
F-MuLV	Friend murine leukemia virus
Foxp3	Forkhead box P3
FSC	Forward scatter
FV	Friend Virus
FVD	Fixable viable dye
g	Gram
Gag	Group specific antigen
GATA-3	Gata binding protein 3
GFP	Green fluorescence protein
gMDSC	Granulocytic myeloid derived suppressor cell
Gzm	Granzyme
HBV	Hepatitis B Virus
HCV	Hepatitis C Virus
HIV	Human Immunodeficiency Virus
HPV	Human papillomavirus
HTLV-1	Human T cell leukemia virus-1
i.p.	Intraperitoneal
i.v.	Intravenous

ICOS	Inducible costimulatory
IDO	Idoleamine 2,3-dioxygenase
IFN-γ	Interferon gamma
Ig	Immunoglobulin
IL	Interleukin
iTregs	Induced Tregs
KLRG-1	Killer cell lectin-like receptor subfamily G member 1
l	Liter
LAG-3	Lymphocyte-activation gene 3
LN	Lymph nodes
L-NMMA	N^G-Monomethyl-L-arginine, monoacetate salt
LTR	Long Treminal Repeat
Mab	Monoclonal antibody
MDSC	myeloid derived suppressor cell
mg	Miligram
MHC	Major histocompatibility complex
ml	Mililitre
mMDSC	monocytic myeloid-derived suppressor cell
mRNA	Messenger RNA

MSV	Murine sarcoma virus
n.s.	Non-significant
NK	Natural Killer cells
Nor-NOHA	N^{ω}-hydroxy-nor-Arginine
NOS	Nitric oxide synthase
Nrp-1	Neuropilin-1
nTregs	Natural Tregs
PAMPs	Pathogen-Associated Molecular Patterns
PBBS	Phosphate Buffered Saline, containing 1.0 g glucose
PBS	Phosphate Buffered Saline
PD-1	Programmed cell death 1
PD-L1	Programmed cell death ligand 1
PE	Phycoerythrin
PE Cy5	Phycoerythrin-Cyanine 5
PE Cy7	Phycoerythrin- Cyanine 7
PerCP	Peridinin-chlorophyll-protein complex
PI	Propidium iodide
PMT	Photomultiplier tube
Pol	Polymerase
PRR	Pathogen Recognition Receptors

RNA	Ribonucleic acid
ROS	Reactive oxygen species
RPMI-1640	Rosewell Park Memorial Institute Medium 1640
RSV	Rous sarcoma virus
s.c.	Subcutaneous
SFFV	Spleen focus forming virus
si	Small intestine
SPF	Specific pathogen-free
SSC	Sideward scatter
STAT	Signal Transducer and Activator of Transcription
Tcon	Conventional CD4+ T cells
TCR	T cell receptor
Tetr	Tetramer
TGF-β	Transforming Growth Factor-beta
Th	T helper cells
Tim3	T cell immunoglobulin domain and mucin domain-3
TLR	Toll-Like Receptor
TNFR	Tumor necrosis factor receptor
TNF-α	Tumor necrosis factor-alpha
TRAIL	Tumor-necrosis-factor-related apoptosis-inducing ligand

Tregs	Regulatory T cells

10.2 Figure list

10.3 Table list

10.4 List of publications:

Akhmetzyanova I, Drabczyk M, Neff CP, Gibbert K, Dietze KK, Werner T, et al. (2015) PD-L1 Expression on Retrovirus-Infected Cells Mediates Immune Escape from CD8+ T Cell Killing. PLoS Pathog 11(10): e1005224. doi:10.1371/journal.ppat.1005224

10.5 Acknowledgements

10.6 Curriculum Vitae